PFC/JA-93-30

Papers Presented at the
IEEE 15th Symposium on Fusion Engineering
by the Alcator C-MOD Group, October 1993.

S. Fairfax and the Alcator Group, W. Beck, H. Becker, V. Bertolino, R. L. Boivin, W. Burke Jr., E. Byrne, R. Childs, J. Daigle, C. L. Fiore, E. Fitzgerald, D. Flannary, T. Fredian, M. Freidberg, T. P. Fuller, J. Goetz, S. Golovato, M Graf, R. S. Granetz, M. Greenwald, S. Horne, A. Hubbard, I. Hutchinson, R. L. Myatt*, J. Paranay, M. Porkolab, C. T. Reddy, J. Rice, J. Schachter, S. Stillerman, Y. Takase, G. Tinios, T. Toland, J. Urbahn, S. Wolfe, X. Zhong.

Plasma Fusion Center
Massachusetts Institute of Technology
Cambridge, MA 02139

* Stone & Webster Engineering Corp.

To be published in Proceedings of IEEE 15th Symposium on Fusion Engineering

This work was supported by the U. S. Department of Energy Contract No. DE-AC02-78ET51013. Reproduction, translation, publication, use and disposal, in whole or in part by or for the United States government is permitted.

PAPERS PRESENTED AT THE IEEE SYMPOSIUM ON FUSION ENGINEERING BY THE ALCATOR C-MOD GROUP OCTOBER 1993

START-UP AND EARLY RESULTS FROM ALCATOR C-MOD
S. Fairfax and the Alcator Group
pp. 1-6

REPAIR OF POLOIDAL FIELD MAGNETS ON ALCATOR C-MOD
William Beck
pp. 7-10

STRUCTURAL BEHAVIOR OF COAXES IN TRANSVERSE MAGNETIC FIELDS
H. Becker, R. Leonard Myatt
pp. 11-13

CRYOGENIC SYSTEM FOR THE ALCATOR C-MOD TOKAMAK
R. L. Boivin, C. T. Reddy and the Alcator C-Mod Group
pp. 14-17

A RELIABLE TEMPERATURE CONTROL SYSTEM FOR THE ALCATOR C-MOD VACUUM VESSEL
William Burke, Eamonn Byrne
pp. 18-21

ALTERNATOR CONTROL SYSTEM FOR THE ALCATOR C-MOD TOKAMAK
Eamonn Byrne
pp. 22-25

DESIGN, CONTROL AND OPERATION OF THE VACUUM AND GAS SYSTEMS FOR ALCATOR C-MOD
R. Childs, J. Goetz, M. Graf, A. Hubbard, J. Rice, T. Toland
pp. 26-29

OPERATION OF THE ALCATOR C-MOD POWER SYSTEM
S. Fairfax, J. Daigle, V. Bertolino, J. Paranay, X. Zhong
pp. 30-33

RADIATION MEASUREMENTS FROM ALCATOR C-MOD INITIAL OPERATION
C. L. Fiore, T. P. Fuller, R. L. Boivin, R. S. Granetz
pp.34-37

DEVELOPMENT OF HIGH STRENGTH ELECTRICAL CONNECTIONS USING COPPER ELECTRODEPOSITION
E. Fitzgerald, C. T. Reddy
pp. 38-40

GROUND FAULT MONITORING IN ALCATOR C-MOD
D. Flanary
pp. 41-44

UPGRADING AND OPERATING OF THE 80 MHz TRANSMITTER ON THE ALCATOR C-MOD TOKAMAK
M. Fridberg, E. Byrne, S. Golovato, M. Porkolab, Y. Takase
pp. 45-48

PERFORMANCE OF THE C-MOD SHAPE CONTROL SYSTEM
S. Horne, M. Greenwald, I. Hutchinson, S. Wolfe, G. Tinios, T. Fredian, J. Stillerman
pp. 49-52

THE DESIGN AND PERFORMANCE OF A TWENTY BARREL HYDROGEN PELLET INJECTOR FOR ALCATOR C-MOD
J. Urbahn, M. Greenwald, J. Schachter
pp. 53-56

Start-up and Early Results from Alcator C-MOD

Stephen A. Fairfax and the Alcator Group
MIT Plasma Fusion Center NW21-111a
190 Albany Street, Cambridge, MA 02139

Abstract

Alcator C-MOD is a compact, high performance tokamak designed to address reactor-relevant issues including diverter operation, confinement, and auxiliary heating. It incorporates flexible shaping of non-circular, diverted plasmas, strong ICRF heating, and many innovative engineering features to achieve high performance in a compact device with modest cost. Like its predecessors, Alcator A and Alcator C, Alcator C-MOD uses cryogenically cooled copper magnets to produce high toroidal fields (9 Tesla at .67 m) and strong ohmic heating (up to 3 MA.) The thick wall of the vacuum vessel, while complicating the normal problems of plasma initiation and control, are relevant to virtually all next-generation designs.

The facility operated briefly in late 1991 and again in early 1992, when a terminal failed on one of the PF magnets. The experiment resumed operations in May 1993. This report describes the start-up and early operational experience, comparing with both design scenarios and previous experience on Alcator A and C. Results from operations during the summer of 1993 are presented.

Introduction

Alcator C-MOD was approved for construction in early 1987. The construction of the facility was completed in October 1991 [1]. A series of system integration tests without cryogenic cooling were performed. The tests were conducted without the cryostat in place to allow observation of magnets and bus. The integration of two dozen major subsystems, including over 50 computers using 3 different operating systems, was remarkably uneventful. Few unexpected behaviors were observed, and the tests, though limited in maximum magnet current and duration by the lack of cooling, resulted in production of a plasma. This accomplishment was significant because it demonstrated the ability to develop the necessary loop voltage and magnetic field null despite the significant eddy currents flowing in the one-piece, thick-walled vacuum chamber and surrounding superstructure. The lack of electrical breaks is prototypical of many future designs.

Work supported by U.S. DOE Contract No. DE-AC02-78ET51013
Manuscript submitted October 28, 1993

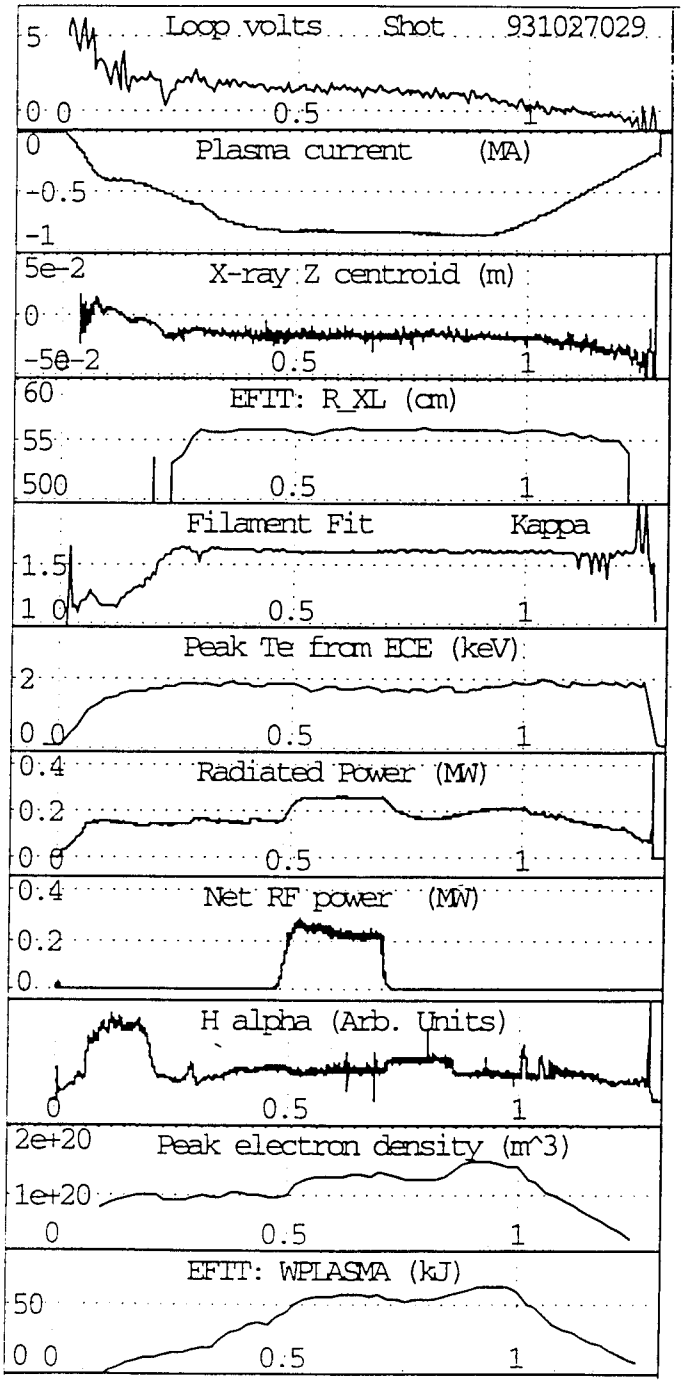

Fig. 1 Alcator C-MOD Plasma Shot #29, October 27, 1993
Note the H-mode transition at 0.8 seconds.

The installation of the cryogenic cooling system and basic diagnostic set required approximately 5 months. The initial cooling of the 150-ton structure to liquid nitrogen temperature was accomplished without incident, and tokamak operations began in March 1992.

The experiment was operating normally on April 10, 1992 when a ground fault was detected on the EF3 magnet system during shot 10. The EF3 upper magnet had suffered a structural failure of the terminal during operation. The associated damage was minimal, but the suspected culprit was the design of the terminal detail. The same approach had been used on 10 of the 13 PF magnets. Disassembly of the machine far enough to remove all the PF magnets required nearly 2 months. Analysis of the terminal [2] failed to identify a definitive mechanism for failure at the operating point, but did show that the design was marginal for full performance operation. Re-design of the terminal resulted in the development of a new technique for bonding copper without loss of strength or stress concentration [3] [4] The design effort, followed by production of 4 new magnets and 20 new terminals, required 6 months. Assembly of the tokamak was completed in 4 months.

The analysis of the failure and production of improved PF magnets consumed most of the engineering and technical manpower available to the project. The staff was augmented by 15 contract engineers and temporary technicians. The initial operating experience had been very instructive. Most systems performed well, but nearly all had identified hardware modifications and/or software upgrades. The cryogenic cooling systems and vacuum systems were completely overhauled [5] [6]. The vacuum vessel heating system was significantly upgraded and the control software completely rewritten [7]. The operator interface for most of the power system was upgraded and the networked engineering control system modified for more rapid and reliable communication of system state changes [8]. The power systems were extensively tested into dummy loads and all converters made fully operational. The testing revealed a minor design flaw that required addition of reactors in the crowbar circuits of 5 power supplies [9]. This flaw would have been difficult to identify in normal operation.

The results of the extensive work on the auxiliary systems during the magnet repair were immediately apparent. The tokamak resumed operation on April 29, 1993. The facility has shown remarkable reliability since that time, with only a single run day canceled in the first 5 months of operation. This degree of availability and performance would have been impossible to achieve if the facility had been operational for the year. It is extremely difficult (and somewhat dangerous) to modify the hardware or software of operating systems.

Initial Operation

Figure 1 shows representative data from a typical shot on October 27, 1993. Plasma current, position, and shape are under feedback control for most of the discharge. This particular shot used feedback on plasma current, plasma position (r and z), x-point location, and separation of the last closed flux surface (LCFS) from the inner wall.

The plasma is initiated (at time = 0 in Fig. 1) by opening 5 thyristor circuit breakers in series with the OH1, OH2U, OH2L, EF1U, and EF1L magnets and power supplies. The loop voltage required for ionization and current rise is typically 4.5 to 6 volts. The power supplies remain in the circuit at all times to provide fine adjustment of the magnet voltages. At approximately 100 msec, the circuit breakers are closed again, and the resulting drop in loop voltage causes a momentary halt in the plasma current rise. The plasma current feedback control compensates for this loss of loop voltage by increasing the power supply inversion voltages, driving the current to 500 kA. The OH1 power supply current reaches 0 approximately 200 msec into the discharge. This supply requires a brief (20-50 msec) interval to switch from forward current to reverse current thyristor bridges. The four OH2 and EF1 converters, used for plasma position control as well as current drive, use circulating current converters and do not pause as their output current crosses 0.

The plasma current continues to rise to the programmed level of 850 kA. The current is held constant until the discharge is deliberately terminated after 1 second. The plasma current is gradually reduced to 120 kA before disrupting.

The plasma position and shape are controlled throughout the discharge. The central panels in Fig. 1 show several measures of plasma shape and position from both soft X-ray centroid and EFIT code results computed after the pulse. The position is programmed a few centimeters below the midplane for proper positioning of the diverter for this shape. The position of the x-point is shown as well. The plasma elongation is held at 1.6 throughout the discharge.

The position control parameters can be set to control inner gap and outer gap instead of inner gap and centroid; outer gap feedback is more useful for matching to the RF antenna. The hybrid computer is central to the Plasma Control System (PCS) [10]. The PCS can combine up to 96 analog input channels to construct up to 16 estimates of parameters to be controlled. The selection of control parameters can be varied from one shot to the next. Desired trajectories of the parameters are drawn or typed by the operator using a graphical computer interface. The estimates are combined with the demands in standard PID loops. The gain of each loop can be varied during the pulse, and the system can

respond to real-time events (e.g. plasma disruptions or failure to initiate) and switch to appropriate alternate control laws (such as a controlled shutdown if there is no plasma.)

Representative plasma diagnostics are shown in the lower panels of Fig 1. The density is not under feedback control in this pulse. Most of the planned diagnostic set is fully operational. The MDS-Plus data system provides convenient displays of raw data and processed results simultaneously. The pellet injector is operational but not used during this run. Ion temperature profiles from Doppler broadening of Argon radiation are available if a small amount of Ar is injected via the gas fueling system during the shot.

Early Results

Breakdown and Plasma Current Rise: The Alcator C-MOD vacuum chamber provides structural support for the PF magnets and internal hardware. The system is designed to carry disruption forces from a 3 MA plasma at 9 Tesla average field disrupting at 1 MA/msec. This resulted in a relatively thick (up to 5 cm) stainless steel wall with no electrical breaks. The chamber is kept near room temperature during operation but is surrounded by a large (up to 66 cm thick) stainless superstructure cooled to 77°K. The L/R time constant for eddy currents is nearly 0.2 seconds. The large eddy currents induced in these components complicate the production of a field null to initiate the plasma.

Many next-generation designs require similar heavy sections near the plasma. The demonstration in Alcator C-MOD of successful plasma initiation and control is an important early result. Detailed knowledge of the magnetic field structure and evolution is required to produce reliable nulls. A set of flux loops and magnetic pick-up coils located inside the vacuum chamber. Two methods of field reconstruction are employed. One uses only toroidally-averaged signals to solve the homogeneous Grad-Shafranov equation in the internal region. The solution at any point can be expressed as a precalculated matrix times the flux signal. The results are accurate to approximately 1 mWb or 1 mT [11]. These signals are used for real-time feedback control of the plasma in addition to post-shot analysis. The second method adds local field measurements to the axisymmetric set to reconstruct the vacuum field outside of the plasma as well as the external magnetic field. The local measurements are sensitive to non-axisymmetric eddy currents but the reduction in accuracy is acceptable.

The magnetic field structure at initiation is shown in Fig. 2, along with hydrogen alpha emission and plasma current. The PF circuit breakers are opened at t=0, and plasma light begins roughly 7 msec afterwards. The contour spacing is 1

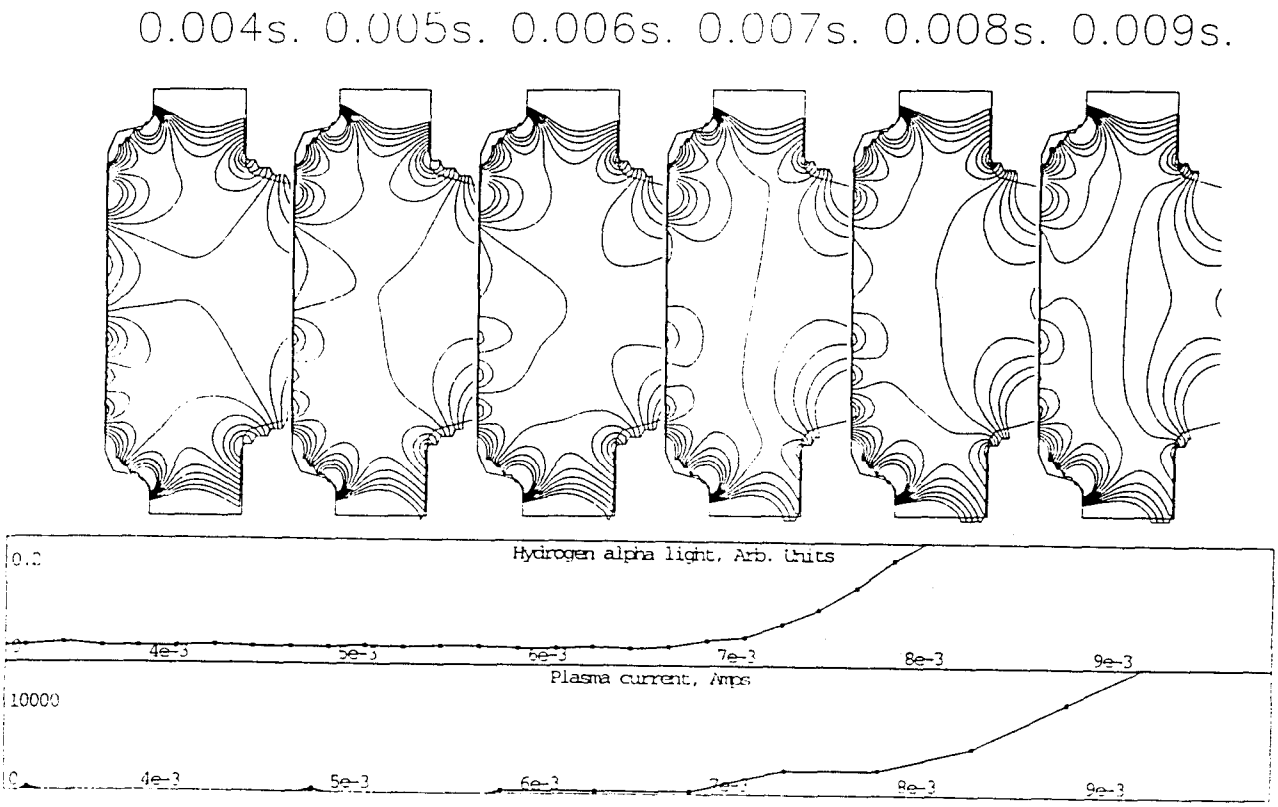

Figure 2: Plasma initiation in Alcator C-MOD. Magnetic flux contour spacing is 1 mWb.

mWb, and the field null fills most of the chamber volume at 6 msec. The proper application of vertical field is critical to obtaining the plasma current rise. The flux plots at 7, 8, and 9 msec show the early evolution of the vertical field.

Figure 3 shows the plasma shape constructed from a filament model at several points in time. The lower traces show the constant x-point position while the outer strike point sweeps most of the diverter plate. While it is possible to start the plasma diverted, the field index required for diverted start can lead to early vertical instability and disruptions. The most reliable start-up is presently obtained with a roughly circular, limited plasma that is gradually elongated and becomes diverted after 200 msec.

Diverter Operation: The tokamak is constructed with 2 diverter areas. The upper divertor is a flat-plate design while the lower uses a more closed geometry. The lower diverter is instrumented with plasma probes, bolometers, cameras, and thermocouples, and gas puff tubes. Early operation has concentrated on developing good control of the x-point position and verification of proper diagnostic operation. The agreement between filament fit predictions of the plasma strike point on the diverter plates and the diverter probes is excellent [12].

The lower diverter area is fitted with a set of tubes and valves that allow gas puffing into the region. Early results show that the power conducted to the divertor plates drops sharply and the radiating region near the separatrix changes shape and location after moderate gas puffs. [13]

Plasma Elongation: The vacuum chamber is capable of accepting plasmas with elongations as high as 2.0. Modeling the plasma vertical stability predicted that the power and control systems would be able to maintain elongations up to 1.8. These predictions have proven to be quite accurate. Elongations up to 1.6 were obtained with relatively little effort. One day of operation devoted to the subject has increased maximum elongation to 1.7. These parameters are more than adequate for the experimental program. Careful tuning of power supply and feedback loop response should allow slightly higher elongations.

Plasma Heating Experiments: A single-strap ICRH antenna [14] is in operation. This antenna is can be moved radially and is protected by an outboard limiter on the adjacent port. The antenna is connected to a tuning system and 2 MW transmitter operating at 80 MHz [15]. Experiments with this antenna will verify predictions of RF coupling to the plasma. Preliminary results show excellent radiation resistance. The system has been conditioned in vacuum to peak voltages in excess of 40 kV, more than enough to handle the full 2 MW output of the transmitter. Some impurity injections are observed but radiated power increases are only a small fraction of the RF power.

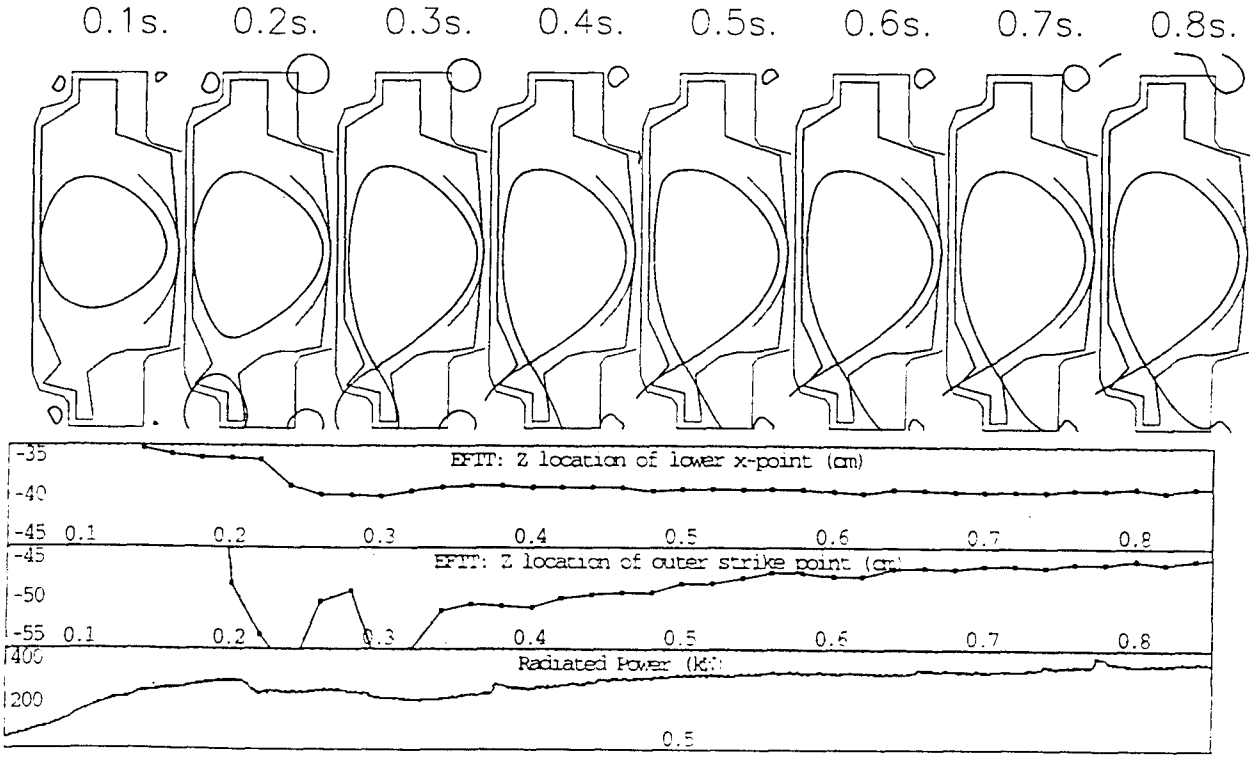

Figure 3: Diverter Operation in Alcator C-MOD.
The diverter forms just after 0.2 seconds.
The outer strike point starts on the "floor" and sweeps upward.

Figure 4 shows a plasma with moderate RF power injection. The net power to the plasma is 500 kW, while the radiation observed by the bolometer increases less than 100 kW.

The single-strap antenna is scheduled to be replaced with 2 dipole antennae. Each of these "two-strap" antennae are rated for 2 MW. These antenna will be fixed to the wall of the vacuum chamber and are not movable. Experience with the single-strap antenna has resulted in the decision to move the 2-strap units 2 cm radially outward from the original planned location.

Pellet Fueling Experiments: The 20-shot pellet injector is operational. The system uses an innovative closed-cycle refrigeration loop to allow remote operation and eliminate consumption of liquid helium. Each barrel can be fired independently, and the system is equipped with pellet velocity measurements and tracking diagnostics [16]. Pellets of several different sizes are available. The soft x-ray arrays and density diagnostics have observed "snakes" on the q=1 surface after some pellet injections [17].

Ohmic 'H' mode: The ASDEX Upgrade experiment has reported H-mode plasmas obtained with Ohmic heating.[18] A series of shots at 700 kA and 3.1 Tesla on Alcator C-MOD produced convincing evidence of H-mode behavior. The thresholds were consistent with the ASDEX scaling law but extended both the input power per unit area and density x toroidal field parameters a factor of 6. Energy confinement was enhanced over 50%. The achievement of H-mode in a machine with metallic walls and no boron coatings or other elaborate wall conditioning is significant for future designs.

Operation at 5.2 Tesla has also produced H-Mode plasmas. Figure 5 shows the transition with a drop in Hydrogen alpha light, an increase in density, plasma energy, and radiated power. The ohmic input power begins to drop as the plasma current is reduced and the plasma goes between H and L-mode several times after 1.0 seconds. This is by far the highest toroidal field reported with H-mode plasmas and occurs at significantly lower ohmic input power than predicted by empirical thresholds laws.

Reliability

The facility has demonstrated excellent reliability to date. Each shot is classified by the engineering operator as either a test or a plasma shot. All shots are further classified as successful or not. The criterion for success is based on engineering performance of the systems. For example, if all systems perform as planned but the plasma disrupts, it is classified as a good plasma shot. If a power supply trips during the pulse and causes a disruption, the shot is classified as a failure.

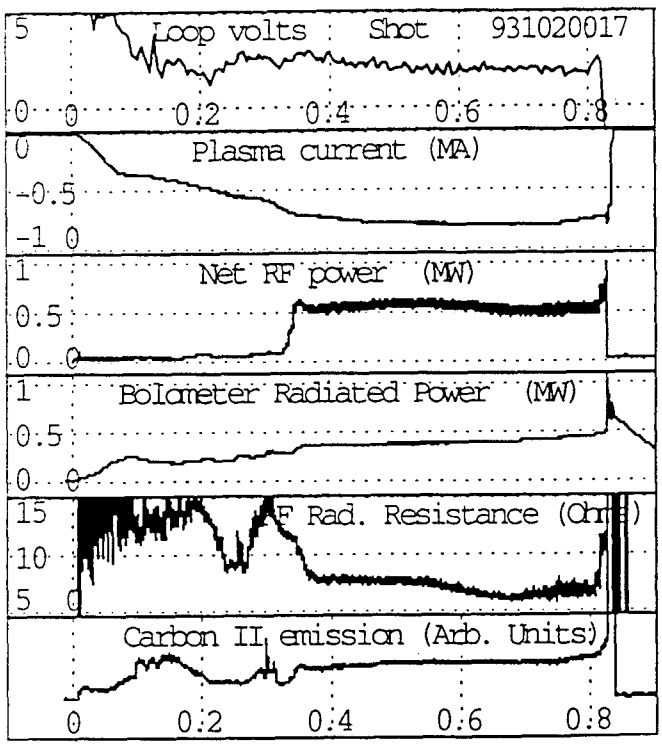

Fig. 4 Alcator C-MOD Plasma Shot #17, October 20, 1993
The net ICRF power is 500 kW.

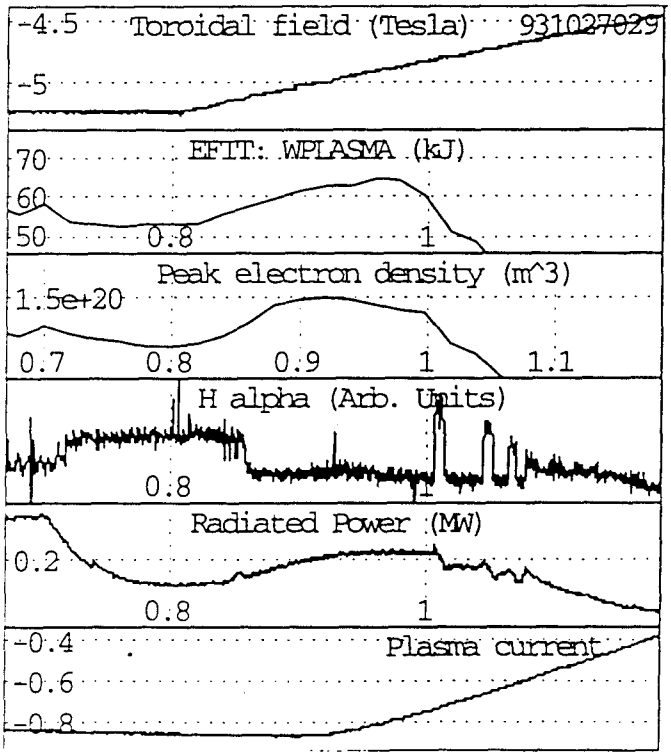

Fig. 5 Alcator C-MOD Plasma Shot #29, Oct. 27, 1993
H-mode transition at 0.85 seconds at 5.2 Tesla

As of October 1, 1993, the system had 1472 plasma shots. Only 75 of these were classified as failed due to systemic problems, operator error, or other reasons. The achievement of 94% reliability in the first 5 months of operation is a new experience for this author. Alcator A and Alcator C did not have the sophisticated computerized database of Alcator C-MOD, but a review of comparable records show that these experiments approached 90% reliability at the end of their operating life.
Two types of failures were responsible for many failed shots on Alcator C. The vacuum circuit breaker system used in the ohmic heating circuit had many moving parts and required substantial maintenance. The system's best reliability was obtained after 3 years of operation when it approached 97% over a 6-month period. Thereafter the reliability decreased as mechanical component wear took its toll.

The design of Alcator C-MOD required 5 PF interrupter circuits rather than the single system used in Alcator C. Reliability much greater than 97% for each of these systems was essential. The maintenance costs associated with 5 systems similar to Alcator C would have been burdensome to our modest budget. A design based on vacuum circuit breakers was contemplated [19], but the concerns over reliability and maintenance prompted the author to choose a new design using only solid-state components. Time and resource constraints prohibited the development and testing of prototype circuits. Two independent simulations of the proposed circuit were used to validate results [20],[21].

The experience with the thyristor circuit breakers has been almost completely positive. The units were operational within 5 days of delivery. A minor problem with a fuse that was not adequately rated for pulsed operation was quickly resolved, and the units have operated over 1600 times without a single failure since May 5, 1993.

Future Plans

The facility will be shut down in early November to install a flywheel on the motor-generator set. This addition will increase the energy available for experiments from 250 to 1000 MJ. (Experiments now require 125 MJ.) The cryostat will be partially dismantled during this period to allow inspection of the superstructure, magnet leads, and bus bars. The 2-strap RF antennae will be installed and the first wall inspected. The facility is scheduled to resume operations in the first quarter of 1994.

References

[1] Fairfax, S.A., and the Alcator Group, "Alcator C-MOD," Proc. IEEE 14th Symposium on Fusion Eng., V2, pp 556-561, ISBN 0-7803-0132-3 (1992)

[2] Fairfax, S.A., and Montgomery, D.B., "Anatomy of the PF magnet failure in Alcator C-MOD," this conference

[3] Fitzgerald, E. and Reddy, C.T., "Development of high-strength electrical connections using copper electrodeposition," this conference.

[4] Beck, W., "Repair of Poloidal Field Magnets on Alcator C-MOD," this conference.

[5] Boivin, R.L., and Reddy, C.T., "Cryogenic cooling system for the Alcator C-MOD tokamak," this conference

[6] Childs, R., Goetz, J., Graf, M., Hubbard, A., Rice, J., and Toland, T., "Design, control, and operation of the vacuum and gas systems for Alcator C-MOD," this conference

[7] Burke, W., and Byrne, E., "A reliable temperature control system for the Alcator C-MOD vacuum vessel," this conference

[8] Bosco, J. and Fairfax, S.A., Proc. IEEE 14th Symposium on Fusion Engineering, Vol 2, pp 782-785, ISBN 0-7803-0132-3 (1992)

[9] Fairfax, S.A., Daigle, J., Paranay, J., Bertolino, V., Zhong, X., "Operation of the Alcator C-MOD power system", this conference

[10] Horne, S., Greenwald, M., Wolfe, S., Tinios, G., Fredian, T., and Stillerman, J., "Performance of the C-MOD shape control system," this conference

[11] Granetz, R.S. and Hutchinson, I.H., private communication

[12] Brian LaBombard, private communication

[13]John Goetz, Private communication

[14] Golovato, S. Bonoli, P., Beck, W. Fridberg, M., "Antennas for ICRF Heating in the Alcator C-MOD tokamak," this conference

[15] Fridberg, M. Byrne, E., Golovato, S., Porkolab, M., Takase, Y., "Upgrade and operation of the 80 MHz transmiter on the Alcator C-MOD tokamak," this conference

[16] Urbahn, J. Greenwald, M., and Schachter, J., "The design and performance of a 20-barrel hydrogen pellet injector for Alcator C-MOD," this conference.

[17] Granetz, R.S., and Irby, J., private communication

[18]Ryter, F., Gruber, O., Büchl, K., Field, A.R., Fuchs, C., Gehre,. O., et al, "Ohmic H-Mode and H-mode power threshold in ASDEX Upgrade," EPS conference, Lisbon, 1993, Part I p. 23 ff

[19] Fairfax, S.A., "The Alcator C-MOD power system", IEEE 13th Symposium of Fusion Engineering, pp 1193-1196, 1989

[20] Fairfax, S.A and Sueker, K.M., "Thyristor DC circuit breakers for Alcator C-MOD", Proc. IEEE 14th Symposium on Fusion Engineering, Vol 1, pp 542-545, ISBN 0-7803-0132-3 (1992)

[21] Sueker, K.S, and Fairfax, S.A, "Design and construction of Thyristor DC circuit breakers for Alcator C-MOD", Proc. IEEE 14th Symposium on Fusion Engineering, Vol 1, pp 546-550, ISBN 0-7803-0132-3 (1992)

REPAIR OF POLOIDAL FIELD MAGNETS ON ALCATOR C-MOD

William Beck
MIT Plasma Fusion Center
190 Albany Street, Cambridge, MA 02139

Abstract

While bringing Alcator C-MOD on line, failure of a solder joint caused an open circuit in one of the PF coils located within the toroidal field magnet. A design review was conducted to analyze the failure and propose possible solutions. The exact reason for the failure was not determined, but the joint may have been weakened by high temperatures during bakeout of the vacuum vessel. Peeling forces also may have been induced by unforeseen temperature gradients and/or magnetic loads. Significant design changes, which are limited to highly stressed PF coils located within the toroidal field magnet, involved repositioning the joint away from the coaxial termination and eliminating the use of solder as a structural element. PF coils external to the toroidal field magnet are not so highly stressed and brazing is acceptable.

The redesign easily accommodates repositioning the joint, but finding a substitute for solder, which was originally selected to avoid annealing the cold worked copper conductor, proved difficult. Localized annealing which occurs in welding and brazing processes eliminated the two most common methods of terminating copper coils. There is not enough space available in the vacuum vessel coil pockets to accommodate mechanical clamping devices. The use of fasteners such as screws and rivets was prohibited due to adverse effects on fatigue life.

Electroforming, a process by which complex parts are formed by electroplating materials such as copper onto an electrically conductive mandrel, was selected to replace soldering the joint. Electroformed copper sheet exhibited superior material properties to those of the C-10700 coil conductor, which has yield strength of 290 MPa. Design changes, development of an electroformed electromechanical joint, and coil manufacturing will be further described.

Coil Description

Alcator C-Mod equilibrium field ring coils are constructed of copper (290 MPa minimum yield strength) 0.863 mm thick ribbon conductor, 0.175 mm Nomex 410 turn to turn insulation coated with B-stage epoxy, G-10 cooling channels, and a fiberglass/epoxy laminate encapsulation. The coils operate in a hostile environment.

Manuscript received October 27,1993. Supported by U.S. DOE Contract No. DE-AC02-78ET51013.

EF-1, EF-3 and EF-C are cryogenically cooled with liquid nitrogen and clamped to the vacuum vessel that at times operates up to 150° C for bake-out and discharge cleaning. The coil set is located within the 9 Tesla toroidal field magnet which makes powering the EF coil package complicated. A coaxial bus is employed to power the coils to minimize net forces on the conductors as they pass through the toroidal field [1]. Access to the coils requires a complete disassembly of the tokamak.

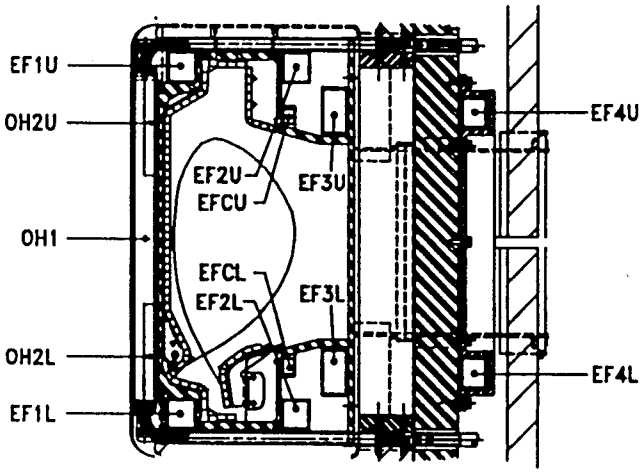

Figure 1

Design Problems

Originally, the coil terminations were fabricated by brazing a shorting strap to the terminal block and the coil end. The first EF-1 coils were completed in this manner but had to be reterminated. The high temperature brazing operation annealed the termination block, and left little strength in the internal tapered pipe threads that connect to the coaxial buses. The softened threads also tended to gall when the coaxial bus was torqued. A damaged terminal block requires a complete disassembly of the reactor for repair.

Repairing the EF-1 coils this first time (about 1 year prior to start-up) was the first experience at ring coil repair. The EF-1 coils had to be stripped of cooling channels and fiberglass/epoxy laminate. The coil ends were peeled back, about one half turn and cut approximately 30 cm back from the termination. The new shorting strap also had to be an extension since the coil ends were shortened. The EF-1 lap

joints were now located approximately 30 cm away from the terminal blocks, where only shear forces are experienced. The terminal blocks and the coil ends were joined by a 95/5 Sn-Ag solder joint. This alloy was selected to replace the brazed joint because of its low melting temperature, 197° C, which prevented recrystallization of the joint components, and high shear strength, 62 MPa. The EF-1 lap joints were sized to keep the average shear in the joint below 2.7 MPa. The design for the remaining ring coils was unchanged except for the substitution of 95/5 Sn-Ag solder.

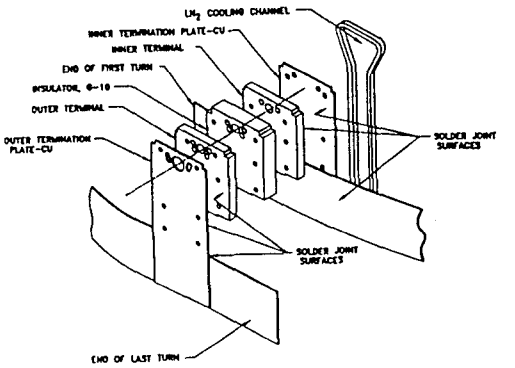

EF3 TERMINATION & COOLING
OLD DESIGN

Figure 2

Soon after bringing the tokamak on line in April 93, the upper EF-3 coil open circuited. The extent of the damage could not be judged immediately because the reactor had to be warmed up and partially dismantled to view the coil. It turned out that the inner shorting strap had completely debonded from the coil, leaving the innermost turn still bonded to the body of the coil. The strap remained bonded to the terminal block and the rest of the terminal block assembly was intact. The laminate wrap also ruptured from the explosion. The laminate was removed from the lower EF-3 termination area and inspected ultrasonically in an attempt to try to explain what happened. The results were compared to the ultrasonic scans completed before installation. Evidence of debonding in the inner EF-3 lower joint was discovered. The EF-1, EF-2, EF-C, and EF-4 coils were also reinspected and no discrepancies were noted. The problem appeared to be common to the EF-3 coils. Differences between the EF-3 and the EF-1 and EF-2 terminal blocks are the height and mass of blocks. The EF-3 coils are required to have two surface cooling. The EF-3 inner shorting strap also had a cooling channel bonded to it to supply liquid nitrogen to the vacuum vessel side of the coil. Temperature gradients caused by the liquid nitrogen flow coupled with magnetic forces may have induced peeling forces [3]. The failure occurred at low power levels. Understanding the reason for the failure was difficult and a review committee was assembled to help uncover the problems. Although the committee was unable to determine the exact failure mechanism, they did make some good recommendations :

1. Eliminate the use of soft solder as a structural element.
2. Position the joint away from the termination blocks where the loads can be more clearly understood.
3. Test the new designs
4. Define acceptance criterion clearly.

Details of these recommendations can be found elsewhere at this conference [3].

ELECTROFORMING :

Joining copper conductors by bridging them together with electrodeposited copper at first glance does not appear to be a very conservative approach to a complicated problem. Brazed joints, common in magnet construction, probably would have met our joint requirements if we could have been certain that the annealed joint region remain bonded to the body of the coil. A test specimen that simulated a strain controlled condition was made by bonding one fully annealed copper strip to six strips of unannealed copper coil conductor with Nomex 410 sandwiched between them. The stack was fatigue tested at 207 MPa for $1x10^6$ cycles submerged in liquid nitrogen before halting the test. The annealed sheet showed no sign of deterioration. Selecting a joining process that would not anneal the copper coil conductor and did not have to rely on the epoxy turn-to-turn bond for its survival, (as with the brazed joint) truly was a conservative approach.

Electroformed sheet was obtained from the A. J. Tuck Co., of Brookfield, CT. Tensile tests were performed and yield strengths greater than 290 MPa were obtained. The high strength is probably due to the extremely fine grain size of the material, organic additives concentrated at the grain boundaries, and plating bath composition [2]. The first fatigue specimen was run at 187 MPa, (the peak stress in the EF coil system) and survived $1x10^6$ cycles before failing near the jaws of the testing machine. More tensile tests were performed and the yield strength of the electrodeposited material was always greater than the coil material. Electroformed joints constructed of the actual coil copper alloys were also tested at room temperature and 77 K. The tensile strength specimens always broke in the coil base metal. The first electroformed joint fatigue specimen did break prematurely after $1.5x10^6$ cycles at 290 MPa due to a surface defect. The presence of aluminum filled epoxy used to bond the parts to be joined to the mandrel was detected microscopically after the break. This defect could not be detected by dye penetrant testing, but would have been easily detected by an ultrasonic inspection. The remaining fatigue specimens were subjected to penetrant and ultrasonic testing followed by microscopic examination. The ultrasonic inspection was reliable and very sensitive to even the slightest surface and subsurface defect. None of the fatigue specimens failed. Life greater than the $2.5x10^6$ cycles required was achieved despite raising the applied stress from

187 MPa to 207 MPa. The Young's modulus of the electrodeposited copper was determined to be 82 GPa by resonance testing. The base metal copper was run as the control for the test resulting in a modulus of 117 GPa. 82 GPa is typical for material produced in a copper sulfate/sulfuric acid solution [2]. The lower modulus should have no significant effect on the joints.

A chemical analysis was also conducted on C10700, C10100, C11000, and the electroformed copper. The results only revealed trace amounts of impurities. The most noticeable difference detected was the high concentration of silver in the C10700. Resistivity measurements were taken at room temperature and 77 K. The resistivity decreased by a factor of six at 77 K which is another indicator of copper purity.

ELECTROFORMED JOINTS

The first step to fabricating an electroformed joint is machining a 15 degree bevel into the conductor ends to be joined [Fig 3]. The ends are then epoxied to a stainless steel mandrel maintaining an appropriate gap between the conductors. A strip of copper foil is positioned to serve as a barrier to prevent the aluminum filled epoxy from running into the joint area. A clamping fixture aligns and supports the conductors to be joined. The beveled tips are bent down into a shallow groove and the foil flattened. The plating is confined to the joint by masking off all areas of the coil inside the tank with vinyl tape. The tape seams are sealed with a vinyl paint.

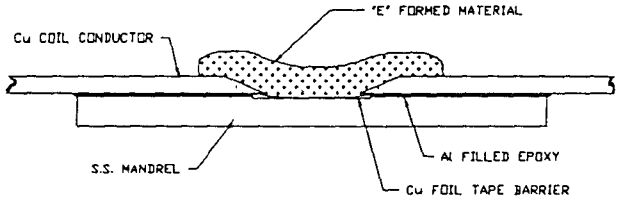

Figure 3

Once cured, the joint is subjected to several proprietary cleaning processes. The joint is inserted into specially fabricated tank containing the plating solution for approximately 40 hours to buildup a 1 mm thickness of copper. The rate of build-up is proportional to bath temperature and current density. Material properties are adversely affected by too high a current density.

The joint requires finishing after it is removed from the tank. Most of the excess copper is removed with hand tools. The conductor is cooled with water to prevent overheating the conductor. After the joint is blended a visual inspection, dye penetrant, and ultrasonic inspections are conducted. Defects less than .5 mm deep were ground out and replated. More serious ones, such as through cracks, which occurred early in production, were cut away and the electroforming process repeated. Most of the defects encountered were found on the mandrel side of the joint and probably caused by small gaps between the tips of the bevel and the copper foil. If a gap is present the plating builds up on each side of the gap until it eventually bridges it forming a crack. Another type of defect often found in the testing phase was hydrogen bubbles. A hydrogen bubble stuck on the joint surface causes a pit to form because the copper can only grow around the bubble. This problem was solved by positioning an air bubbler below the joint. The air bubbles rise along the joint surface dragging away the hydrogen. Laminations were not encountered in the electroforming process. All cracks discovered were aligned normal to the inspection surface making them easy to detect.

NEW DESIGN

Major coil design changes required the use of a high strength electroformed joint located away from the termination block where the loads are understood to be tensile or compressive. A new shorting strap was fabricated to adjust the position of the joint. The EF-1 and EF-3 coaxial buses were replaced with larger ones due to high stresses on the inner conductor within the terminal block. The coaxial geometry ends at the terminal block exposing the inner conductor to high magnetic stresses [1]. A stainless steel reinforcement plate was also added to react the magnetic loads induced on the inner coax, and to provide means for the terminal block to be bolted on instead of soldered.

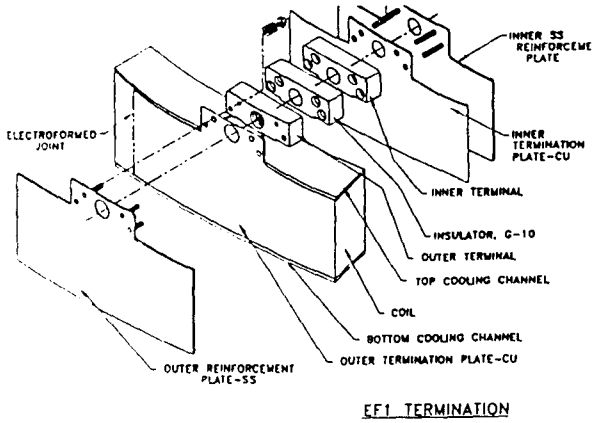

Figure 4

A gap was also manufactured between the terminal blocks to minimize thermal stress in the shorting strap between the coil and the terminal block.

Repair Process

Repairing the coils required a complete disassembly of all components external to the vacuum vessel. The coils were stripped of the fiberglass/epoxy case and the coil ends were peeled back to remove the soldered terminations. A compression test was performed on all of the coils by attaching a chain fall diametrically across the coil in series with a dynomometer. The upper and lower EF-3 coils were seriously debonded. EF-3 upper was 50 percent more flexible than predicted, and EF-3 lower was twice as flexible as predicted. The problem was thought to be caused by a loss of tension during the coil winding process. Prior to the EF-3 failure, a diametral compression test was not part of the coil receiving inspection. It was necessary to replace both EF-3 coils. After the new coils were wound the diametral compression test was repeated and both coils were accepted. The top and bottom surfaces of the new EF-3 coils were sealed with thermally conductive epoxy (as are all of the coil heat transfer surfaces) to prevent turn-to-turn arcing while promoting good heat transfer to the liquid nitrogen. A dynamic high voltage test was performed on the coils to insure that the coils were properly sealed and to make sure that no turns were shorted. The coils were wrapped with plastic tape to seal the body of the coil, leaving the ends exposed for electroforming.

Electroforming the shorting straps to the coil ends required precision to keep the coaxial connections in the terminal blocks concentric. The inner joint was joined first to establish a reference for the outer joint fit-up. The time required to produce two joints average about two weeks once a routine was established. Each joint was dye penetrant, ultrasonically, and visually inspected as were the fatigue specimens. Defects found were removed and the joint was replated to meet the thickness requirement ± .05mm.

Once back at M.I.T., the coils were cleaned, inspected, and high voltage tested before construction. The terminal blocks and the shorting straps were silver plated to insure good electrical contact. A fit-up of the coil terminations and the cooling channels was conducted so that the channels could be scribed in place for trimming. The position of the terminal blocks was also established and the blocks were fastened to the stainless steel reinforcement plate. The hex nuts were tack welded to the studs to prevent them from backing off. The terminal block assembly was keyed to the cooling channel below it, and it was necessary to bond that cooling channel and the coil ends simultaneously to the body of the coil. The remainder of the cooling channels were bonded to the coil after clamping the terminal blocks in place. Another high voltage test was conducted to insure electrical integrity of the coil. The coil case was formed by wrapping the coil with three half laps of a B-stage fiberglass/epoxy laminate. It was then vacuum bagged and cured for 24 hours at 70° C. Four thermocouples were installed between the second and third layers to monitor cooling performance. A high voltage test was repeated before the static pressure, cooling, and diametral compression acceptance tests. As each coil was completed it was carefully fit-up to the vacuum vessel. A reference plane was established from the inside surface of the mounting plates so that the bearing pads could be trimmed to fit properly against the vacuum vessel. The coil was lowered enough to insert the pads along with B-stage epoxy sheet. The coil was then raised, clamping the pads in place against the vacuum vessel throughout the cure. The fit-up operation was repeated for each coil and the tokamak was reassembled.

Reparing the poloidal field coils was a difficult task. It took more than a year to complete the job with one third of that time spent on research and development. Not knowing exactly what caused the failure forced a complete engineering review of the coil system. C-MOD is now on line for physics operation.

References

[1] H. Becker "Coax Stresses in Transverse Magnetic Fields", this conference.

[2] William H. Safranek, *The Properties of Electrodeposited Metals and Alloys*, 2nd edition, American Electroplaters and Surface Finishers Society.

[3] S. Fairfax, D. Montgomery, "Anatomy of the PF Magnet Failure in Alcator C-MOD", this conference.

Structural Behavior of Coaxes in Transverse Magnetic Fields

H. Becker
Massachusetts Institute of Technology, Plasma Fusion Center
Cambridge, MA 02139

R. Leonard Myatt
Stone & Webster Engineering Corporation, working at
Massachusetts Institute of Technology, Plasma Fusion Center

ABSTRACT

The ALCATOR C-MOD tokamak employs poloidal field (PF) coils inside the toroidal field (TF) coils. C10100 copper coaxial current leads pass radially through an 18 tesla toroidal field to reach the terminals of the ohmic heating (OH) coil. In addition, there are radial and poloidal fields on the order of 2 tesla near the OH terminals. The 50 kA lead currents interact with those fields to produce 900 kN/m forces which act in opposite directions on the coaxial conductors. The net load is zero on the conductor pair. However, the internal forces and moments cause stresses in the outer conductor tube that depend strongly on the size of the air gap between the tube and the insulation. Analysis indicates a peak stress of 430 MPa for a 0.19 mm air gap. The stress field is complicated by a 90 degree bend to vertical at the terminal block. Internal loads in the bend region lead to bourdon tube behavior, which produces longitudinal bending stresses in the coax. The coax must resist fatigue failure for reversed 50,000 pulses with a Safety Factor of 10. Ironically, this component is considered innocuous, and rarely given such attention, simply because there is no net load on a coax in a transverse field.

INTRODUCTION

The coaxial conductors for the ALCATOR C-MOD PF coils were designed with the usual regard for current capacity and temperature rise. The failure of the EF3 ring coil terminal initiated an extensive review of the coil designs. That included identification of every conceivable stress field in the coils and terminals, and analysis to support redesign where required.

One item for investigation, that surfaced during that review, was the nature of the stresses in the coax induced by the interaction of the oppositely directed Lorentz loads from the currents flowing in a transverse magnetic field. An elementary strength-of-materials calculation was performed for the coaxial lead which carries 50 kA in an 18 tesla toroidal field to the terminals of the OH coil. The simplified approximation indicated a peak stress of 500 MPa at the inside surface of the outside conductor (tube).

That analysis did not consider the resistance to tube deformation provided by the inner conductor (bar). It also did not account for the insulation (nominally, G-10) around the bar, or for the effect of a gap between the insulation and the tube. It was apparent that a finite element analysis was required to include these effects and define the influence each would have on the stresses in the conductor cross section.

Manuscript received October 11, 1993. This work was supported by the U.S. Department of Energy.

The PF coil coaxes run radially (that is, normal to the machine vertical axis) from the buses outside the machine to the coil terminals. The OH coax was bent to vertical on a small radius to meet the terminal plate structure. As a result, bourdon tube behavior would occur in the loaded tube. The bend caused the tube cross section to deform to a quasi-ellipse, which would accentuate the bourdon tube action. It would raise the bus end of the coax. Restraint of that movement would lead to longitudinal bending stresses in the tube.

The tube bending process caused the tube wall thickness to increase on the inside of the bend, and to decrease on the outside. The small bend radius and the thickness changes would cause the tube current to hug the inside of the bend. The centers of the tube and bar current paths would not be coaxial in that region. Interaction of the currents with vertical and radial fields would institute couple action that would twist the conductor. It would result in cyclic wrenching of the attachment to the terminal plates.

The toroidal field diminishes inversely with machine radius along the coax from the terminal plate to the bus. The gradient near the terminal would cause 3-D stresses that could impact the maximum tresca stress. The terminal plates would tend to resist the cross section deformation, leading to additional 3-D stresses.

That describes the total problem in the C-MOD OH coax. Discussion of all those effects appears in the OH stress report now being completed. This presentation is confined to delineation of the behavior in the straight section. That applies to all the other PF coil coaxes, which are not bent near the terminals. The use of some results from the OH analysis is intended only to illustrate the nature of the problem.

STRESS DISTRIBUTIONS

Nominal dimensions of the C10100 conductors are shown on Figure 1. The coax was fabricated by sliding the insulated bar into the tube. The air space between the conductors was potted with epoxy cement, which theoretically would eliminate all air gaps. Best estimates of the actual initial air gap, g, during operation indicate that it probably would be less than 0.076 mm (0.003"). The calculations covered the range from zero to 0.19 mm (0.0075"). The postulated insulation modulus range was from 7 GPa to 44 GPa.

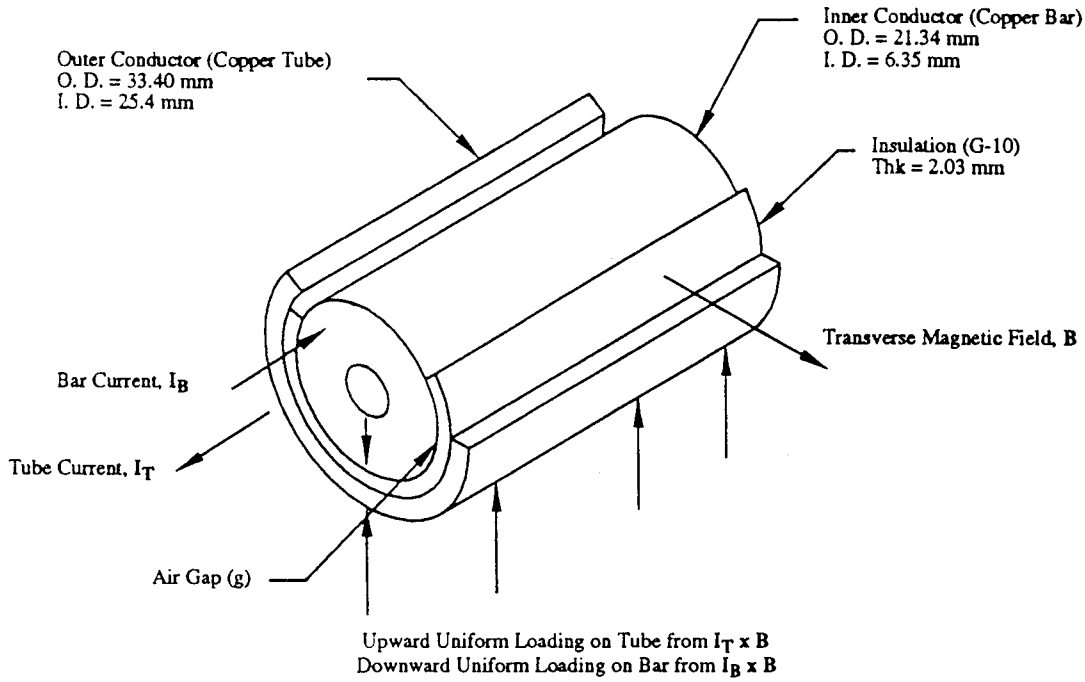

Fig. 1 Coaxial Cable with Current , Magnetic Field and Force Directions

The current and external transverse magnetic fields were assumed to be distributed uniformly over the conductor cross sections. Self field effects were neglected, as were those arising from relative motion between the conductors under load. The analysis was confined to the effects of gap size and insulation stiffness.

A simple calculation reveals the potential magnitude of the problem. The OH 50 kA current in the 18 tesla field leads to a uniform loading of 900 kN/m along the coax, oppositely directed in the tube and bar. At the midplane of the tube section, half of the 900 MN/m force is carried by the two tube wall thicknesses. This causes an average tensile stress of 56 MPa in the tube, independent of gap size or insulation stiffness. Most of the stress would be expected to arise from tube wall bending as the cross section ovalizes. It is not necessary to perform calculations to see the significance of the tube-bar interaction.

Fig. 2 shows the finite element ANSYS [1] model. Not shown are the frictionless gap elements that separate the insulation from the inside surface of the tube and the outside surface of the bar. The gap size relates to the gap before loading. It is the sum of the two spaces, which are exaggerated in the plot to show the three structural elements of the model.

The initial gap size, for each analysis, ranged between zero and 0.19 mm. Difference in the thermal expansions of the copper lead and the G-10 insulation allows the gap to change when the coax is cooled from 293K to 77K. The analyses considered a variation in the insulation modulus extending from pure epoxy to G-10 to twice that of G-10.

A series of computer runs was dedicated to establishing a finite element grid that produced converged stress results. The mesh shown in Fig. 2 is a result of this optimization process.

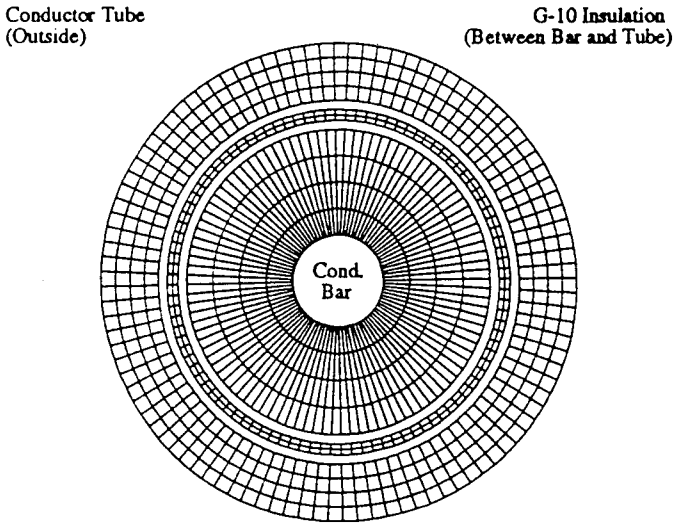

Fig. 2 The Finite Element Model

In the first of two series of computer runs, the insulation modulus was chosen at 22 GPa (typical of G-10 insulation), and g was varied. Fig. 3 shows the tresca stress contours for a g of 0.0025 mm. The stress field is superimposed on an exaggerated image of the deformed conductors. Stresses peak on the inside surface of the tube, at the 4 and 8 o'clock positions in the tube cross section. The insulation remains in contact with the conductors over about half of the circumference. For all g values, the tube peak stresses are on the inside surface of the tube, and below the separation points. As g increases, the azimuthal extent of the contact region decreases and the tube bending stress increases. That results in increased peak stress, as shown in the summary tresca stress plot of Fig. 4. Since there is no surface contact at the peak location, the tresca and first principal stresses are the same.

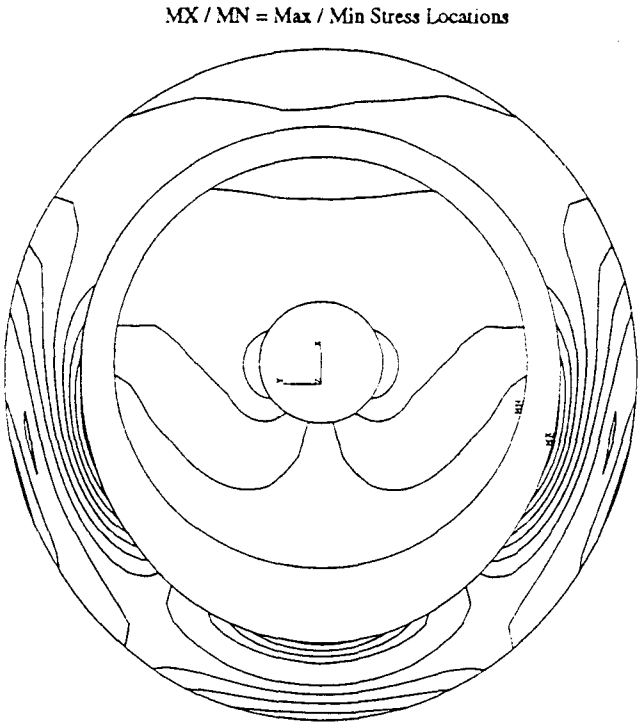

Fig. 3 Tresca Stress Contours, Zero Initial Air Gap

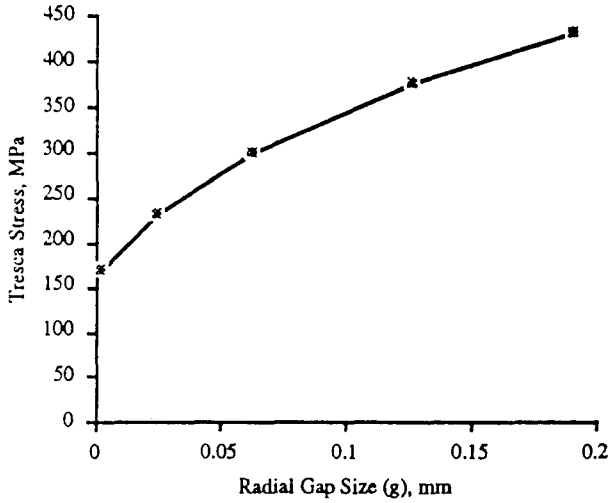

Fig. 4 Tresca Stress in the Tube vs. Initial Gap Size

In the second series of computer runs, the stress sensitivity to variations in insulation Young's modulus was studied. A 1.6 percent peak stress decrease was found for a modulus change from 7 GPa to 44 GPa, with a nominal gap of 1/8 mm. The change was 18 percent for a g of 0.0025 mm.

The stress range in Fig. 4 portends a strong influence of gap size on fatigue life, N. It was assessed by employing 77K fatigue data from [2]. The relation was found to be as follows:

$$N = 225\,(g)^{-2.69} \qquad (1)$$

As an example, at a g of 0.0762 mm (0.003"), the estimated number of cycles to failure is 230,000. The fatigue life is reduced dramatically to only 58,000 for a g of 0.128 mm (0.005"). That is a 1/4 life ratio for a 5/3 gap ratio.

CONCLUSIONS

If a coaxial conductor is carrying large currents in a transverse magnetic field, the internal stresses should be calculated and the coax life should be assessed. The high sensitivity of fatigue life to the initial air gap size indicates the desirability of assessing carefully the Factor of Safety for coax design.

REFERENCES

1. ANSYS 4.4a, Swanson Analysis Systems, Inc., Houston, PA.

2. N. J. Simon, E. S. Drexler, R. P. Reed, "Properties of Copper and Copper Alloys at Cryogenic Temperatures," NIST Monograph 177. U. S. Department of Commerce, Technology Administration, National Institute of Standards and Technology, February, 1992.

CRYOGENIC SYSTEM FOR THE ALCATOR C-MOD TOKAMAK

R. L. Boivin, C. T. Reddy and the Alcator C-Mod group
Plasma Fusion Center
Massachusetts Institute of Technology
Cambridge, MA 02139

ABSTRACT

Alcator C-Mod is a compact tokamak (major radius 66 cm), designed to operate at high toroidal magnetic field (up to 9 Tesla), and high plasma current (up to 3 MA). The coils and the tokamak structure must be cooled to liquid nitrogen temperature in order to withstand the pulse-induced mechanical and thermal stresses (e.g. 316 LN steel has higher strength at LN_2 temperature). Operating at low temperatures has also the advantage of reducing the required voltage and power from the power supplies thus significantly reducing their cost. This report will describe the design of the cryogenics delivery system which must remove up to 300 MJ of heat from the tokamak in 20 minutes. Details of the various components (tanks, valves, pump) will be presented along with the cooling scheme of the coils (poloidal field [EF], toroidal field [TF] and ohmic heating [OH]) and of the structure. We will also report on the PLC-based control system which regulates the cooling efficiency for the various components. This will include details about the extensive instrumentation required for feedback control. The interaction of the cooling system with other tokamak subsystems will also be described.

INTRODUCTION

Like its predecessors at MIT, the Alcator C-Mod experiment is a liquid nitrogen (LN_2) cooled tokamak operating at high field, high plasma current, and at high density. Such capabilities require a compact design, which in turn requires an extensive supporting structure and limits access to internal parts. The set of coils (all cooled by LN_2) required to form the internal field structure consists of a field magnet, 3 ohmic solenoids and 10 poloidal field coils (5 above and below the midplane).

In this compact design, the forces generated by forming the toroidal magnetic field are greater than what the magnet can withstand by itself [1]. Consequently, a surrounding stainless steel structure was designed to contain the expanding force of the TF magnet during a tokamak pulse. That structure is made of 2 covers (upper and lower), 66 cm thick, 1.45 m in radius, joined together by a cylinder, 15 cm thick, 1.45 m radius, 2.35 m high. Before starting operation, these components must be cooled at a safe rate, calculated to be approximately 2°C/hr, using thermal stress analysis. A total of approximately 10 GJ is removed during that process which usually extends over a 5 day period.

During the experimental phase, (i.e. when the tokamak is pulsed) the cooling system must be able to remove the heat generated in the coils and by the heaters which keep the vacuum vessel at room temperature. At peak performance, this represents approximately 300 MJ which by design must be removed in approximately 20 minutes.

We will report first on the major components of the cooling system. Details of the internal cooling scheme for the coils and the structure will also be described, with the instrumentation and control system constituting the last part.

COOLING LAYOUT

A. Liquid Nitrogen

We designed the delivery system to be able to carry 120 liters per minute from the two outdoor storage tanks to the system pump. The main unit is a 80,000 liter tank kept at a pressure of 420 kPa, backed up by a 35,000 liter reserve tank. In the case of an emergency (problem with the main tank), the reserve tank has been designed to supply enough GN_2 to purge the machine for warm-up, or enough LN_2 to cool the machine after a bakeout. Remote operation of the feed line valves allows easy switching between the tanks. The valves are manufactured by the True Torq corporation, meet cryogenic specifications and have the NEMA 4 approval rating for outside service. An external emergency solenoid valve is also in line and would shut off the supply of LN_2 if the building oxygen level drops below safe levels. In order to optimize the quality of the liquid nitrogen, an actively evacuated supply line (< 1 kPa) was installed for most of the feed line lengths. This line is approximately 50 m long, and is protected from overpressure by Circle Seal 700 kPa pressure relief valves.

The LN_2 is then directed to the tokamak cryostat through a Bauman pneumatic valve. In the cryostat the liquid nitrogen goes through several phase separators and is then directed through a primary filter to the sump, located below and aside from the cryostat, where the immersed pump is located. It is advantageous to have the feed line enter the cryostat before the sump for two reasons: first, the cold vapors help to cool the machine in the initial stages of the cooldown and second, the film boil-

This work was supported by US DOE Contract No. DE-AC02-78ET51013. Manuscript submitted Oct. 12^{th}, 1993

ing is reduced before it enters the pump chambers. The pneumatic valve is linked through a simple feedback loop to a differential pressure transducer, which signals when a proper liquid level has been reached.

Located inside the sump, the pump and motor are an integral unit, eliminating the need for a shaft seal. It is fully immersed and capable of delivering up to 300 liters per minute at 250 kPa. The liquid is then pumped through the secondary filter system and on to the valve manifold. The manifold consists of 18 electrically actuated ball valves, designed for cryogenics operations, and are manufactured by Worcester Controls). The valve actuators have an internal feedback system which matches position with the demand from the PLC. Immediately after the valves, pressure transducers monitor the pressure in individual cooling circuits and are transmitted to the PLC. From there, Teflon tubes carry the liquid nitrogen to the various coils and structure. Teflon tubing was selected for its flexibility at cryogenic temperatures and its non-conductive properties. Finally, any excess liquid nitrogen is returned to the bottom of the cryostat where it drains to the sump and is recycled.

B. Gaseous Nitrogen

Nitrogen gas is used to keep the internal components of Alcator C-Mod moisture free, and to purge liquid nitrogen from the magnetic coils during operation. Outside the building liquid nitrogen enters a passive 1,000 m^3/min heat exchanger where it is converted to room temperature gas. The control of the coil purge is a simple solenoid valve activated approximately 2 minutes before a plasma shot.

COMPONENT COOLING

A. Poloidal Field Coils

The 10 EF coils (5 upper and 5 lower) are built on the same basic design. The laminar copper conductor is wrapped on itself several times [3], and forms a ring varying in radius from 0.52m for EF-1 to 1.52m for EF-4. A cooling channel has been machined in the G-10 plate which lies on top (bottom) of the upper (lower) coils, the exception being with EF-3 which, requiring more cooling, has cooling channels on both sides. The liquid nitrogen circulates in the cooling channels and cools the copper through a layer of electrically insulating but thermally conducting Stycast epoxy. Turbulators (small bumps imbedded in the epoxy) have been added to the surface to increase the heat transfer between the coil and the LN_2.

Liquid nitrogen is fed into the coil through the inner conductor of the electrical coaxial connection, and for some of the coils through additional cooling tubes. The flow is then directed to both sides of the coil and exhausts on the opposite side.

B. Ohmic Heating Coils

The OH solenoid consists of three electrically separate coils wrapped outside the TF core, inside the vacuum vessel inner wall[4]. Because of space restrictions and the relatively small size of the conductor itself, the coil is mainly cooled by immersion. A 3mm gap was designed between the conductor and its outer casing, where the liquid nitrogen enters in contact with the coil. The liquid nitrogen is fed into the casing through the coils coaxial connections (2 at the top, one at the bottom) and through an additional feeding line at the bottom. Gaseous and excess liquid nitrogen exhausts at the top of the coil where it then flows to the bottom of the machine and to the cryostat.

C. Toroidal Field Coil

The toroidal field magnet is modular; the 120 turns are grouped in 20 components, each one being separated in 4 straight sections: the core, the upper and lower radial arms and vertical legs[1]. The core (also referred as the central column) is cooled by immersion on its inner and outer sides, with the nitrogen exhaust coming at the top between the radial arms.

The radial arms are cooled through channels machined in their G-10 cover plate. The liquid nitrogen is supplied to each arm with two 0.6 cm copper tubes, which directs the flow towards the front and the back of the arm. On the top (or the bottom) of the radial arms, 2 holes were machined allowing the gaseous and excess liquid to exit the coil, just below (or above) the upper (lower) cover, and be directed towards the outside of the tokamak.

The vertical outside legs are cooled through a G-10 cooling jacket epoxied over the turns of the coil. The liquid nitrogen flows from bottom to top and exhausts through the main cylinder to the bottom of the cryostat.

D. Superstructure Cooling

There were major concerns about thermal stresses resulting from cooling by immersion the top surfaces of the upper and lower covers in liquid nitrogen. Rapid cooling of just one surface could result in extremely high stresses through the thickness of the material. In order to reduce these stresses, a thermal resistor was designed to cool them more uniformly and more slowly. Working with the Girton manufacturing company, we designed dimpled stainless steel cooling plates that fit our tight clearance specifications. The LN_2 enters the plate through two 1cm supply lines and exhausts through one 1.25 cm drain tube. A slightly compressed layer (0.6 cm) of insulating polyimide foam (manufactured by Solimide) placed between the cooling plates and the covers reduces conductive heat transfer. This thickness has been chosen as to obtain a maximum of 2°C/hr cooling rate, passively protecting the integrity of the supporting structure.

INSTRUMENTATION

The instrumentation required to monitor and control the cryogenics system is rather extensive, with mainly temperature and pressure measurements required. Temperatures are measured directly by thermocouples (all of type E), and also using coil resistances. The combination of those two techniques allows comparison between local and global readings, and permits a minimum of redundancy in case of malfunctions.

Since all coils are made of the same copper alloy (C10100), their average temperature can be obtained using their resistance. The latter is measured using the 4 wire technique in which current and voltage are measured simultaneously. Using the known dependence of the resistivity of copper as a function of temperature, coil temperature can be computed, typically once a minute. Because of the modular composition of the toroidal field magnet (TF), the resistance of the coil is also broken into 360 segments, which allows the monitoring of the joints but also of the core temperature, independently of the outer portion of the coil[5].

The thermocouples are distributed around the tokamak, on coils and on the structure. Each poloidal field coil has 4 thermocouples attached to its external surface (at the LN_2 inlet, outlet, and midway on the left and on the right), electrically insulated from the coil itself. On some of them (EF1, EF2, EF3, upper and lower coils) an additional thermocouple has been installed on the electrical coaxial connection to monitor its proper cooling. The poor accessibility to the 3 Ohmic solenoids (center of the tokamak) prevented the installation of thermocouples inside the coil itself, so only the electrical coaxial connection was instrumented. For the same reason the toroidal field magnet (TF) core could not be directly instrumented with thermocouples, although the 60 legs and arms have one on each[5].

The stainless steel supporting structure is also instrumented with thermocouples attached to both internal and external surfaces using Stycast epoxy.

Because of the relatively large number of thermocouples, it was necessary to multiplex the different signals (for a total of 49 for the coils, 60 for the TF, and 55 for the structure) through 2 scanners, one commercial (Matrix, rated for 500V) and one built in house for the TF magnet (rated for 5000V). Signals are then sent to the Allen-Bradley PLC for processing, with an overall update time of one minute.

CONTROL SYSTEM

Since access to the tokamak and its subsystems is severely restricted during operations (either by radiation, electrical or other hazards), remote operation is essential. In addition, a high level of automation is sought in order to expedite cooling and to reduce the need for continuous operator attention. As for the other tokamak systems this was done using a PLC-based system (Allen-Bradley 5/25). Information is relayed to the control room through fiber optic communication. Coil temperatures (resistance and thermocouples) and the average of the structure thermocouples are recorded (once every 20 minutes) and sent a VAX (Dec Corp.) for archiving once a day. In addition, coil temperatures are recorded just before and after each pulse (archived also on the VAX).

In considering the various regimes in which the tokamak is operated, we designed the control system to be functionning in one of 4 mutually exclusive modes. These internal modes (SLEEP, PRECOOL, BAKEOUT and OPERATE) correspond to different cooling regimes and perform specific task.

In SLEEP mode, no cooling is performed. The control system monitors temperatures and purges all the coils with room temperature GN_2, to prevent formation of ice anywhere in the internal parts of the tokamak.

The PRECOOL mode was designed to cool, at a given rate (2°C/hr), the supporting structure, which represents approximately 10 GJ in heat removal. This operation is only required a few times a year, typically after a maintenance shutdown of 4 days or more. The goal is to attempt an uniform cooldown of all the main components in order to avoid differential thermal stress, and loss of contact in electrical connections by differential thermal expansion.

At regular intervals, and especially after a vacuum vessel vent, it is desirable to bake the first wall to a temperature above 100°C in order to remove water and other impurities in the vacuum chamber. However, the coils are not designed to withstand such temperatures and must be cooled. In the BAKEOUT mode, the coils are cooled to a temperature near -25°C, not too cold as to reduce the efficiency of the bake. Such conditions can be maintained for 2 to 5 days continuous, depending on the vacuum vessel cleanliness. The coil temperature is maintained through a simple feedback algorithm which matches LN_2 flow through each coil (or cooling circuit) with measured temperature. Experience has shown that it is necessary to continue cooling 6 to 8 hours after the end of vessel bakeout, in order to allow all the internal components to cool to a safe level for the coils.

Finally, the OPERATE mode has been designed to control cooling during pulsed tokamak operations. Prior to any pulse the coils have to be cooled to a temperature near LN_2 boiling point (-196°C). Just before the pulse, cooling is stopped and all the coils are purged with GN_2; the presence of LN_2 during a pulse could rupture the coil case. Immediately after the pulse, cooling is re-initiated (recool phase). The next shot is permitted when all coil temperatures are below established setpoints

(i.e. typically -165°C for most of the coils). Since the coils are very different in size, in cooling efficiency, and in flow characteristics, the control system tries to maintain a given cooling rate (approximately 130-175°C/hr, up to 300°C/hr at peak performance). This permits a more equilibrated distribution of LN_2 among the 18 cooling circuits, attempting to prevent any coil to lag behind during cooling. This is especially important considering that the flow impedance of LN_2 goes down with temperature, i.e. colder coils will cool more quickly than a warmer one for the same manifold pressure. When a given coil is cold (typically 15-20°C above LN_2 boiling point), the control system switches to a maintain temperature algorithm, which requires considerably less LN_2, allowing any lagging coil to catch up, reducing the inventory of LN_2 inside the machine, and reducing the impact of unwanted cooling on the vacuum vessel and seals. The presence of liquid on the vacuum vessel, and especially on the horizontal port flanges were found to cause vacuum leaks. The diagnosis of the problem is, however, very difficult, mainly because of the unaccessibility of the areas in question. Leaks and/or unexpected flow patterns, combined to a tight environment, which prevents the installation of additional shields for the flanges, are the principal factors.

Finally, at all times, independently of the internal mode, the control system attempts to maintain a positive pressure (with respect to the atmospheric pressure) in the cryostat of approximately 37 Pa, in order to avoid the formation of ice inside the machine. The PLC controls a proportional valve which feeds GN_2 to the cryostat (and through the coils during SLEEP mode and just prior to a pulse) using a simple feedback algorithm matching measured pressure with valve opening.

ACKNOWLEDGMENTS

The Alcator C-Mod cooling system has been the result of the work and ideas of a lot of people from the Alcator C-Mod group, unfortunately too many to be named individually. We wish to acknowledge their contribution, knowing that such an enterprise would not have been successful without the contribution of every one of these individuals. We also acknowledge the special contribution of A. Zhukovsky of the Francis Bitter Magnet Laboratory in the design of the cooling system.

REFERENCES

[1] W. Beck, "Alcator C-Mod Toroidal Field Magnet Assembly",Proc. 14^{th} Symposium of Fusion Engineering, 1991

[2] W. Burke and E. Byrne, "A reliable temperature control system for the Alcator C-Mod vacuum vessel", this conference.

[3] W. Beck, "Repair of Poloidal Field Magnets on Alcator C-Mod", this conference.

[4] J. Daigle, "Fabrication of Alcator C-Mod ohmic heating coil and coaxial bus", Proc. 14^{th} Symposium of Fusion Engineering, 1991

[5] W. Burke, "Temperature control and magnet instrumentation in Alcator C-Mod", Proc. 14^{th} Symposium of Fusion Engineering, 1991

A RELIABLE TEMPERATURE CONTROL SYSTEM FOR THE ALCATOR C-MOD VACUUM VESSEL

William Burke and Eamonn Byrne
MIT Plasma Fusion Center, Cambridge, MA 02139

ABSTRACT

In Alcator C-MOD, a complex magnetic field is used to hold a hydrogen plasma in a vacuum. In normal operation, the magnets and support structure are cooled to liquid nitrogen temperature (-200 °C) to take advantage of the reduced resistivity of copper and the increased strength of stainless steel at cryogenic temperatures. However the vacuum vessel, which is surrounded by the cold magnets, must be kept relatively warm (20 °C) to maintain the integrity of the vacuum seals. Once C-MOD has begun operation, the temperature control system must operate continuously for months at a time.

The temperature control system includes 454 heaters of various types with a nominal electrical load of 250 kW. A programmable logic controller (PLC) monitors 472 K-type thermocouples to measure vacuum vessel temperatures and controls the heaters via banks of solid state relays. The relays by themselves can only permit an on-off control of the heaters. The PLC software makes it possible to implement a superior proportional-plus-integral (PI) control scheme with electrical load leveling. The PLC also provides data logging and on-line diagnostic capabilities not as readily available in a hard-wired system.

The construction of C-MOD is described briefly with an emphasis on thermal considerations. The temperature limits for the various components and the overall performance requirements for the vacuum vessel temperature control system are discussed. The design of the temperature control hardware and software is presented in some detail. Problems discovered during the initial C-MOD run period, which required changes in the heaters and controls, are described. Some of the faults and failures that plague any large system with hundreds of active components, thousands of connections, and miles of wire are also discussed.

CONSTRUCTION OF ALCATOR C-MOD

The drawing in Figure 1 shows a cross-sectional view of Alcator C-MOD. The machine is nearly symmetric around the center line and around the mid plane. The magnets and the structural components are included in the top half of the figure, but are left out on the bottom to show the vacuum vessel more clearly.

The TF magnet encloses the vacuum vessel and most of the other magnets. The OH coils are wound on the core of the TF magnet, facing the inner cylinder wall of the vacuum vessel. Eight EF magnets are mounted on the vacuum vessel, four on the top and four on the bottom. The massive structural components, i.e., the retaining cylinder and the top and bottom covers, clamp the entire assembly together. A large fiberglass dewar keeps the machine cold. Ten large horizontal ports, and twenty smaller vertical ports provide access to the vacuum vessel. The ports must pass through the TF magnet and either the cylinder or the covers to reach outside the dewar.

Fig. 1 illustrates one of the problems with the compact design of C-MOD. There is very little free space between the vacuum vessel and the magnets for heaters or thermal insulation. Typical clearances are between 0.5 and 2.0 centimeters. A polyimide foam is used for thermal insulation

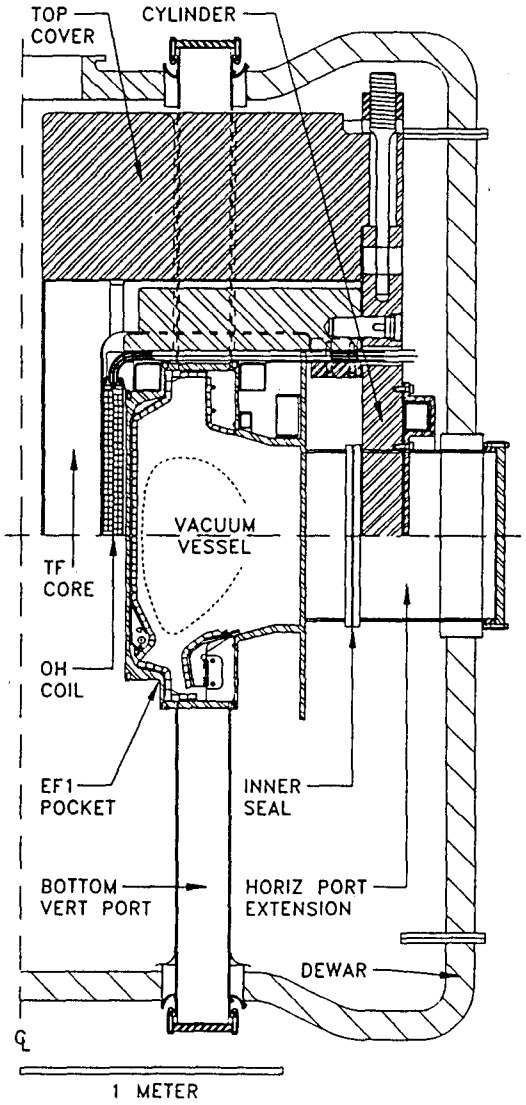

Fig. 1 Cross section of Alcator C-MOD

Manuscript received October 13, 1993. This work supported in part by DOE Contract No. DE-AC02-78ET51013.

wherever feasible. The outer wall of the vacuum vessel, the horizontal and vertical ports, and the EF coils are wrapped with the foam. However, there is no thermal insulation between the OH magnets and the vacuum vessel.

Thermal Parameters

The thermal parameters of C-MOD are summarized in Table 1. The heat capacity of the magnets and support structure is ten times larger than the heat capacity of the vacuum vessel. Thermal time constants are on the order of 10 minutes, so control system response times on the order of one minute should be acceptable.

TABLE 1. C-MOD THERMAL PARAMETERS

Warm Components: Mass and heat capacity of the vacuum vessel.	**8690 kg**	**4.2×10^6 J/°C**
Cold Components: Mass and heat capacity.	**132000 kg**	**5.7×10^7 J/°C**
Covers, cylinder, etc.	108,000 kg	4.7×10^7 J/°C
TF magnet.	18,000 kg	7.1×10^6 J/°C
OH and EF Magnets.	6100 kg	2.4×10^6 J/°C
Area and thermal resistance between the vacuum vessel and the rest of the machine.	**49.5 m^2**	**3.8×10^{-3} °C / W**

OPERATING REQUIREMENTS

C-MOD operations require three primary utility systems: vacuum vessel heating (Heat), cryogenic cooling (Cryo)[1], and torus vacuum pumping (Torvac)[2]. They must work well together for C-MOD to be successful.

The time between a vacuum break and plasma operation is typically seven to ten days. The machine starts at room temperature with the vacuum chamber at atmospheric pressure. It must be pumped for several hours before bakeout can begin.

The Heat system is used to bake the vacuum vessel for two or three days to remove traces of water vapor, solvents, and other impurities. The bake temperature is limited to 150 °C by the use of Teflon insulation and coil forms inside the vessel. The Cryo system must be active during bakeout to insure that all magnet temperatures remain below 50 °C. The epoxy used in the coils deteriorates at higher temperatures.

When the bakeout is complete, the vacuum vessel temperature is brought back to 20 °C and the Cryo system can start to cool the machine. The cooling rate must be kept below 2 °C per hour to limit thermal stress in the cylinder and the covers. Full cool down typically requires five days. The Heat system must be on line during this time to maintain the integrity of the vacuum seals.

Once cool down is complete, plasma operation can begin. During a plasma run, the vacuum vessel temperature is typically set at 20 °C with the magnets and structure at -200 °C. The large surface area between the vessel and the rest of the machine allows for a substantial heat flow. Approximately 50 kW of the electric heating and 20 liters per minute of LN_2 cooling are required to maintain the proper temperatures.

It is necessary to disable all of the heaters for about 10 seconds during plasma shots and power supply tests. The heaters induce 60 hertz noise on some of the more sensitive diagnostics. The heaters inside the TF magnet would also be subject to **J x B** forces if they were energized at the same time as the magnet.

Availability and Reliability

The Cryo system is usually turned off between plasma runs, i.e., nights and weekends. However, the Heat and Torvac systems must run continuously for months at a time. If the Cryo system shuts down, the magnets and structure take 10 to 14 days to return to room temperature. However, if the Heat system shuts down, the vacuum vessel temperature will fall at almost 1 °C per minute. Within one or two hours, the vacuum seals will begin to fail. Cleaning and reconditioning the vacuum vessel after a serious leak could cost the experimental program several weeks.

The time required to tear down and rebuild C-MOD is at least three months, not including the time for any repairs. The reliability of the heaters and all other components inside the machine is critical.

HEATER SYSTEM DESIGN

A block diagram for the Heat system is shown in Fig. 2. The heaters and thermocouples are installed on the vacuum vessel in the C-MOD Cell. The PLC and the other control and power equipment are located in the Power Room just outside the cell. The operator console for the Heat system is in the Control Room.

Heaters and Thermocouples

Most of the vacuum vessel heaters (430 out of 454) are Kapton-foil construction with a pressure sensitive acrylic adhesive on one or both sides. The heaters are less than 0.2 centimeters thick. This was an important consideration given the tight tolerances and limited space available in C-MOD. The heaters are also flexible; they can follow the simple curves of the vacuum vessel quite well. All of the heaters are designed with conservative power rating of 7.5 kilowatts per square meter.

The heaters must cover as much of the vacuum vessel as possible. Approximately 30 different shapes and sizes were required, with power ratings of 60 to 2200 watts. Standard heaters were used in a few places, but most of the heaters were custom designed for C-MOD. The installed heaters cover 36 square meters, 75% of the surface of the vacuum vessel. This represents a nominal electrical load of 250 kilowatts.

Heaters are attached to the vacuum vessel with acrylic adhesive. The same adhesive is used to attach the foam insulation where space permits. All of the custom heaters were designed with integral K-type thermocouples. Thermocouples for the standard heaters are spot-welded to the vessel as close to the heater as practical. All heater and thermocouple leads are routed along the surface of the vacuum vessel to the nearest port, then exit the dewar along the port.

Designs for all of the custom heaters specify two heating elements and two thermocouples. If a heating element or thermocouple is damaged during machine assembly or fails in operation, the spare may still be usable. The large number of heaters also provides a measure of redundancy. The loss of a single heater, or even several heaters at separate locations, should not compromise the performance of the Heat system significantly, and probably would not justify disassembly of the machine.

The performance of the Kapton-foil heaters has certainly been acceptable so far. Stainless steel cable heaters, which were added to the horizontal port extensions to protect the inner seals, have not worked as well. This problem will be discussed later.

Electrical Power

As shown in Fig. 2, there are four sources of 480 VAC 3-phase power available for the Heat system: two independent utility feeds and two emergency diesel generators. The diesels start automatically within one minute after a power failure. The transfer switches automatically select whichever power source is on line. This design allows the Heat system to survive power failures, and also allows one or both of the utility systems to be shut down for maintenance.

The Heat system should continue to operate though most faults. However, there are some failure modes, such as a relay failing closed, for which it is better to disable all the heaters and let the vacuum vessel freeze rather than let a

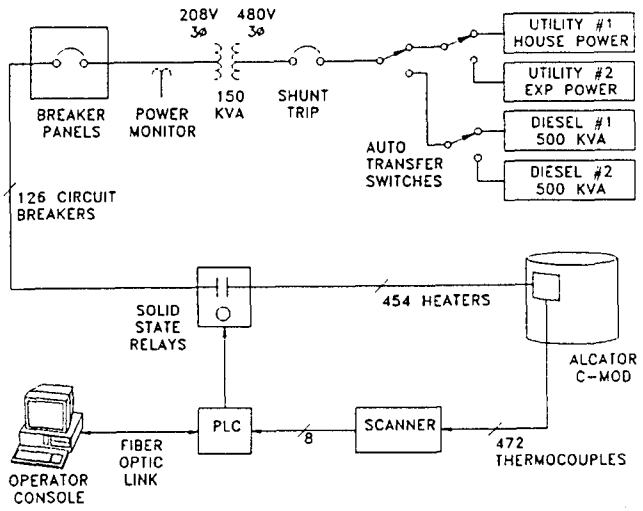

Fig. 2 Block diagram for the C-MOD vacuum vessel heater control system.

heater or another internal component overheat. The shunt-trip breaker provides this capability. The breaker can be tripped under PLC control, but it must be reset manually.

A 150 KVA transformer converts the 480 VAC input to 208 VAC 3-phase power for the heaters. Current transformers on the output monitor power consumption.

The Heat system requires approximately 50 kilowatts for normal operation, and up to 90 kilowatts peak power during a vacuum bake. The available power is more than adequate. However, the heaters represent a nominal load of 250 kilowatts. This means that all of the heaters can not be turned on simultaneously. Individual heaters can be on with a 100% duty factor, but the average and instantaneous duty factor for all of the heaters must not exceed 60%.

Power is distributed to the heaters via 126 single-phase, 30-ampere circuit breakers. Each breaker supplies either one large heater or a number of smaller ones.

Control System Hardware

The Allen-Bradley PLC is an industrial computer that accepts a variety of modules to handle input, output, and communications. The Heat PLC has a larger I/O count than any other C-MOD system, but the tasks it has to perform are fairly simple. The PLC must read vacuum vessel temperatures using a thermocouple scanner, and control the heaters using banks of solid state relays.

The PLC thermocouple module takes eight inputs and requires two seconds per reading. The scanner handles 70 channels with 8 inputs per channel, for a total of 560 inputs. The Heat system uses 472 thermocouples for control. All of the unused inputs are short circuited. The PLC needs 140 seconds to take a full set of temperature readings.

The PLC can only turn heaters on or off using relays. However the PLC is fast enough to simulate proportional control. The scan time for the Heat system PLC is 40 milliseconds. This is essentially the time required for the PLC to check each input, each output, and each instruction once. This is much faster than the fastest response time of the vacuum vessel. The PLC also handles faults, alarms, and interlocks, as well as miscellaneous functions, such as power monitoring.

The operator console for the Heat system is a personal computer that communicates with the PLC via a fiber optic link. The console is used for entering temperature set points and displaying vessel temperature and heater duty data. All of the control functionality for the Heat system is in the PLC. The system will run properly with the operator console shut off or disconnected.

Control System Software

PLC programs are written in ladder logic. The Heat system program has 600 instructions, or rungs, which take up 6000 words of memory. An additional 10,000 words are required for the data tables used to store input and output values, state information, and system parameters.

The PLC implements a proportional-plus-integral control algorithm for the heaters in software. The PLC reads vacuum vessel temperature every 140 seconds. It compares the measured values to the set points for each heater, and then calculates the error, the integral of the error, and the duty factor for the heater. All of these values are stored in data files.

Heaters are controlled with 1% resolution in an eight second timing cycle. For example, a heater at 25% duty will turn on for two seconds out of every eight. Heaters are assigned to one of six timing groups. The starting time for the groups is staggered to spread the electrical load more evenly.

Heaters are also assigned to one of three temperature control zones (ports, coils, and walls). This allows heaters near coils to be set lower during a bakeout, and heaters on ports to be set higher during normal operation. The timing groups and the temperature control zones for each heater are stored in data files.

Paragon 550 from Intec Controls is used as an operator interface and for data acquisition. It validates set points and other data that are entered from the console. It can provide tabular and graphic displays of temperatures, duty factors, and power consumption. The Paragon software also retrieves data from the PLC and processes it for archiving.

Advantages of Software Based Control

Software-based control for the C-MOD Heat system has been an unqualified success. It has provided excellent flexibility and availability.

When the Heat system came on line in 1991, it used an on-off control algorithm with one temperature control zone. Temperature regulation and load leveling were marginally acceptable. The real improvements in system performance all came in the software. It was not necessary to touch a single wire or a screw.

Software can be changed while the system is running. Simple changes can be made on line. Major modifications, or even a complete redesign, can be programmed off line. For example, the programming for multiple temperature zones required several weeks, but the Heat system was up and running the whole time. After the new software was tested off line, it was installed in the running system in less than 15 minutes.

OPERATING EXPERIENCE

C-MOD suffered a few serious setbacks during its initial run period in 1992. Some combination of design, manufacturing, and operating errors resulted in a catastrophic failure of one of the EF coils after ten weeks[3]. This incident required a complete disassembly of the machine, and resulted in a one year shutdown. Less spectacular but only slightly less serious problems were discovered in the heat system.

Inner Cylinder Failures

Eight large heaters (47 cm x 62 cm, 2200 watts) were used to cover the inner cylinder of the vacuum vessel. The clearance between the inner cylinder and the OH coils is 0.6 centimeters. There is barely enough room for heaters and wires; there is no room at all for thermal insulation. Intuition suggested that the thermal loading would be fairly uniform, so a large heater would be acceptable. However, one of the inner cylinder heaters failed during the first full temperature bake, after just two weeks of operation. Three more heaters failed within the first ten weeks.

A careful thermal analysis determined the cause of the failure. The heaters do not extend to the ends of the inner cylinder, so the heat losses at the ends will always be higher than in the middle. In addition the EF1 coil pockets were not heated at all; this exacerbated the problem. Finally, the thermocouple controls for the heaters were located near the ends, where temperatures were lower. During bakeout, the top and bottom of the inner cylinder were regulated at 150 °C, but the middle reached peak temperatures of 250 to 300 °C. This was hot enough to destroy the heaters and several magnetic diagnostic loops inside the vessel.

The shut down to repair the EF coils also provided an opportunity to work on the inner cylinder heaters. The eight large heaters with integral thermocouples were replaced with 44 smaller ones and 52 spot-welded thermocouples. Heaters were also installed in the EF1 pocket.

Inner Seal Heaters

There have been continuing problems with intermittent vacuum leaks on C-MOD. The leaks are correlated with high cooling rates and have been localized to the inner seals on a few of the horizontal ports.

The ports and port extensions are heated. However, the flanges that make the inner seal were not originally heated, insulated, or instrumented. We assumed that liquid nitrogen leaking on the flanges caused large temperature gradients and compromised the seal.

During the shut down, two thermocouples (top and bottom) and a stainless steel cable heater were attached to the inner flanges on all ten port extensions. This has not been a success.

Three of the cable heaters did not survive the assembly process. All ten heaters have since failed. Even when the heaters were working, they did not solve the seal problem. Instrumentation indicates that there is always a gradient between top and bottom of the flanges, perhaps from convection in the dewar. The cable heaters, which heat the flange uniformly, have no effect on the gradient.

[1] R. Biovin and C. Reddy, "Cryogenic cooling system for the Alcator C-MOD Tokamak," This conference.

[2] R. Childs, J. Goetz, M. Graf, A. Hubbard, J. Rice, T. Tolland, "Design, control, and operation of the vacuum and gas systems for Alcator C-MOD," This conference.

[3] S. Fairfax and D. Montgomery, "Anatomy of the PF magnet failure in Alcator C-MOD," This conference.

ALTERNATOR CONTROL SYSTEM FOR THE ALCATOR C-MOD TOKAMAK

Eamonn Byrne
Plasma Fusion Center
Massachusetts Institute of Technology
Cambridge, MA 02139

Abstract

The Alcator C-MOD tokamak can expend over 500MJ in a single pulse. The primary power source for this experiment is the upgraded Alcator C alternator. Over the years the alternator has undergone several modifications to make it more suited for pulsed operation and in the near future the energy storage of this 40 year old alternator will be increased from 500MJ to 2000MJ with the addition of a 75-ton flywheel. After 25 years of utility service and 8 years of pulsed operation the alternator is still in good condition. However, in order to insure many more years of reliable service every effort must be made to reduce electrical, thermal and mechanical stresses. This means the alternator must be interlocked with the power supplies (7 in all) so that it can protect itself from excessive armature current should any one fail. It also necessitates monitoring many of the critical temperatures, pressures and safety backup systems so that either operator intervention or an orderly shut-down can prevent serious problems. This report will describe how the Alternator control system has been modernized with the addition of a Programmable Logic Controller (PLC) in conjunction with a networked, PC based Supervisory Control And Data Acquisition (SCADA) package. The report will discuss the design, commissioning and operational experiences of the new control system.

Introduction

The Alternator, built by General Electric, was commissioned in 1952 for Consolidated Edison in New York. It was taken out of service and donated to the Plasma Fusion Center in 1977. Over those 25 years it ran nearly continuously. In its new role, for Alcator C, it operated in pulsed mode generating up to 250MJ once every 20 minutes. Demand can exceed 500MJ during an Alcator C-mod pulse. The cyclic stresses resulting from this type of operation and the impact associated with failures and downtime demanded that cooling, heating, lube oil, seal oil and control systems had to be upgraded. In the past operators routinely logged system information by hand. This necessitated a 20 minute walk-through of the alternator building inspecting temperature and pressure gauges. A mechanical data logger was also used for recording RTD readings but this was susceptible to noise problems and required considerable maintenance.

Supported by U.S. DOE contract No. DE-AC02-78ET-51013.
Manuscript received October 12, 1993.

It is clear that to minimize failures and downtime the operators must have clear and reliable access to critical system information. By automating routine tasks, providing real time alarming and trending, and recording system performance potential problems can be foreseen and prevented.

General

Consistent with the overall Alcator C-MOD control system architecture[1] Allen Bradley PLC-5's were utilized as the primary industrial controller. These programmable logic controllers are field proven to be reliable and flexible industrialized controllers suitable for small and large systems. They allow for easy integration of control systems which are distributed in nature by the use of a variety of remote I/O interface modules. In conjunction with the PLC's, a PC based graphical operator interface and data acquisition package was required. In all, three PC's are required for the system. One is located adjacent to the existing control cabinets for centralized control and will be used for system start-up, shutdown and trouble shooting. A second, to be installed in the new sound proofed and air conditioned control room, will duplicate the first in functionality and will be used for normal daily operation. This new environment will afford a higher level of safety as well as comfort. Noise levels fall between 80-85dB and operating temperature is between 85-100 ^{o}F in the alternator building. The dangers associated with high power and high voltage will be increased due to the longer coast-down time as a result of the new flywheel. The third PC, separated by fiber optic cable, is located in the C-MOD control room and allows the Alcator C-MOD operator to control the alternator during shot cycles. System status including speed, excitation, mode of operation and summarized faults are displayed. The PC based interface packages available on the market are not as mature as the industrial controllers. Several packages were reviewed in 1991 most of which provided control capabilities such as PID and sequence control, but their role will be limited to that of operator interface and data acquisition only. Paragon 550[2] was chosen at that time because it offered networking capability, ease of use and one of the lower costs.

System Design

The primary objectives of the control system are:

- enhance system protection via hardwired and PLC controlled interlocks.
- monitor system temperature, pressure and vibration.
- provide flexible alarming, trending and recording of process variables.
- integration into the overall C-MOD control system for remote control and synchronization.
- minimize operating and system costs.
- minimize stresses on the machine by reducing cycling stresses and avoiding critical speeds.
- simplify start-up and shut-down procedures.

The PLC system is intended to provide additional system protection rather than total protection. Much of the time invested over the years has concentrated on improving system reliability and particularly improving personnel and equipment safety. This has resulted in a hardwired relay logic safety system that is tried, test and approved. Excessive vibration, heat, pressure or contact failures are interlocked as appropriate for personnel safety and equipment protection. Backup pumps, diesel generators, Uninterruptable Power systems (UPS) and/or system shutdown can all be initiated automatically. This hardwired protection relies on actuators such as limit switches, pressure switches, relays, thermostats and interlocks provided by a wide variety of instrumentation and control equipment. Hardwired interlocking should always be used as the first level of protection in designing a "fail-safe" system. However, faulty actuators, wiring errors, cable damage, or unforeseen failure modes can inhibit such protection. Temperature or pressure actuated switches may lack sensitivity or may not allow adjustment for varying operating conditions. It is in this context that we utilize the PLC for second level or backup protection. System protection is enhanced by monitoring process information and setting appropriate alarm and trip values in the PLC. The PLC-Paragon combination allows this data to be presented in real time and in a context sensitive format. Alarm and trip set points can easily be modified via the operator interface to better match operating conditions. Different limits can also be loaded automatically during pre-heat, start-up or shutdown modes to account for changing operating conditions and avoid unnecessary alarm annunciation. The improved sensitivity, flexibility and interface can reduce stresses and damage by annunciation of problems before they become critical. Clear and timely fault annunciation allows more time for operator intervention.

Standard analog output modules are used to control the alternator speed and excitation in preparation for a pulse. Running at full speed heats the alternator gas seals to 170 ^{o}F, ten degrees below the recommended limit. By running at reduced rpm in-between shots, the gas seal temperature can be lowered to 160 ^{o}F thereby increasing the safety margin. Operating costs can be reduced at the same time as a result of the lower windage and friction losses. The PLC controls the alternator speed over the range of 1400-1800rpm (A maximum performance pulse should decelerate the alternator to about 1500rpm). The control room operator sets the shot and the in-between shot alternator speed via Paragon. Referring to figure 1 the objectives are to reduce the gas seal operating temperature by running at as low a speed as possible between shots, but also to minimize stress cycling and vibration. This is accomplished by setting the in-between shot speed slightly higher than the anticipated post shot speed (including the speed increase due to acceleration of the alternator as a result of the toroidal field power supply going into inversion). If the in-between shot speed is set lower than the post shot speed we incur additional stress cycling. If it is less than or equal to the post shot speed excessive vibration can result in the 2000HP motor. This results from shifting of the rubber inserts in the motor-alternator coupling if no torque is applied to the shaft by the motor.
The time to full speed can also be matched with the required cooling time for the coils to ensure that the alternator is ready for scheduled shots. Stresses can also be minimized by ensuring that the alternator does not dwell at critical speeds causing excessive vibration.

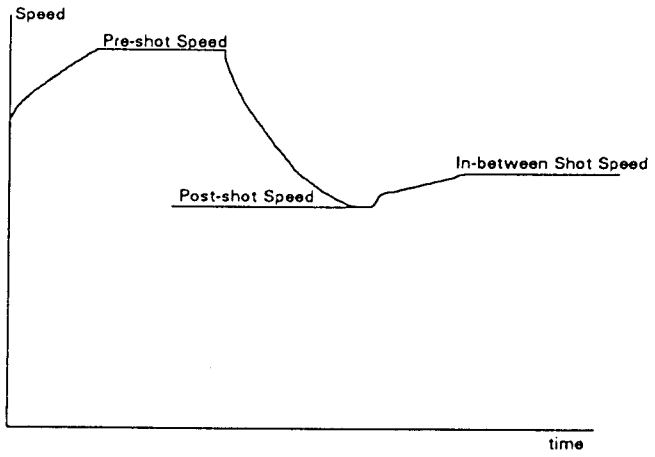

Figure 1

Control of the excitation is employed for personnel safety and equipment protection. Synchronization of the excitation with the shot cycle reduces the time at high voltage and interlocking with the power supply systems ensures that excitation is removed in the event of serious faults. This protects the power supplies as well as the alternator.

The following signals are monitored:

66 RTD's (six 100Ω Platinum, & sixty 10Ω Copper)
7 Vibration sensors
20 pressure sensors
13 current transformers (CT)
alternator voltage
alternator speed
128 DC inputs (approx.)
96 AC inputs (approx.)

In determining the system I/O it is important to evaluate what signals are required and to allow for maximum flexibility and expandability while minimizing system costs. Looking at cost factors we realize that the greatest impact on system cost results from the relatively high price of analog modules, particularly the dedicated RTD modules. In a typical power plant the alternator control system would monitor only one of the many embedded RTD's which would be representative of the stator temperature (this would be selected during commissioning). Given that the heating, cooling and lubrication systems for the alternator have all undergone major changes and given the unique nature of operation, it is important to monitor all 18 of the embedded RTD's. This helps the operators to better understand the radial and axial temperature distribution under various operating conditions. It also pin-points areas of maximum thermal stress. The cost of using dedicated modules to monitor all of the RTD's, vibration sensors, pressure sensors, and CT's would approach $22,000. To cut costs a multiplexor was employed to reduce the PLC module count. The six flywheel bearing RTD's (100 Ω Platinum) were wired to a dedicated RTD module and all of the 10Ω Copper RTD's, pressure sensors, vibration sensors and CT's were interfaced to the PLC via a Matrix Corporation[3] Model 1701 low level scanner. The signals were divided into 3 groups (see figure 2) to provide flexibility in changing the system configuration should the need arise. These groups are RTD's(temperature), 0-10VDC signals (vibration and CT's) and 0-100mV DC signals(pressure). Pressure transducers with a 0-10VDC or 4-20mA output could have been selected but considerable savings were realized by opting for the 0-100mV model and using an in-house 2 channel instrumentation quality amplifier. While the use of a multiplexor reduced the update rate of the signals it resulted in savings in the order of $15,000.

RTD Interface

Perhaps the most crucial aspect of multiplexing the 10Ω RTD's was insuring accurate lead length compensation. This compensation is built into the PLC RTD module (cat. No. 1771-IR), but it is necessary to insure that the modified cabling does not introduce lead resistance imbalances. This could arise from poor soldering, bad connectors or contact resistance associated with the reed relays that make up the multiplexor. The initial installation made this quite clear. The edge card connectors supplied with the multiplexor were low quality and produced contact resistance which was significantly large and time varying. We are mainly concerned with relative temperature measurements, so fixed errors could be compensated or tolerated but not erratic or time varying ones.

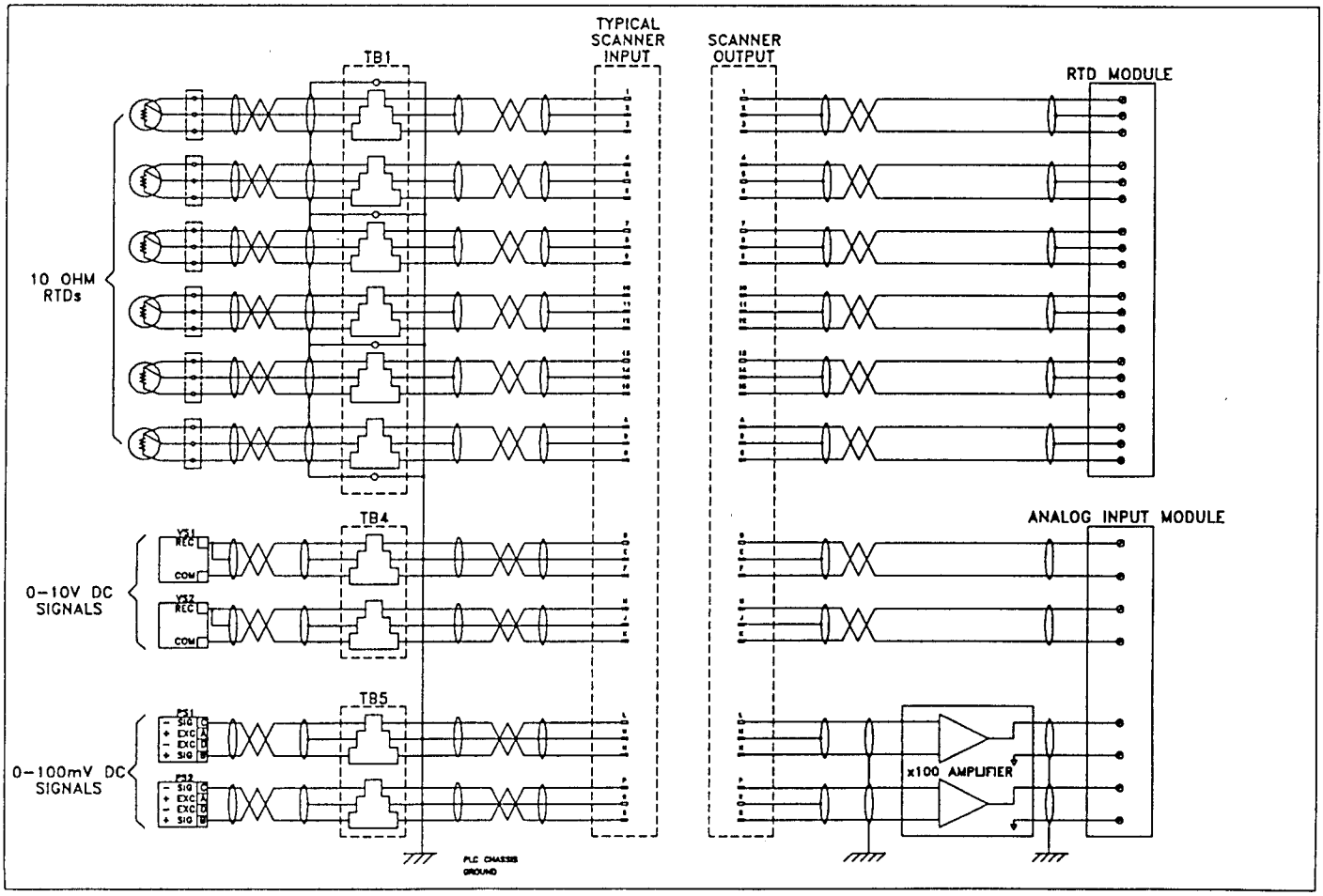

Figure 2

To remedy this situation new cables were made with superior edge card connectors. The connector pins were gold plated and greater pressure on the pins increased the ampere rating to 5 amps. The excitation current for the RTD's is only 1mA. Unfortunately close inspection of the temperature data revealed that the contact resistance of the new connectors was still unstable, resulting in intermittent errors in the order of 2 to 5 percent. In order to enhance alternator protection by implementing alarming and tripping for orderly shutdown, it is necessary to eliminate spurious readings and reduce errors to less than one percent.

Reviewing the situation it was clear that eliminating the intermittent component of the contact resistance associated with the edge card connector and the multiplexor would be very difficult. Other connectors and multiplexor models were considered as potential solutions but would require considerable additional investment. It was also desirable to utilize the Matrix scanner to reduce spare part inventory as the same model is employed for thermocouple applications on other C-MOD systems. The solution was to replace the measurement of resistance using a bridge circuit (i.e. the RTD module) with a 4-wire measurement technique. This required the addition of a simple 6 channel amplifier and minor wiring changes - see figure 3.

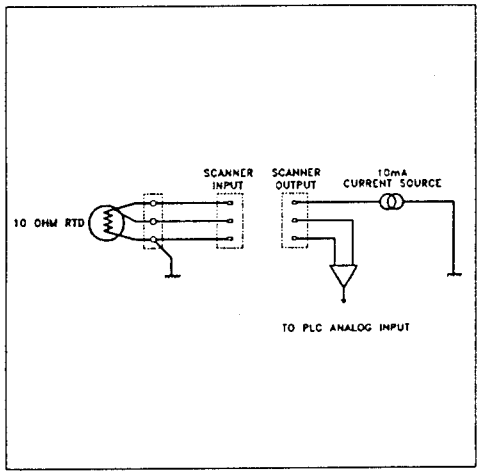

Figure 3

A current source drives 10 mA through the scanner and the RTD and utilizes the alternator frame as a return path. The ground actually substitutes as the fourth lead necessary for a true four wire measurement. The voltage generated across the RTD is measured using the two remaining leads. Varying contact resistance associated with the current carrying lead will result in a change in the voltage drop across the connector but will not effect the measurement as no current flows in the current sensing leads. A standard analog input module is used in place of the RTD module which measures the amplified RTD voltage. The amplifier design incorporates a DC offset to improve the dynamic range of the measured signal such that 0-3.9VDC corresponds to 0-100 ^{o}C. Our measurement is sensitive to the RTD lead length because the RTD's are not true 4-wire devices Each reading will have an offset equal to the resistance of the lead between the RTD and the ground termination. In practice this only effects the RTD's embedded in the windings which have lead lengths of 15-30 feet. As stated earlier this is not a significant problem and is easily corrected in the PLC program.

Summary

Historically the alternator system has undergone numerous modifications and upgrades. This trend will continue with the addition of the flywheel and plans to automate the labor intensive startup and shutdown procedures. It is important to incorporate this dynamic nature of the system into the control strategy. This means setting up the hardware, software and documentation in a modular and flexible format to allow for easy system upgrades without incurring unnecessary expense or the risk of system downtime. Even though problems were encountered with the multiplexing of the RTD's this flexible approach paid off by facilitating a relatively easy upgrade. The latest upgrade to a PLC based control system has already greatly enhanced system operation. Laborious operator tasks have been reduced and unreliable data logging equipment has been replaced. The data acquisition and trending, combined with the graphical operator interface, has provided a more accurate, reliable and meaningful man-machine interface. Operators and engineers can better analyze system and sub-system performance with a view to reducing costs and improving reliability. Also the distributed interface simplifies system operation by assigning control where and when it is needed. This minimizes the need for communication between the control room operators and the operators in the alternator building, an issue which has proved to be troublesome in the past. While many tasks still remain the inherent modularity of the PLC and the flexibility designed into the system should facilitate relatively easy modifications well into the future.

Acknowledgments

The success of the alternator control system upgrade is founded on the insight and dedication of many people. I would like to thank S. Fairfax, J. Bosco, J. Rosati, M. Rowell, K. Rettman, F. Sibelli and D. Harris for their contributions and commitment to the project.

References

[1] J. Bosco, S. Fairfax "The Alcator C-MOD Control System" Proceedings of the IEEE 14th Symposium on Fusion Engineering.

[2]Paragon is a registered trademark of Intec Controls Corp., Walpole, MA 02081

[3] Matrix Corporation, Indianapolis, Indiana 46241

DESIGN, CONTROL AND OPERATION OF THE VACUUM AND GAS SYSTEMS FOR ALCATOR C-MOD

R. Childs, J. Goetz, M. Graf, A. Hubbard, J. Rice and T. Toland
Plasma Fusion Center
Massachusetts Institute of Technology
Cambridge, MA 02139

ABSTRACT

The torus vacuum system for the Alcator C-Mod tokamak is composed of two 1000 l/s vertical axis turbomolecular pumps and one 8" cryogenic pump. Since the vacuum vessel port connections are inside a liquid nitrogen dewar and are subjected to large temperature gradients during cooling, a double seal arrangement with inner Helicoflex seals and outer indium coated copper seals has been implemented. The gas fueling system provides mixtures of six supply gases to an array of fill valves with complete flexibility of gas mixture and feed location. Fully remote operation and monitoring of the vacuum and gas systems is required and has been implemented using a Programmable Logic Controller. Design details, test results and operational experience are presented.

INTRODUCTION

The vacuum system for the Alcator C-MOD fusion experiment is responsible for maintaining a low base pressure and high degree of cleanliness in the torus vacuum chamber. Alcator C-MOD is a compact, high field diverted tokamak with a plasma volume of typically 1 m^3 and a vessel volume of 4.03 m^3. Almost all of its plasma facing surfaces are composed of molybdenum. The vacuum pumping system has a total pumping speed of over 5000 l/s, and is described in section II. One of the greatest engineering challenges in the vacuum system was designing seals for the diagnostic ports which could withstand the large thermal gradients imposed by proximity to liquid nitrogen-cooled coils. The design and testing of these seals is discussed in section III.

The gas fueling system, which is closely linked to the vacuum system, is required to fill the torus with experimental gases to the pressure needed for plasma breakdown and density control, as well as for discharge cleaning. A key design feature is its flexibility, which allows mixtures of any of six supply gases from each of several fill locations. This is important for radiative divertor experiments, minority ion heating and impurity transport studies. Details of the system are given in section IV. Both the vacuum and gas systems are controlled remotely, enabling pumping and fill operations to be carried out from the control room. Section V outlines the hardware and software used to implement these functions.

This work was supported by US DOE Contract No. DE-AC02-78ET51013. Manuscript submitted October 14, 1993.

II. VACUUM HARDWARE

The vacuum pumping system, shown schematically in Fig. 1, is attached to an extension on one of the horizontal ports of the vacuum chamber and consists of two turbomolecular pumps and one cryogenic pump with associated backing pumps and valving. A rotary vane mechanical pump provides backing of the turbo pumps and roughing of the vacuum chamber. This pump is a Leybold D60A rated at 17 l/s and, with a 50 mm roughing line, can pump the torus to 1 Torr in approximately 30 minutes. The turbo pumps are both Leybold TMP1000 rated at 1000 l/s for hydrogen with ISO NW250 inlet flanges. Above the turbo pumps are adaptor headers to the ISO NW320 components used for the rest of the pumping line. Connected to the headers are ceramic electrical breaks manufactured by Ceramaseal Inc. These are attached to mitered elbows which have a short bellows section built in to reduce shock to the electrical breaks during tokamak operation. ISO NW320 VAT Series 10 gatevalves make the final connections to the port extension.

The two pumping stacks make a common connection to the mechanical pump with separate foreline isolation valves. The left hand turbo stack has an additional set of valves that provide a roughing bypass circuit. For the roughing operation, the foreline valves to the turbo pumps are initially closed and SV2 and SV3 are opened. When the chamber reaches 500 mT, SV2 is closed and a VAT CF63 butterfly valve (SV4) which is controlled via a stepping motor, acts as throttle valve to control the gas load to the turbo pump. Once the pressure differential across the gate valve GV1 is reduced to 0.1 Torr, it is opened for maximum conductance.

A separate cryopump system is attached to a port located on top of the port extension between the turbo pump stacks. It consists of a CF200 VAT Series 10 gate valve, ceramic electrical break and gauging header, and a CTI Onboard 8 cryogenic pump. An Alcatel Microtorr molecular drag pump system provides safe, "dry" regeneration of the cryopump. The cryopump system was added after initial operation showed the need to provide more pumping speed (typically 3500 l/s) for condensibles like water, carbon dioxide, and methane and is used during off hours to help "clean up" after a run.

Pressure monitoring at points throughout the pumping station is provided by Convectron gauges from atmo-

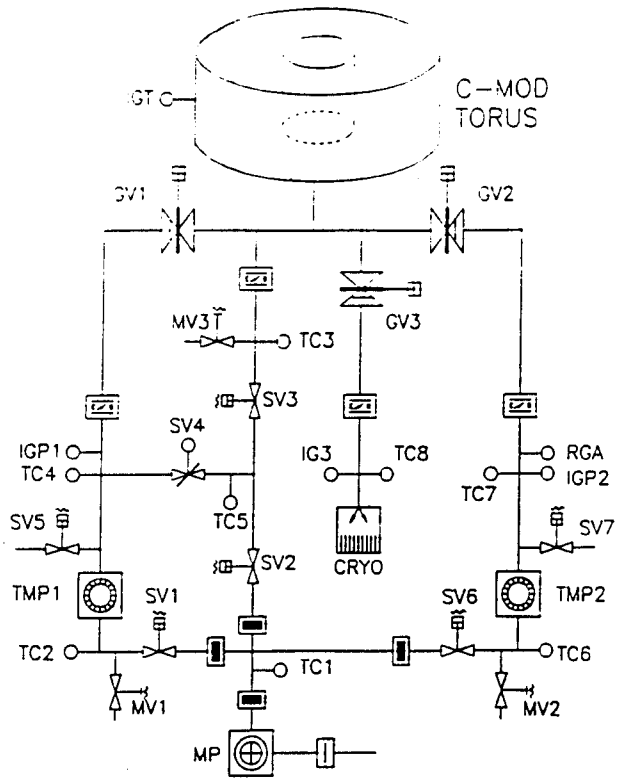

Fig. 1 Schematic of the vacuum pumping system

sphere down to 10^{-3} Torr, and nude BA gauges from 10^{-3} Torr down to 10^{-10} Torr. An Ametek/Dycor System 1000 quadrupole mass spectrometer RGA provides status of the condition of the vacuum and initial leak detection. More sensitive leak detection is accomplished using a helium mass spectrometer leak detector.

III. DESIGN AND TESTS OF FLANGE SEALS

The C-MOD vacuum vessel is of solid stainless steel construction to withstand large mechanical forces associated with 9 T operation. There are one horizontal and two vertical diagnostic ports in each of the 10 sectors of the machine. The horizontal ports are 20.3 cm wide and 62.9 cm tall, in a 'racetrack' shape, and are located inside a cryostat which serves to insulate the cryogenically cooled coils. The smaller vertical ports have a 'teardrop' shape, with radii of 4.6 and 2.4 cm at the two ends and a length of 20.9 cm. They are located at the end of 1.2 m long vertical extensions through the mechanical structure. Since both sets of flanges are inaccessible once the cryostat and radiation shielding blocks are in place around the vessel, development of reliable seals for these non-standard cross-sections was critical.

The primary vacuum seal for the horizontal racetrack flanges is a custom made two layer "C" crossection Delta seal with internal spring, manufactured by Helicoflex, Inc. A pair of indium coated copper wires serve as secondary

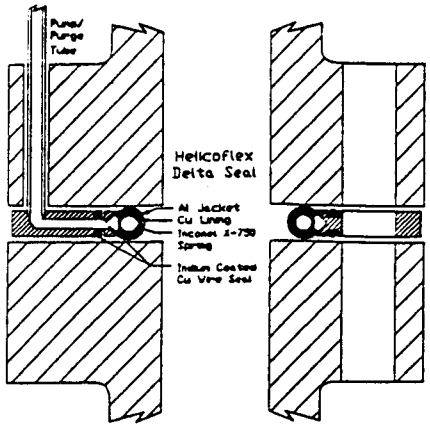

Fig. 2 Helicoflex Delta seal flange assembly

seals, and are imbedded in grooves machined into the limiter centering ring which supports the primary "C" seal. Two small tubes on the top and bottom of the limiter centering ring that pass through the outer flange provide access to the volume between the primary and secondary seals for evacuating, purging and leak testing the seals. The flanges are then fastened to the main vacuum chamber with 84 3/8-24 bolts torqued to 40 ft-lb. Smaller Helicoflex seals are used for the vertical ports and external horizontal flanges. Standard Helicoflex Delta seals are also used on pumping stacks in place of the usual ISO Viton o-ring seals.

In order to reproduce the environment of the flanges on the actual machine, that is, exposure to liquid nitrogen or cold vapor which gives rise to large temperature gradients, two port extensions with race-track flanges were bolted together and placed inside a small cryostat. The volume was then pumped with a 450 l/s turbo pump and the double seal volume was set up to be either evacuated with a small roughing pump or purged with helium. The flanges were instrumented with thermocouples on the sides, top and bottom. A helium mass spectrometer leak detector was attached to the foreline of the turbo system. The port extensions and flanges were able to be baked up to 150 C with heaters.

Several cooldown tests were performed where liquid nitrogen was introduced into the cryostat, and the flange temperature and seal pressures were monitored. A typical result is seen in Fig. 3a and 3b, where the pressures in the double seal region and inner volume, and the temperatures at the top and bottom of the flange are shown as a function of time. At 50 minutes the bake of the port extensions and flanges was started. At 80 minutes liquid nitrogen cooling was initiated. At 160 minutes the outer indium seal failed and the double seal region reached atmospheric pressure. At this time there was a 150 C temperature difference across the flange. At 170 minutes the

pressure inside the test chamber began to rise and the cooling was turned off. The Helicoflex seal then quickly resealed and shortly thereafter the indium o-rings also resealed. Several cooling cycles have been performed with similar results. The outer and inner seals fail when there is an excessively large temperature gradient across the flange but reseal when the flange is warmed up or direct contact to LN_2 is stopped.

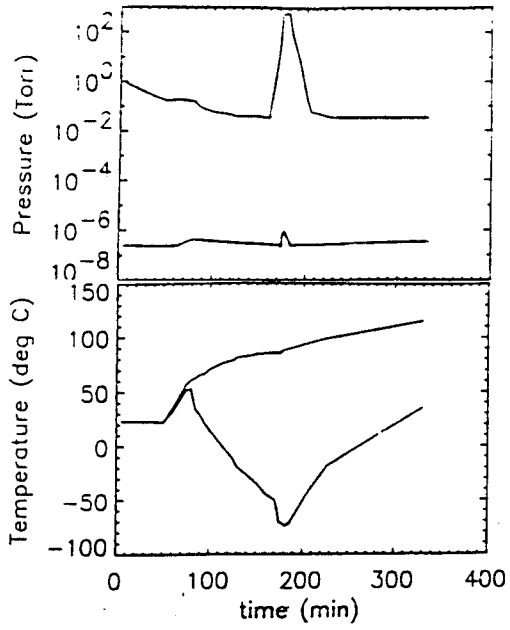

Fig. 3 Time history of chamber and seal pressures (a) and upper and lower flange temperatures (b) during flange cooling tests.

Operational experience with the seals on C-MOD reflects the results of the above tests. Under most conditions the flange seals have performed well, with RGA measurements showing that the vessel base pressure, typically 3 x 10^{-8} Torr is dominated by outgassing of methane, water and other gases rather than by leaks. However, there have been events, associated with increased LN_2 cooling to the PF and TF coils, which have resulted in one or more horizontal seals opening temporarily. Thermocouple measurements show that at these times temperature differences across the flange exceed the safe level of 150 C. It is inferred that liquid is contacting part of the flange. Pumping or purging of the secondary seal has helped minimize the effects of these leaks. Improvements in the insulation around the flange are being developed to keep liquid away from the seal.

IV. GAS FUELING SYSTEM

The gas fueling system consists of the hardware and software necessary to control and monitor the flow of all gases required for the experimental program of the tokamak. The system allows for ultra-pure gases or mixtures of gases to be introduced to the tokamak for pre-filling, fueling, and experimental gas impurity studies. The hardware can be considered in four separate sections: (i) the supply gases, (ii) the mixing and storage chambers, (iii) a molecular drag pump and associated vacuum hardware for purging, and (iv) the valves which interface the system with the tokamak vacuum vessel.

The system is capable of providing up to six different high-purity supply gases to various locations in the tokamak. The gases can be delivered in pure form or in any mixed ratio desired. This mixing is done in six 4-liter holding plena connected to the supply bottles through a common manifold. Purity of any single gas in this manifold is maintained with a molecular drag pump which is capable of pumping out the system from atmospheric pressure to a pressure of less than 10^{-2} Torr in about 5 minutes. The tokamak interface consists of five piezoelectric valves mounted at various locations on the side, top, and bottom of the machine. There are also 28 capillary tubes located in the divertor regions (both upper and lower) which are externally connected to fast pneumatic valves. These capillaries are fed by two of the six plena, allowing for complete flexibility of the gas mixture and feed location.

V. REMOTE CONTROL AND MONITORING

Both the torus vacuum pumping station and gas fueling system must be controlled and monitored remotely, from the machine control area. The experimental cell is inaccessible to personnel during tokamak operation, due to electrical and radiation hazards as well as potentially low oxygen levels. The control functions are implemented using a Programmable Logic Controller (PLC) located in the cell, which is linked via optical fibers to a PC in the control room. The PLC, which we refer to as 'TORVAC', is an Allen-Bradley PLC-5/25 processor. Each of the pumps, valves and gauges in the system is hardwired to input and output modules in the PLC rack, enabling its status to be monitored and, where appropriate, controlled. Since the gas hardware is located in a different part of the cell from the pumping station, its I/O modules are in a remote, electrically isolated rack but controlled by the same PLC.

The control logic is programmed into TORVAC using the PC. The philosophy used is to make the hardware 'fail-safe' as far as possible, to prevent equipment damage and especially accidental venting of the torus. Operations such as pumpdown are carried out following the commands of knowledgeable operators, but checks are included for each

step to guard against errors or hardware problems. For example, a turbo pump cannot be turned on unless its backing pressure is in the correct range and cooling water flow and temperature status signals are present. If at a later time one of these conditions is violated, or a power outage occurs, the pump automatically shuts off and valves close to isolate it from both the machine and the roughing pump. After a delay, the turbopump volume is vented. Analogous logic exists for each active component. An important aspect of the "fail-safe" design is in the wiring of components such that any interruption of cables, fibres, power supplies etc. results in the same state (usually a signal going low) and will be interpreted as a fault.

The operator interface to the vacuum and gas control systems is through a commercial Paragon software package (Intec Controls Corporation) on a PC. Several graphical display screens have been developed which show the status of components and the pressures at various points. Commands are initiated by toggling switches or entering setpoints, and the operator has immediate feedback (for example, change in colour of a component) on the action taken. Fault messages or audible alarms draw attention to any problems with the system. The Paragon software package also has the capability to display and store time histories of selected parameters, which has proven very useful in tracking pressure trends. These are transferred once a day to the C-MOD data storage system, where they can be easily accessed by any user on the VAX network.

The control room user interface for the gas system allows for automatic filling of each of the six plena with a specified mixture of gases before each experimental run day as deemed necessary by the operators. The specified plenum is first vacuum purged and the desired partial pressures are added. Mixing is performed by adding the smallest partial pressure first and proceeding until until all gases are added. Pre-filling of the tokamak before each experimental discharge is also performed automatically from any pre-selected piezoelectric valve. A target pre-fill pressure is maintained by a PID feedback algorithm implemented through the PLC, which controls the voltage applied to the piezoelectric valve. The feedback gains have been adjusted so as to make the system critically damped. The feedback loop calculates and updates every three seconds and is capable of reaching and holding the target pressure within about two minutes of the initiation of the fill. Fast control of the fueling gas during the discharge is achieved using the Plasma Control System hybrid computer [1]. Independent hybrid computer signals can be sent to up to three of the piezoelectric valves at the same time, enabling fast puffing of different gas mixtures at different locations during the same shot. This is routinely done to provide argon for ion temperature studies and minority fuel gas for RF heating experiments as well as to achieve the required electron density waveform. The configuration of the gas system is transferred to the C-MOD data system after each shot.

Similar PLC/Paragon control is used for other machine systems such as heating, cryogenics and power supplies [2,3,4]. Since there are many interrelationships between such systems, this facilitates the transfer of data. Critical status information is passed between PLCs on fiber optic links, while other parameters are shared between PARAGON programs via a PC network. A good example is the electron cyclotron discarge cleaning procedure. This is controlled from the vacuum PLC since it involves gas prefill and pressure feedback. It also requires sweeping of TF current, which is run by a separate PLC. In addition, temperatures on several other systems must be monitored to assure that no coils or internal vessel components are overheating. A fault on any of these systems is communicated to TORVAC, which shuts down discharge cleaning in a controlled sequence.

CONCLUSIONS

The vacuum pumping system designed for the Alcator C-MOD tokamak has performed as expected and has provided a base pressure of 3 x 10^{-8} T in the vacuum chamber. Helicoflex Delta seals designed for the port flanges have been shown in both laboratory tests and actual operation to be leak-tight except when temperature differences across a flange exceed 150 C due to contact with liquid nitrogen, and have resealed when warmed up. While similar sealing systems have been used on other tokamaks, eg [5], none have been subjected to as severe environmental conditions. We have demonstrated the abilility to operate a complex vacuum and gas fuelling system using remote, PLC control. The systems have proven highly reliable, shutting down safely after power failures and other faults. There has been very little experimental downtime due to vacuum problems, while the flexible fueling capability is routinely exploited.

REFERENCES

[1] S. Horne et al, this conference.
[2] W. Burke and E. Byrne, this conference.
[3] R. Boivin and C. Reddy, this conference.
[4] S. Fairfax, J. Daigle et al, this conference.
[5] D.H. Mullany, M.A. Mozeleski and R.B. Fleming, J. Vac. Sci. Technol., A 1 (2), p. 1331, 1983

ACKNOWLEDGMENTS

We would like to thank Joe Bosco for his contributions to setting up PLC control, Ed Fitzgerald for assistance with seal development and Earl Marmar for guidance on ECDC procedures.

OPERATION OF THE ALCATOR C-MOD POWER SYSTEM

Stephen A. Fairfax, Joseph Daigle, Vincent Bertolino, Jeffrey Paranay, XiWen Zhong
MIT Plasma Fusion Center
190 Albany Street, Cambridge, MA 02139

ABSTRACT

The energy storage and power conversion system for Alcator C-MOD is designed to supply up to 500 MJ to the experiment at peak powers in excess of 300 MVA. The experiment requires flexibility in the control of magnet currents to achieve simultaneous shaping, ohmic drive, and position control with a small set of uncompensated PF magnets. The relatively modest budget and limited manpower make issues of maintenance and reliability extremely important to the eventual success of the experiment.

These requirements resulted in a power system design with many unique features. A total of 11 conversion systems power the 14 magnets of the tokamak to provide nearly complete flexibility in plasma shaping and control. Five thyristor circuit breakers are used to initiate the plasma. Four of the PF converters utilize circulating current configurations to maintain plasma position control as the magnet currents pass through zero. The TF converter incorporates transformer tap-changing circuitry to reduce alternator loads during peak demand periods. Many converters have solid-state fuse loss and conduction monitor circuits that allow continued operation when only 1 device in a parallel bank fails. The same circuits detect commutation failures and protect the converters from these potentially destructive faults.

Unique design features can sometimes lead to new and unforeseen problems in operation or maintenance. This report will discuss the initial operating experience of the Alcator C-MOD power system from preliminary acceptance testing through plasma operations. The performance of the thyristor circuit breakers, commutation and conduction monitor circuits, circulating current power supplies, and tap-changing TF supply will be presented and compared with expectations. The overall performance and reliability of the power system will be examined as well.

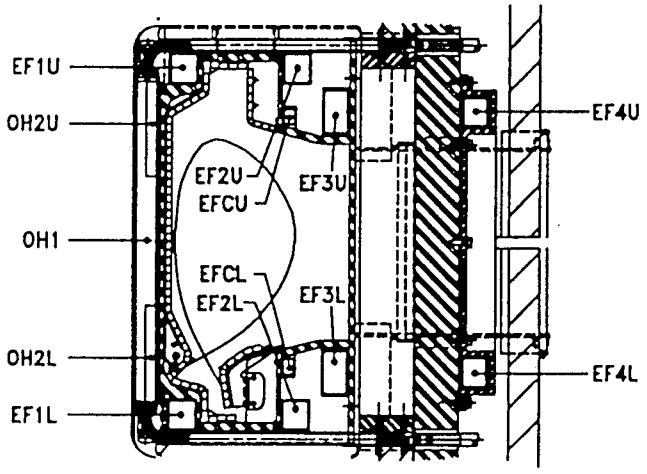

Figure 1

INTRODUCTION

Alcator C-MOD was originally proposed in 1985 [1]. After several reviews and some revisions [2], the project was approved in early 1987. Several aspects of the power systems design have been presented previously [3,4,5,6,7]. The tokamak core and power systems installation were completed in October 1991. The experiment has been in routine operation since April 1993, accumulating over 1500 plasma pulses at the time of writing. Power is provided by a 41-year old alternator/flywheel feeding custom converters.

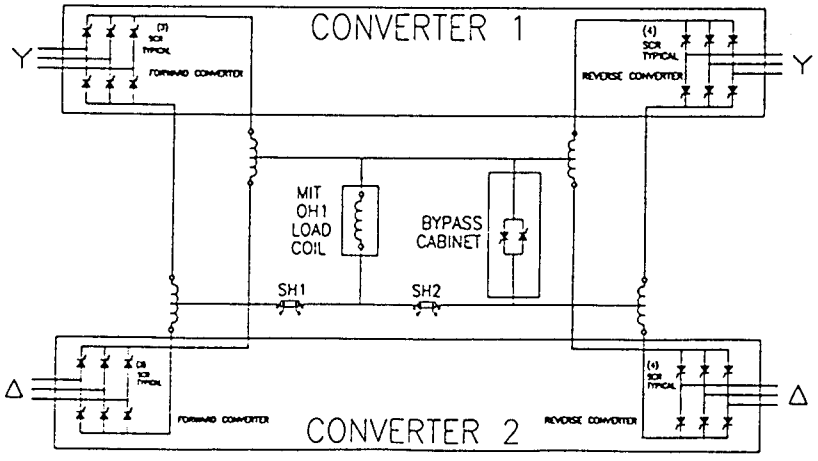

Figure 2

Supported by U.S. D.O.E. Contract No. DE-AC02-78ET51013

CIRCULATING CURRENT POWER SUPPLIES

Seven of the fourteen Alcator magnets require operation with reversing current. Figure 1 shows a cross section of the plasma chamber with the magnets identified. The OH1 magnet and EF4 series pair supply primarily Ohmic drive and vertical field, respectively. Other magnets, especially the EF3 pair, also provide these functions without the need for reversal. It is therefore permissible and economical to allow momentary interruptions in the flow of current to the OH1 and EF4 magnets. The power converters for these magnets utilize dual, opposite-polarity bridges as shown in Figure 2. Only one bridge at a time is enabled. Figure 3 shows voltage and current traces for a typical reverse current pulse in the OH1 power supply.

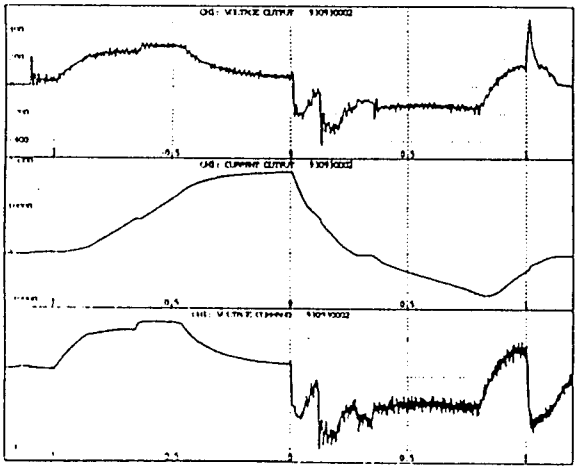

Figure 3

The four OH2 and EF1 magnets, play critical roles controlling vertical position and shape of the plasma. The currents in these magnets may not be interrupted during the plasma without risking a vertical disruption. The power supplies for these magnets are designed to circulate current through both bridges at all times. The circulating current is not actively regulated in these power supplies. The magnitude of the circulating current is limited by operating the opposing thyristor bridges at nearly identical output voltages. The voltage command to the bridges is biased to increase the circulating current when the load current is less than 15% of the maximum rated value. Figure 4 shows the load current and voltage traces in the OH2 power supply. Figure 5 shows the current in the forward and reverse bridges (the shaded area represents circulating current).

The circulating current and lockout dual converters were designed and built by Robicon, Pittsburgh PA [8], except for the EF4 unit, which was constructed at MIT from 5 TMX converters.

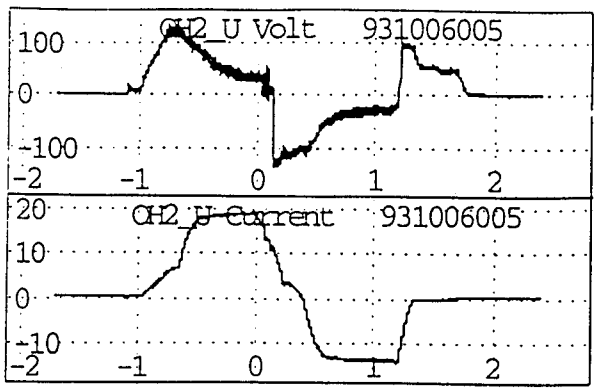

Figure 4

The reverse current bridges were enabled in September, 1993 after installation of extra reactance in the crowbar paths of each power supply. Bipolar output current requires a bipolar crowbar to protect the magnet and converter in the event of a gross malfunction during a pulse. Full-power testing showed that operation of the crowbar circuits would blow fuses in the bridge SCRs. The bridge SCR gate pulses are blocked when the crowbar is fired, so the bridge SCRs and fuses need to survive a single pulse of fault current. The reactance in series with the crowbar limits the magnitude of the fault pulse enough to prevent damage to either thyristors or fuses.

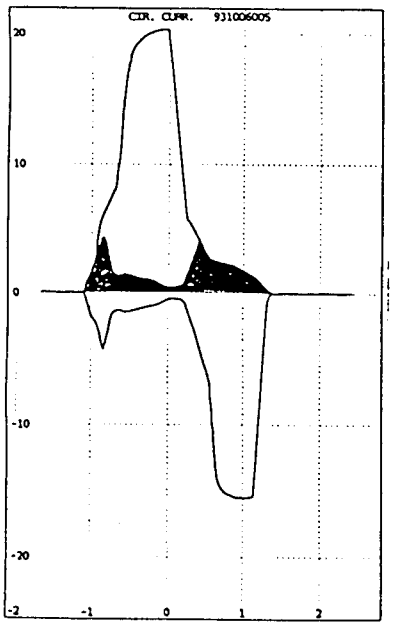

Figure 5

Thyristor Circuit Breakers

The thick, electrically continuous walls of the Alcator C-MOD vacuum chamber support the electromagnetic loads of the entire PF magnet set. Plasma start-up is best accomplished with relatively low voltage in order to limit the effects of eddy currents in the steel of the chamber and surrounding superstructure. Start-up voltages are still a factor of 4 or more above those required for normal operation. A total of 5 magnets require a brief pulse of high voltage to start the Alcator C-MOD plasma.

The number of magnet circuits requiring a pulse for plasma initiation make reliability and low maintenance a key attribute. The modest voltages (4 kV maximum in OH1) allow the use of solid-state rather than electromechanical interrupting elements. The design of these units has been adequately documented elsewhere [3,7]. The units have proven to be simple and reliable in operation. They have been operated to produce plasma nearly 1000 times since installed, with only a few failures in that interval. The switch SCR fuse rating in the 50 kA, 2 kV OH2 units was changed after several opened in normal service. The logic of the commutation and conduction monitor circuits was altered (see below.) No other change or service has been necessary.

Commutation and Conduction Monitor Circuits

The TF, OH1, and EF1 converters utilize a new and unique method of monitoring the operation of parallel SCRs in a pulsed bridge. Each parallel device is operated in series with a resistor sized to drop approximately 5 volts at maximum device operating current. The LED of an optocoupler is connected across this resistor. Any current pulse large enough to develop more than 2 volts across the resistor, turns on the LED. The optically isolated current pulses are compared with the gate pulses for that phase group. PROMs are programmed with acceptable current flow patterns so as to allow operation with 1 device not functioning long enough to complete the pulse in progress. Phase groups indicating 2 or more parallel paths malfunctioning cause the power supply to shut down immediately. Current flow not synchronized by gate pulses is indicative of commutation failure during inversion. This fault causes the bridge SCR gate pulses to be blocked and the crowbars to fire.

Each phase group's status is checked for each firing of its associated SCRs. The status signals are sent to auxiliary boards that qualify the signals based upon output current (the LED signals are not reliable below 30% rated output current), pulse start and end. Commutation failures are immediately flagged regardless of output current.

The circuits have worked well, particularly at preventing the destructive effects of commutation failures. The previous Alcator C TF converters lost hundreds of SCRs and fuses to the effects of single-phase operation resulting from commutation failures. The long L/R times of the cryogenically cooled Alcator magnets exacerbate the damage during these faults.

The commutation and conduction monitor circuits operate in a hostile electromagnetic environment. Full power testing resulted in changes to improve noise immunity. The power supply voltage command signals are slewed rapidly for plasma position control. It was necessary to change the initial design of the phase group circuits timing signals. The firing pulse for the next phase group is required in order to know when to expect the current to have been commutated out. These changes were challenging logistically because of the 108 printed circuit boards involved.

TMX power supplies

A rack of twelve TMX power supplies delivers current to EF2, EF4 and EFC magnets. Each TMX has been supplying 300V at 3KA and inverting reliably since start-up of C-MOD. Initially these power supplies were controlled with six SCRs on the primary side of the power transformer. During relatively fast changes in phase angle control, high AC currents were observed. The cause of this problem was found to be a characteristic of the phase-lock-loop gate drive circuit. When the delay command is changed, there is a momentary imbalance in the gate pulse lengths. This imbalance causes a net DC across the transformer primary and using a two-series-controlled-bridge configuration on the secondary alleviated the problem. Other benefits gained by this circuit are two quadrant capability and twelve-pulse ripple at any given output voltage.

The versatility of using a rack of small power supplies was proven earlier this year. A test required more voltage for the EF2 magnets. In a matter of hours, each source was changed from two TXMs in parallel to three in series. The original plan was that each power supply be a black box which could be connected to others in any configuration. Each box received its own command and delivered its own output. Sharing in both series and parallel configurations was a problem until a master regulator was developed. One master power supply now controls the SCR gates in up to two auxiliary power supplies.

Tap-changing TF Supply

The TF power supply was designed with tap-changing circuitry to reduce alternator load at peak toroidal fields while still providing acceptable current rise and fall times [9]. Two separate SCR bridges are implemented, one with 1550 VDC open-circuit output voltage, the other with 900 VDC. The "high tap" bridge carries the entire output current as it is raised from 0 to 150 kA. The high tap bridge is then gradually phased back so that both bridges conduct for output currents 150 to 220 kA. The low tap carries the output current during flat-top and when ever the output exceeds 220 kA. The transformers for the TF supply use extended delta primary

windings to achieve a $\pm 15^{0}$ phase shift for 12-pulse operation. This allows the secondaries to be tapped-Y windings. The only other complication of the tap-changing scheme lies in phase control during inversion and in SCR conduction monitoring circuits.

The auto-tap changing circuits have been tested extensively at currents up to 50 kA but have not been used as yet on the actual TF magnet. The reasons are logistical rather than technical. Present operation is almost exclusively at 5.3 Tesla, corresponding to 148 kA. The low-tap SCRs have adequate thermal capability for the full load current in this range. The small incremental effort to test the tap changing regulator circuitry with the actual load has been deferred in favor of work on the PF power supplies. The TF auto-tap changer is presently scheduled to be operated into the TF magnet the week of November 1, 1993.

VARISTOR PROTECTION NETWORKS

Silicon Carbide varistor networks are connected in parallel with each PF magnet. These networks provide passive protection of the magnets from excessive voltages. Each network is sized to handle the full stored energy of the associated magnet at design current. Silicon carbide varistors are preferable to zinc oxide in this application. Zinc oxide has a sharper "knee" in the I-V curve, corresponding to a higher exponent in the equation $I = k V^{n}$ that describes most varistors. The exponent for silicon carbide ranges from 4-5, while for zinc oxide it is generally 8-10. While the higher exponent provides more positive voltage limiting, it makes it very difficult to parallel devices. Silicon carbide is easily connected in parallel. Commercial units with 20 disks in parallel, rated for discharge energies of 500 kJ, are priced at roughly $1000/unit.

Each network is monitored by a Rogowski coil and magnetic reed switch. any significant current flowing through the protection network is automatically detected by a routine dispatched by the MDS-Plus data system after each shot. A warning message is sent to the engineering operator indicating which network is conducting and the peak current.

No gross failures have occurred in the PF system that required the varistors to dissipate all of the magnet's stored energy. There have been several cases where the varistors limited the applied voltage to a magnet. There has been no damage to the networks or problems associate with them.

GROUND FAULT FUSES AND MONITORING

Each magnet is grounded through a 20 amp, 5000 volt indicating fuse. The philosophy is to provide a ground on the magnet at all times, but not to allow large ground fault currents to flow. In the event of a ground fault, the fuse indication forces all power supplies to invert and then open the circuit breakers. This technique avoids the expense, maintenance, and failure modes of grounding switches rated for full power supply current. The system worked as planned when the EF3U magnet failed in operation [10].

CONCLUSION

The Alcator C-MOD power system utilizes a number of innovations to achieve high performance and reliability with minimal cost. The thyristor DC circuit breakers, conduction monitor circuits, and circulating current power supplies have all performed well in the first five months of operation. The best indicator of engineering system reliability is the number of plasma shots attempted and aborted. A total of 1549 plasma shots were attempted between May 1, and October 1, 1993. Only 77 shots failed due to engineering system problems. Power system trips were classified as the cause in 60 of these failures. The achievement of over 96% successful operation of 11 magnet power systems in the first five months of operation is a good indication that the basic design and philosophy is sound. The repairs and maintenance requirements of the power system have been minimal, allowing the staff to concentrate on increasing the capability of the system. We look forward to achieving even greater reliability as we gain experience with the system.

REFERENCES

[1] Alcator C-MOD Proposal, PFC-RR-85-18

[2] Addendum to Alcator C-MOD Proposal, PFC-RR-85-18

[3] Fairfax, S.A. "The Alcator C-MOD Power System," Power Engineering, October 1989, Knoxville, TN, pp1193-1196

[4] Fairfax, S.A. and Sueker, K.M., "Thyristor DC Circuit Breaker for Alcator C-MOD," and "Design and Construction of Thyristor DC Circuit Breakers for Alcator C-MOD", IEEE 14th Symposium on Fusion Energy, San Diego, CA October 1991, pp 542- 546

[5] Paranay, J., "TMX Power Supplies for Alcator C", IEEE 14th Symposium on Fusion Energy, San Diego, CA October 1991, pp 533

[6] Murphy, J. "Flywheel", IEEE 14th Symposium on Fusion Energy, San Diego, CA October 1991, pp 556

[7] Sueker, K.S. and Fairfax, S.A., "Construction of Alcator C-MOD Thyristor DC circuit Breakers," IEEE 14th Symposium on Fusion Energy, San Diego, CA October 1991, pp 546

[8] Robicon, Division of High Voltage Engineering Corporation, 100 Sagamore Hill Road, Pittsburgh, PA 15239

[9] Sueker, K.H, "Auto-tap Changing Power Supply for Alcator C-MOD," IEEE Symposium on Fusion Engineering, 1989 pp

[10] Fairfax, S.A., and Montgomery, D.B. "Anatomy of PF Magnet Failure in Alcator C-MOD", this conference.

RADIATION MEASUREMENTS FROM ALCATOR C-MOD INITIAL OPERATION

C. L. Fiore, T. P. Fuller†, R. L. Boivin, R. S. Granetz
Plasma Fusion Center
Massachusetts Institute of Technology
Cambridge, MA 02139

ABSTRACT

Operation of the Alcator C-Mod experiment, a compact high field tokamak, resumed in April, 1993. This experiment is ultimately expected to produce neutron rates of 5×10^{15} n/s for 1 second long pulses at 20 minute intervals. The radiation detection system is comprised of a number of components for examination of specific aspects of the resulting ionizing radiation fields. Six fission detectors and 2 BF_3 counters which are mounted inside two moderator stations are used for detecting the global neutron production on each shot. Environmental thermoluminescent detectors (TLD's), sensitive to both neutrons and γ-rays, are placed at distributed points both inside and outside of the facility. Self-reading dosimeters (SRD's), neutron bubble dosimeters, and film badges are also used to check the daily and monthly radiation production. Portable instrumentation capable of integrating the radiation signals from short pulse operation is available in order to survey biological shield penetration leakage. Tracerlab area monitors have been installed to measure the activated background levels in the test cell. Details of these systems are discussed, and the initial measurement results are presented.

INTRODUCTION

The Alcator C-Mod high performance tokamak experiment has recently begun operation at the MIT Plasma Fusion Center in Cambridge, MA. The experiment combines a compact design with high field operation (9T) [1] to achieve reactor relevant plasma operation. The experiment is designed to achieve densities of $1.5 \times 10^{21} m^{-3}$, and operate at temperatures in the 4-8 keV range. Neutron rates up to 5×10^{15} n/s are anticipated.

Measurement of ionizing radiation from the experiment must cover a wide range of types and intensities. During a tokamak pulse, for example, the dose rate could reach 20 Rem/s from neutrons and 1 R/s from x- and γ-radiation[2]. Dose rates produced in the test cell by bremsstrahlung of runaway electrons are expected to reach even higher levels, as has been observed in other tokamaks [3].

The neutron flux in the experimental cell will cause component activation in many of the surrounding structures. Once the neutron fluence begins to cause activation in the test cell, the area must be monitored for low level γ emission at all times so that personnel doses can be maintained as low as is reasonably achievable.

The purpose of this paper is to describe the elements of the ionizing radiation measurement systems used on Alcator C-Mod and to present the results from the current phase of operation.

SHIELDING CONFIGURATION

The experimental test cell is constructed from reinforced concrete. The walls are 1.5 m thick, the floor is 1.0 m and the ceiling is 1.2 m in order to attenuate the neutron and γ radiation produced by the experiment. During operation, access to the experimental cell is prohibited to within a minimum distance of 4.6 m outside of the cell concrete walls. The north wall abuts the power room, which is also restricted during operation.

The tokamak is surrounded by an igloo structure. It is constructed of concrete which contains boron frit as an aggregate. The resulting mix has 0.5% boron by weight. It is 0.6 m thick. There are large openings at each port used for diagnostic access.

NEUTRON MEASUREMENTS

The neutron diagnostic system for Alcator C-Mod is capable of measuring the total fusion yield over the full range of deuterium operation. The diagnostic was designed for a neutron source rate which could vary from 1×10^{11} n/s at $T_i = 1$keV and $\hat{n}_e = 1 \times 10^{20} m^{-3}$, to 1×10^{16} n/s for $T_i = 6.5$keV at $\hat{n}_e = 1 \times 10^{21} m^{-3}$[3]. To achieve this coverage with detectors operated in the count rate mode, four separate detectors located in each of two moderator stations are used. Three of these are fission chambers containing 1.68g, 0.075g and 0.004g U^{235} (93%) respectively. The fourth is a BF_3 long counter.

The detectors are distributed in two identical moderator stations, each of which is located in the vicinity of Alcator C-Mod as shown in Fig. 1. Moderator 1 (detectors 1-4) is placed on the floor underneath the center of the tokamak inside the igloo structure which surrounds the experiment. Moderator 2 (detectors 5-8) is placed at the horizontal midplane of the experiment near a large opening in the igloo structure which accommodates the toroidal field busswork. This position takes advantage of the increased neutron flux through the side port. Variations in the sensitivity caused by structural changes in

This work was supported by US DOE Contract No. DE-AC02-78ET51013. Manuscript submitted October 12, 1993.

†MIT Radiation Protection Office.

the area can be determined by comparison with the signal from the moderator station inside the igloo.

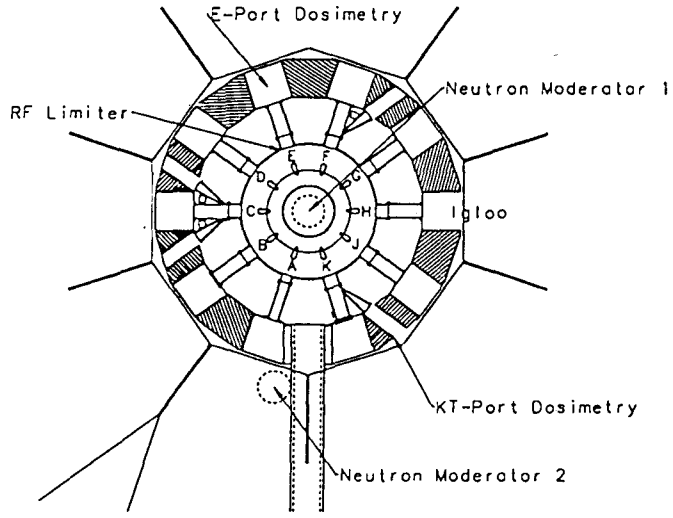

Fig. 1. Location of neutron detectors for Alcator C-Mod. The moderator shown in the center is located on the floor underneath the experiment. It contains channels 1-4. The second moderator is on the diagnostic stand near A-port and contains channels 5-8.

The most sensitive neutron detectors have been absolutely calibrated using an NIST traceable Cf^{252} source of strength 1.01×10^8 n/s as of the most recent calibration date. The least sensitive detectors will be calibrated from the more sensitive ones as higher neutron rates are achieved. Further description of this system and its calibration can be found in [4].

The neutron source rate as a function of time during the plasma pulse is readily obtained with resolution of 10 ms at source rates of 5×10^{10} n/s and above, as is demonstrated in a typical deuterium discharge in Fig. 2. The total neutron production for each shot is obtained and summed to provide a daily neutron inventory.

Bubble dosimeters (Siemens-Gammasonics)are used in addition to these neutron detectors in order to obtain a daily dose rate. These depend on a neutron induced phase change in a superheated liquid imbedded in a polymer to produce visible bubbles proportional to the human dose equivalent. They are insensitive to x- and γ-radiation. These are counted daily and reset.

Neutron and γ sensitive thermoluminescent dosimeters (TLD's) are located throughout the site to obtain monthly or quarterly neutron dose rate information.

A portable neutron monitor (SNOOPY) is used to check neutron rates from the Cf^{252}source used in calibrations and for checking shielding leakage.

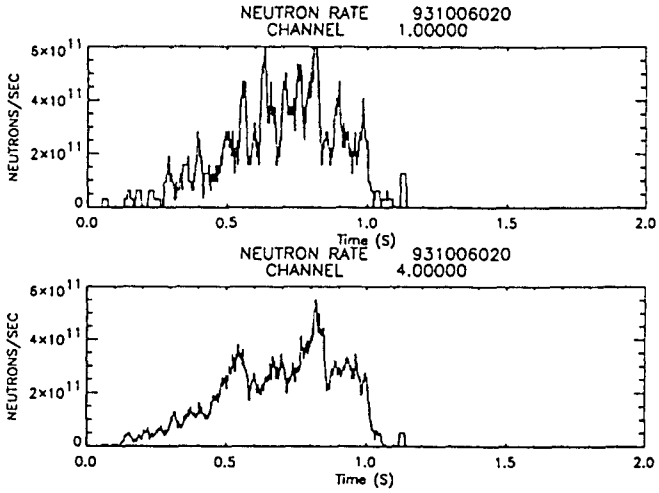

Fig. 2. Neutron rate as a function of time as measured on 2 of the neutron detectors. Channel 1 is a 1.68 g U^{235} fission chamber and channel 4 is a BF_3 detector. Both are located in a moderator station located directly under the center of Alcator C-Mod.

X- and γ- RADIATION DETECTION

The daily dose from x- and γ-radiation is monitored using self-reading dosimeters (SRD's) distributed around the Alcator C-Mod experimental cell, as shown in Fig. 3. Film badges which are read monthly are located at the same sites. The TLD's mentioned previously also measure the dose from x- and γ-radiation.

To date, the main source of ionizing radiation in the cell has been from bremsstrahlung x-rays produced by runaway electrons striking a limiter on port E of the tokamak. An uncalibrated NaI detector is used to monitor the time evolution and relative intensity of this radiation.

A Tracerlab area monitor system has been installed in the facility to monitor the basic ionizing radiation from activated machine and diagnostic components. Several hand held Frisker units and radiation meters are used to search for hot spots and contaminated areas. No activation has yet been detected outside of the experiment. It is expected that internal elements (particularly in the area of the limiter) will show some activation when they are accessed during the next major vacuum break.

RESULTS

A. Neutrons

The first plasma currents in excess of 300 kA of this run period were produced in late May of 1993. Operation proceeded in hydrogen gas until August 19, when the first deuterium gas was introduced. There was only one day of deuterium operation in August.

Photo-neutrons (produced by γ,n reactions near the limiter) were observed by the neutron detectors and bubble dosimeters when hard x-rays resulting from runaway electron bremsstrahlung were produced. These result in

an asymmetry in the bubble-dosimeter readings between the E-port and KT-port locations, since the rf limiter is located on E-port. The KT-port location is on the opposite side of the tokamak from the limiter. There is also a difference of a factor of 2 in the apparent neutron rate measured from the two neutron moderator stations because of the localized source. This can be seen in Fig. 3, which compares the neutron rate from ahard x-ray dominated hydrogen discharge obtained from the neutron moderator station underneath the igloo (Channel 4) to that measured on the midplane side (Channel 5).

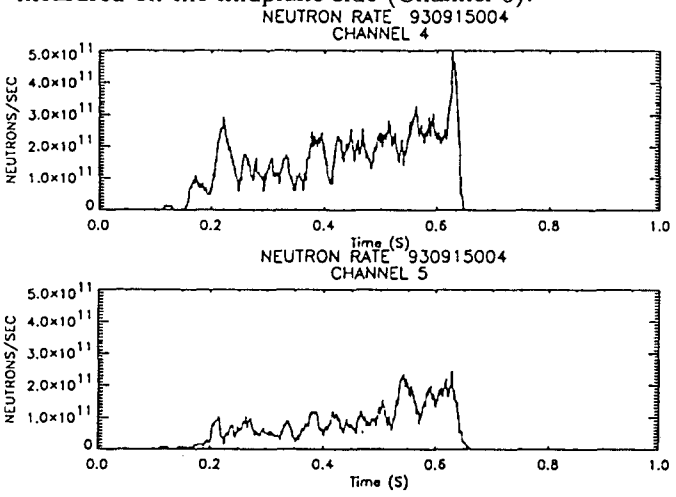

Fig. 3. Comparison of neutron rate obtained from side and bottom neutron detectors during a runaway electron dominated hydrogen discharge. The difference indicates that the photo-neutron source is localized.

Typically, the apparent neutron rate measured from photo-neutrons produced during runaway electron dominated discharges is of the same magnitude or larger than that observed from well behaved deuterium plasmas. It is therefore important to establish that runaway electrons are not present before utilizing the global neutron measurement in further analysis of the physics data. These photo-neutrons, however, contribute to the measured dose rates in and around the experiment, to component activation, and to the experimental neutron budget. Establishing an actual rate of production of these is difficult because their energy distribution is unknown. (All calibrations have been done with a Cf^{252}source which has an energy distribution similar to a D-D fusion spectrum.)

The total measured neutron production for the deuterium operation in September is 1.01×10^{13}. The expected cell neutron dose rate which was calculated in [2] for a neutron production of 5 $\times 10^{15}$ neutrons is 20,000 mRem. Thus the expected in cell neutron dose from the month of September is 40 mRem. The neutron dose rate determined from the bubble dosimeter on E-port was 46 mRem (Table II). The KT dose rate was only 14 mRem for the same period. The discrepancy is qualitatively consistent with the assumption that half of the neutron total results from photo- neutrons produced near E-port. The KT port bubble dosimeter is located in a small opening in the concrete igloo, so that the observed neutron dose is more collimated than at the other location and consequently less sensitive to scattered neutrons.

The γ dose calculated in [2], primarily resulting from n,γ reactions in the structures surrounding the experiment, would have resulted in a dose of 2 mRem from this neutron inventory.

B. Ionizing Radiation Dose Measurements

The location of the dosimetry measurements in the Alcator C-Mod cell is shown in Fig. 4. In addition to these, TLD's are located throughout the site, both inside and outside of the building. No measurements above background have been observed outside of the experimental cell to date.

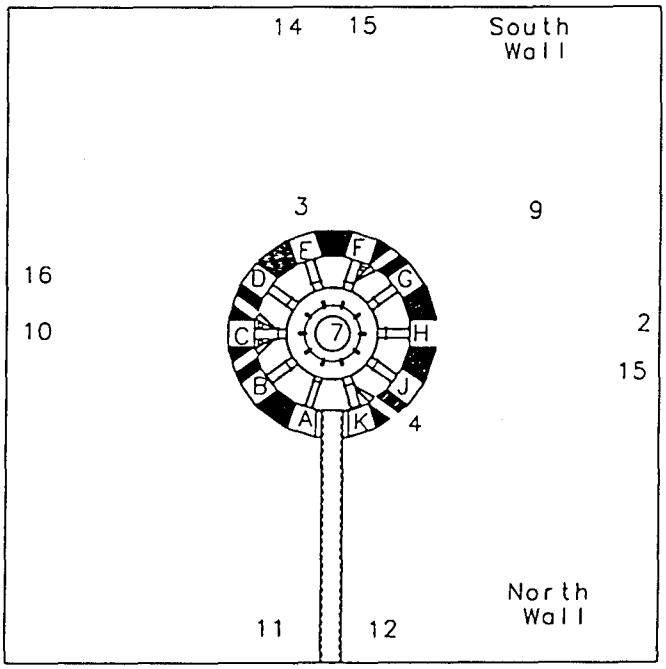

Fig. 4. Location of dosimetry for radiation measurements listed in Tables I. and II. The drawing is to scale, with the cell walls 15.25 m on each side.

The cell dose rates are presented in Table I, as measured by several types of dosimeters. The bubble dosimeters were not added until July 15, so they do not represent the full neutron dose rate for this operating period. Neutron sensitive TLD's were co-located with the γ sensitive TLD's, but due to continuing problems with algorithm development, the initial readings are erratic and not considered to be reliable indicators of the area dose rates.

Only 1 day of deuterium operation occured during this period, which contributed less than 2 mRem to the

dose measured by the bubble dosimeters. The remaining neutron dose is from photo-neutron production. This is responsible for the large difference in magnitude between the E-port and KT port measurements.

The asymmetry of the x- and γ-ray radiation measurements also results from the bremsstrahlung from runaway electron production. There is a factor of 10 difference between the dose rates measured on E-port compared to those on KT-port. Similarly the dose rates measured on the East and South walls are higher than those on the North and West.

Table I. Alcator C-Mod Dose Rates (mR)
5/15/93 to 8/31/93

Location	SRD mR	Film mRem	Bubble mRem	TLD(γ) mRem
1 Control Room	56	min.	-	min.
2 West Wall	78	40	-	21
3 E Port	19,295	14,050	337	-
4 KT Port	2,402	2,020	32	-
5 Room 156C	48	min.	-	min.
6 Power Room	47	min.	-	-
7 Under Igloo	168	50	-	-
8 Room 156B	66	min.	-	min.
9 G-Stand	329	310	-	-
10 East Wall (U)	223	120	-	191
11 North Wall (L)	-	-	-	24
12 North Wall (U)	-	-	-	77
13 West Wall (U)	-	-	-	77
14 South Wall (L)	-	-	-	135
15 South Wall (U)	-	-	-	174
16 East Wall (L)	-	-	-	73
17 Room 156A	-	-	-	min.
18 Room 156D	-	-	-	min.

The results from the operation in September are listed in Table II. Operation commenced after a short break on September 15. Of 11 operating days (runs), 6 were done using deuterium. The measured dose rates continued to be dominated by radiation from bremsstrahlung of runaway electrons. As was indicated in the previous section, the γ dose rate expected from the observed level of neutron production was only 2 mRem. The TLD(γ) measurements were not available for the September operation.

The SRD measurements for KT port occasionally included offscale readings, which results in underreporting of the dose from this dosimeter. The TLD detectors were not read at exactly the same intervals as the film and the SRD's, which results in some discrepancies in the reported doses.

Table II. Alcator C-Mod Dose Rates (mR)
9/1/93 to 9/30/93

Location	SRD mR	Film mRem	Bubble mRem
1 Control Room	35	min.	-
2 West Wall	30	10	-
3 E Port	6,551	4,530	46
4 KT Port	895	1850	14
5 Rm 156C	40	min.	-
6 Power Room	15	min.	-
7 Under Igloo	0	min.	-
8 156B	10	min.	-
9 G-Stand	65	180	-
10 East Wall	41	50	-

CONCLUSIONS

Measurements of the ionizing radiation from the Alcator C-Mod experiment indicate that the dose rates from the current level of operation result primarily from the bremsstrahlung of runaway electrons at a limiter which was installed to protect the rf antenna. Neutrons are a minimal contributor to the operational doses at this time. The thermal neutron production is currently 4 orders of magnitude lower than that which is expected when the experiment reaches full power operation. No dose rates above background have been observed outside of the experimental cell.

ACKNOWLEDGMENTS

The authors wish to acknowledge the assistance of Joe McCormick and John Mumley at the MIT Bates Linear Accelerator for operation of the TLD program. They also thank Earl Marmar for installing and operating the uncalibrated hard x-ray detector.

REFERENCES

[1] S. Fairfax, Alcator Group, "Start-up and Early Results from Alcator C-Mod.", this meeting.

[2] C. L. Fiore, "Alcator C-MOD Final Safety Analysis", PFC/RR-89-8, June, 1989.

[3] H. Knoepfel and D. A. Spong, "Runaway Electrons in Toroidal Discharges", Nuclear Fusion 19, (1979) p.785.

[4] C. L. Fiore, R. Boivin, R. S. Granetz, T. Fuller, and C. Kurz, "Status of the Neuron Diagnostic Experiment for Alcator C-Mod", Rev. Sci. Instrum. 63, (October, 1992) p.4530.

DEVELOPMENT OF HIGH STRENGTH ELECTRICAL CONNECTIONS USING COPPER ELECTRODEPOSITION

E. Fitzgerald, C.T.Reddy
Plasma Fusion Center
Massachusetts Institute of Technology
Cambridge, MA 02139

ABSTRACT

The poloidal field coils on the Alcator C-Mod Tokamak are manufactured from C107 or C110 half hard copper strip. A copper C10100 flag is joined to the ends of the coil turns in order to transfer the current from the coaxial leads. The coil design requires that any joint made between the flag and the coil turn be as strong, statically and in fatigue, as the coil strip. Standard methods such as welding, brazing and hard soldering would reduce the tensile strength by annealing the copper in the area of the joint. A soft solder connection with a full lap joint was not considered due to a premature failure in an initial test. In investigating alternative joining methods, tests were performed on samples of electrodeposited copper provided by the A.J. Tuck Co., of Brookfield, Connecticut. The tests showed that the joint met C-Mod structural specifications at 77K. Encouraged by these results, M.I.T., embarked on a testing program involving electroformed butt joints. Through an extensive engineering program, reliable electroformed joints were obtained in production. The production engineering involved the construction of a special facility to control the process parameters. Details are presented here for duplicating this facility.

INTRODUCTION

Electrodeposition is not new [1]. The application of ED in high strength joints is. Producing these joints required close cooperation between M.I.T., and the A.J. Tuck company. In order to produce reliable connections on the Alcator C-mod PF coils, systems engineering of a new facility was required. These systems included: preparation of the coils and flags for joining, design and fabrication of an ED facility, implementing process control procedures, production of the joints under quality control, inspection procedures, and finally return of coils to M.I.T., for final inspection before installation. After completing the new facility and implementing the new production techniques, the coils were shipped to the Tuck company.

The details of electrodeposition are not proprietary, but the chemical composition of the plating bath is. It is not necessary to know the fluid composition in order to use it in a well controlled process to produce a joint with desirable electrical and mechanical properties.

PRODUCTION PROCESS

The preparation for the electroforming process involves immersing the copper joint in various liquid solutions. The results from earlier testing concluded that the best method to electroform the joint was in a vertical position. As a result of this we were now required to design a containment system with an integral seal to accept the copper coil and to prevent the leakage of the various solutions. Neoprene rubber was the best choice for the seal material because of its chemical resistance and its durometer. Two designs were prototyped and tested. The most user friendly seal was chosen and refined. The tanks and the other major components were also made of chemically resistant materials including polypropylene and stainless steel. The tanks were redesigned to accept the neoprene seals. The process also required that there be enough room in the tanks for a bagged titanium basket to hold the copper anode briquettes, a quartz immersion heater and an air sparger. This air sparger aids in mixing the copper sulfate solution and by directing the airflow over the surface being plated to help eliminate the hydrogen bubbles released at the cathode.

By gathering information about the process from A.J.Tuck, we were able to replace the large tanks used in the initial cleaning process with a much smaller funnel tank. This not only increased reaction time, but also decreased the volume of hazardous material handled by personnel. The weights of the coils ranged from 300 lbs up to 1700 lbs and their diameters ranged from 2.8 ft. to 6.35 ft.. To minimize damage to the coils we chose to position the coil with an automotive engine lift and move the solutions to the positions they were needed. This was accomplished with a hydraulic lift table rolling on a track assembly. The track system insured precise positioning while maintaining a level solution surface. A solution pump was used to transfer the plating solution from the main reservoir to the smaller tanks. Once the position was set and locked, the hydraulic table raised the solution until the seals were engaged and the joint assembly was fully immersed in copper sulfate.

A temporary e-forming facility had to be designed and fabricated on site because the larger coils would not fit through the access doors of the A.J.Tuck company. A prefabricated building approximately 10' x 20' was purchased and delivered to the company. The building was then modified to accommodate the major components needed to complete the high strength electroformed joints. The necessities for the e-forming process are deionized water, electricity, pressurized filtered air, and a controlled heat source. These were incorporated into the design from the outset. This facility had to meet strict environmental guidelines in order to prevent ground contamination. Actions were immediately implemented to prevent chemical spills. These included catch basins around all the plating tanks as well as chemical resistant paints and sealers applied to the flooring surfaces. Safety precautions such as eye wash stations, goggles, aprons and gloves were available and worn by all personnel involved.

MANFACTURING TECHNIQUES

The coil and the flag were machined to a taper of 150 degrees. Tapers less than 90 degrees should be avoided because planes of weakness develop at the junction of the crystals growing from the sides of the materials being joined. This corresponds to a report by J.W. Dini of the Lawrence Livermore National Laboratory that suggested that parts being joined by electrodeposition be machined with a taper of at least 120 degrees and preferably greater [2]. The following steps were then taken to insure each coil was prepared and manufactured within the control parameters agreed upon between M.I.T., and the A.J. Tuck Company. The temporary joint was fabricated according to the process described below. The inner and outer flags had to be positioned on the coil at the same point, and opposite each other. The coax block is then mounted between them. In order to get precise alignment a dummy coax block was used and clamped to the coil. Alignment and curvature of the flags relative to the coil material was now acceptable. The coil was cut with a 15 degree taper using a miniature vertical milling machine. The flag was placed on the alignment jig and marked for cutting. A second mark was scribed approximately .100 inches behind the first. Through empirical observation a space about five times the thickness of the material is provided for the ED copper to grow. This provides a void of about .170 inches between the coil material and the flag. Mill the flag at the second line with a 15 degree angle. The ends of the flag and coil turn should be turned down to a knife edge to provide good electrical contact to the copper tape interface and to provide .020 growth on the back of the joint. The growth and any contamination in this region is then removed during the finishing process. The coil turn and the flag now have a space of .170 inches. We now had to develop a temporary joint that would be electrically conductive, didn't contaminate the solution, and was strong enough to be forced through the seals. We designed a multi-layer system consisting of a stainless steel plate for strength, conductive epoxy for bonding the stainless to the copper and a copper tape interface to prevent epoxy contamination in the joint. An alignment jig was used to insure the coil and flag were in parallel to each other during the epoxy set up. After the epoxy has set up, vinyl tape is applied to any copper that will be exposed to the plating solution except for the 1/2 inch exposed joint. A final cleaning is then performed prior to the electrodeposition process.

Our primary analytical tool for monitoring the copper sulfate bath was the Hull cell test. The Hull cell test consists of a miniature plating tank which uses a sample of the solution to copper plate a brass coupon. Visual inspection of the plated sample provides an indication of the range of the bath as well as a qualitative analysis of brighteners (organic additives). This test will also reveal any solution contamination. The brightener additives account for the mechanical strength of the plated copper. The area of the joint to be plated was calculated based on a current density of .03 amps/sq. cm.. The power supply is then adjusted to the calculated current. Repeat the Hull cell test after the solution transfer to the plating tank. The following procedure was developed and resulted in the successful fabrication of sixteen high strength joints. The electroform cleaning and activation sequence is presented here.

1. A minimum of four people is necessary to start the process.
2. The copper sulfate tank must be on the drip pan with the drain tub.
3. Burnish the neoprene seals on the plating tank, this helps to ease the coil and flag terminal through them.
4. Transfer the copper sulfate plating solution from the reservoir to the plating tank.
5. Connect an electrical wire to the flag, have a flag to coil jumper wire available.
6. Scrub joint to be electroformed with a toothbrush and potash/detergent mix.
7. Connect PVC container to flag/coil (make sure flag/coil bottoms out on seals.
8. Tighten hose clamp on top of PVC container.
9. Close valve on the PVC container.
10. Fill PVC container with deionized water (check for leaks, small leaks are ok).
11. Drain PVC container valve.
12. Set up power supply and ammeter.
13. Fill PVC container with hot alkaline electrolytic cleaner.
14. Place alkaline electrolytic cleaner bucket under PVC container.
15. Install reverse current electrode, set power supply to 6 volts.
16. Agitate cleaner mixture with the electrode for 40 seconds.

17. Drain alkaline electrolytic cleaner into bucket.

18. Rinse with deionized water.

19. Reverse electrical leads, preset rectifier to .8-1.0 amperes into a dead short.

20. Spray joint with 50% HCL solution.

21. Rinse with deionized water.

22. Close PVC container valve.

23. Place copper activator drain tub under PVC container.

24. Fill PVC container with copper activator (approximately two liters).

25. Time for 40 seconds.

26. Drain copper activator into tub.

27. Close PVC container valve.

28. Rinse with deionized water.

29. Drain, remove PVC container.

30. Spray joint with 10% sulfuric acid solution, continue spraying until joint is immersed in plating bath.

31. Start raising tank on lift table.

32. Two people guide flag/coil into seals.

If time elapsed after draining copper activator solution to immersion in plating bath exceeds 60 seconds then we must stop the plating and repeat the copper activation procedure. If the activation process is O.K. then the plating bath is tested. Plating the flag/coil joint takes approximately six days to have the proper thickness of copper plate.

Quality Assurance Tests

Daily Hull cell tests were performed on the plating tanks. Solution adds made in accordance with Hull cell test results. Daily visual inspection of the copper growth and temperature readings were recorded. Current density and air sparger location were also closely monitored. After full growth was complete and excess copper was removed from the joint area a dye penetrant test was performed. This is followed by an ultrasound inspection. If all these conditions were satisfied then the coil was prepared for shipment.

REFERENCES

[1] Metal Finishing Guidebook and Directory, 1993.

[2] Joining by Plating, J.W. Dini, Lawrence Livermore National Laboratory Livermore, CA 94550.

GROUND FAULT MONITORING IN ALCATOR C-MOD

David Flanary
Consultant to the Plasma Fusion Center*
Massachusetts Institute of Technology
Cambridge, MA 02139

ABSTRACT

The Alcator C-MOD tokamak has a complex AC power distribution system to power diagnostic equipment, magnet power, vacuum, heating, and cryogenic control. During a 9 Tesla pulse, the existence of ground loops between these systems can cause damage or compromise the performance of the associated equipment. The real-time detection of these ground loops in the grounding system is crucial to the productive operation of the tokamak.

The ground fault monitor is capable of detecting ground loops with an impedance as high as 10KΩ. This monitoring system utilizes current transformers and a multiplexed driver/sensor architecture to monitor each of the 20 ground lines that are connected to a star point ground in the C-MOD cell. Continuous monitoring is accomplished without breaking ground wire connections. The star ground cable to earth ground is monitored to detect ground leakage paths that circumvent the star ground point.

A synchronous demodulator circuit is utilized to detect the driver signal in a noisy environment and in the presence of 60 Hz leakage current. The detector output is linear for fault impedance values in the range of 100KΩ to 100Ω. The detection of 60 Hz leakage current is possible with the use of an alternate measurement mode.

The monitor runs continuously to detect faults as they occur. Outputs are monitored in the control room via a fiber optic interface. Control room functionality includes data logging of fault conditions, overrides, and alarms. A manual operating mode and instrument rack display panel can be utilized by the operator for tracking down ground faults. A diagnostic circuit is available to perform a "self-test" function, which verifies proper monitor operation and locates defective circuitry down to the component level.

BACKGROUND

The "star point" ground system in Alcator C-MOD is designed to eliminate ground loops (faults). The traditional method of checking for ground faults is to disconnect individual ground lines from the ground terminal at the star point and, using an ohmmeter, measure the resistance to earth ground. The value measured is the resistance value of the ground loop. Each ground line has to be measured seperately. This process is both time consuming and dangerous. Disconnecting the ground lines poses a potentially lethal situation to the technician assigned to the task. A faulty circuit could introduce line voltage onto the ground line. If the technician were lucky, one ground fault would be present at a single time. Identical resistance readings would be present on the two grounds. At this time the operations personnel would search the cell area served by these grounds in search of the connection that was causing the ground loop. A review of the activity in that area would further locate where the offending ground connection could have been introduced.

Anyone familiar with this process would understand the need for a monitoring system that could detect ground faults as they occur, without human interaction, and leaving the ground wiring intact.

Some ground faults are of a relatively simple nature, such as having two instrument racks in different sections of the platform being connected to each other with shielded coaxial cables. Many ground faults are difficult to detect. Heater elements inside the vacuum vessel would occasionally short to the vessel wall. Aluminum foil insulation can create intermittent connections between grounds.

In addition to ground faults occurring between the power sections of the cell, there could also be ground loops between the section ground and earth ground, circumventing the star point. A common problem is having instrumentation contacting the aluminum trough covers, which are earth grounded. Other paths could be found by connecting to "house power" in the experiment labs adjacent to the cell or in the bottom of the cell. The potential for faults that bypass the star point require that the monitor also check the earth ground connection for ground loops.

The original requirements specification for the monitor called for the detection of ground faults between the vacuum vessel, the TF magnet, major engineering and diagnostic systems, and each section of the diagnostic stand. Ground lines are brought from each of these components of the tokamak cell to a star point which is connected to earth ground. Faults as small as 10K ohms were to be detected. A PLC interface would report faults at the control room.

The design of the ground fault monitor was begun in December, 1992. The basic concept of the design was to use a method of AC coupling a sine wave signal into a ground line and detecting the signal current. The flow of current means a conductive path is present. This basic method had been used on the tokamak at the Lawrence Livermore Lab.[1] A limited amount of documentation was available from this project, but it served as a starting point for the design.

An experimental circuit was built and demonstrated by the end of December. This breadboard circuit monitored one ground line only. Alcator was scheduled to be reassembled in late February, 1993. It was determined that the primary

need during the reassembly was to have the "machine" (vacuum vessel) ground monitored more than any other ground line. As an interim measure, the breadboard circuit was installed on the machine ground. A simple threshhold comparator circuit on the sensor output detected a fault condition which sounded an audible alarm immediately upon the connection of a ground fault. This loud chime soon became a familiar sound to those working in the cell.

The design of the full scale monitoring system utilizes design and assembly techniques that are beneficial to the task of simultaneous designing and building. A standard electronic instrument packaging system that was designed for other Alcator projects was utilized that included a Eurocard backplane and an I/O panel for signal distribution[2]. It was decided to wirewrap the pc boards on commercially available 6U size vector boards. This allowed for changes in the design without having to deal with the excessive lead times involved with pc board layout and fabrication. The digital logic circuits were designed using the standard 22V10 programmable logic devices (PLD) and CUPL software that helped reduce circuit size, minimize assembly time and improve documentation.[3] Netlists generated by a schematic capture program were used by the technicians in wirewrapping the circuits. The result was a very low number of errors in the assembly process. All of the electronic components are housed in a standard 19 in. instrument rack.

ANALOG CIRCUIT DESCRIPTION

The ground fault monitor must be capable of performing the basic function of making resistance measurements between ground lines which are all connected to each other at one end, the star point. Measurements must be made while leaving the ground connections intact, and comply with electric wiring codes. One method to accomplish this is to drive an AC voltage onto a ground line with a transformer and sense that driven AC current with a current sensing transformer (see fig. 1).

In order for the monitor to operate in the range desired (detecting faults from a short circuit down to 10KΩ), a number of factors had to be considered in the analog circuit design:

- Driver CT turns ratio
- Driver signal amplitude
- Sensor CT turns ratio
- Sensor Amplifier Gain
- PLC A/D converter input range and resolution

The AC driver function is accomplished with a commercially available current transformer (CT), normally used for measuring AC current. Using a CT allows the ground wire to pass through the center core of the transformer with no discontinuity or added interconnect that would violate electrical codes.

The driver circuit uses a 1 KHz sine wave to act as a driver signal. The choice of this frequency was somewhat arbitrary. The important factor was that it be significantly higher than 60 Hz so that it can be differentiated from leakage current. A higher frequency may cause problems with radiating noise in the electrical system. This frequency is compatible with the CT used for the driver and the sensor. A low turns ratio for the driver CT is desired so that the voltage level from the driver isn't reduced more than necessary. A GE 200:5 (40:1 ratio) CT was chosen. The maximum output of the driver amplifier circuit using standard 24 volt power supplies is +/-20V. This voltage and turns ratio results in a $1V_{p-p}$ signal on the ground line. The CT acts as a voltage source with the current in the ground line being a function of the fault resistance. The drive signal must not be too large or else the resulting voltage induced on the ground line would interfere with the instrumentation connected to that line.

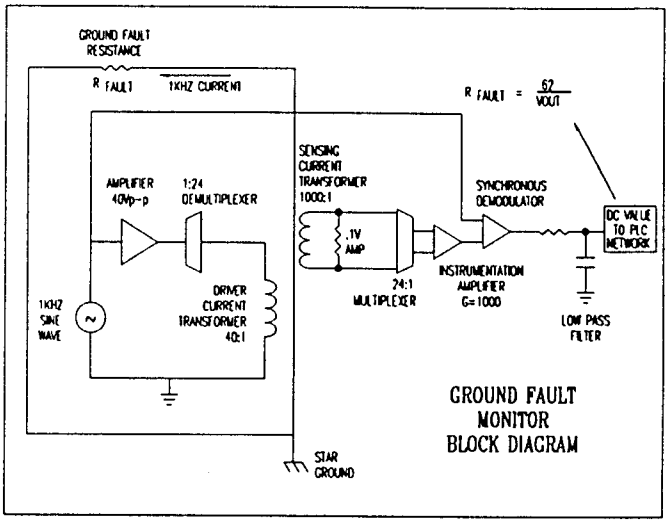

fig. 1 Functional Block Diagram

An amplitude stable oscillator, which is required for accurate measurements, generates the sine wave which drives a high voltage, high current op-amp. The op-amp output is current limited to 400 mA_{p-p} to prevent destruction of the device, and/or the multiplexor switches, which could occur if the oscillator were to fail and the op-amp would drive the inductive load of the CT with a DC current. With this current limit value, the output waveform does not start to clip until the fault resistance is less than 0.5Ω, a value which is not a factor in the electrical system with long wire lengths and resistive interconnects. When the op-amp drives a pure inductive load, the output can oscillate at high frequency. To increase stability, a capacitive load was added to match the inductive load. A small series resistance was also added.

One driver circuit is used to drive a total of 24 different ground lines. This requires a multiplexor that is robust enough to handle the voltage and current output of the amplifier. A small (8 pin DIP) package "Photo Voltaic

Relay" is used. An array of these devices performs the switching from channel to channel. These devices have optically coupled TTL compatible inputs for control. The presense of a large current in a ground line could induce a high voltage on the driver side of the CT. This possibly destructive situation is eliminated with the use of an MOV device at the CT terminals to suppress any transients.

A sensor CT is in series with the driver CT on each ground line. It has a 1000:1 turns ratio and calls for a 100 ohm burden resistor in parallel with the winding, which creates a current to voltage converter with a ratio of .1Volt/Amp.

The 100 ohm burden resistor, the CT, and two diodes for over-voltage protection are mounted to a PC board. 24 of these boards, along with 24 driver CTs are mounted to a wall-mounted panel between the power cable duct and the star point.

The 2 wire sensor output is brought to the instrument rack via shielded cable. The shield is grounded at the backplane only. This signal goes through a 24:1 differential multiplexor before reaching the instrumentation amp, which has high gain, very high input impedance, and a high common mode rejection ratio. The sensor signal can be as small as 10μV for a 10KΩ fault resistance. This voltage is generated by the sensor CT from a current of 100 nA. As the input bias current of the instrumentation amp (AD624C) can typically run at 15 nA, extra care must be taken to ensure that the input nodes of the amplifier have equal dc paths to ground so that the bias currents do not flow through the 100 ohm burden resistor and the resistance of the multiplexor. The difference between the bias currents is the input offset current which, when flowing through the source resistance, results in a voltage offset. At a gain of 1000, the input offset voltage must be kept to a minimum. Lowpass filtering at the input must use small capacitance values to prevent phase shifting.

The sensed signal requires a means of filtering that will eliminate all but the 1 KHz drive signal. A problem with this method is that all AC current will be sensed by the sensing transformer, including 60 Hz noise which can be many orders of magnitude larger than the AC drive signal.The amplified signal goes to the AD630 synchronous demodulator where it is demodulated by using the driver as a sync signal. In order for the driver signal to be in sync with the sensor signal, there must be no phase shift. Phase shift can be caused by having a reactive load in the sensing path. This is one reason why extra care must be taken in design the sensor/mux circuit. Capacitance between ground lines is a situation that cannot be removed as easily. The heating elements lining the vacuum vessel walls caused approximately 2μf capacitance between the heater ground and the vessel ground. There was also a phase shift on the "earth" ground line. These phase shifts are corrected using a channel selectable phase shifter that utilizes a PLD and analog switches to decode the mux address into switch settings that can place the correct RC value into a phase shift circuit. Figure 2 shows the output of the amplifier (top) and the output of the demodulator (bottom) with a 1KΩ fault present.

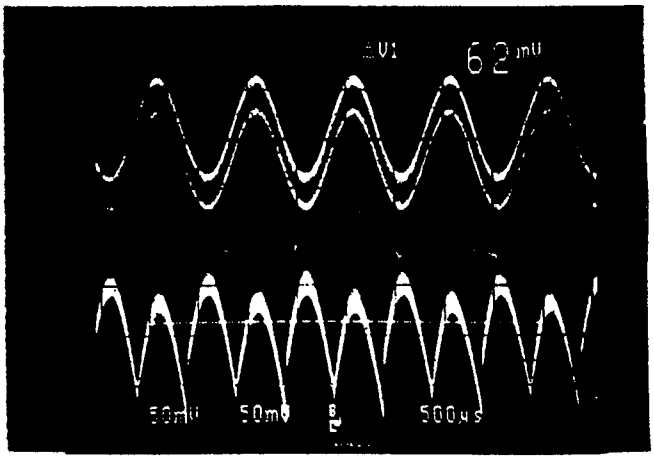

fig. 2 Amplifier (top), Demodulator (bottom) outputs

The AD630 output is filtered by a lowpass filter to create a dc voltage. The fault resistance is computed with the equation:

$$R_{fault} = \frac{62}{V_{out}}$$

This function is valid for faults ranging from 30 Ω down to 100KΩ. At 100K, a high precision meter is required. The specification has been degraded to 10KΩ to as an error margin.

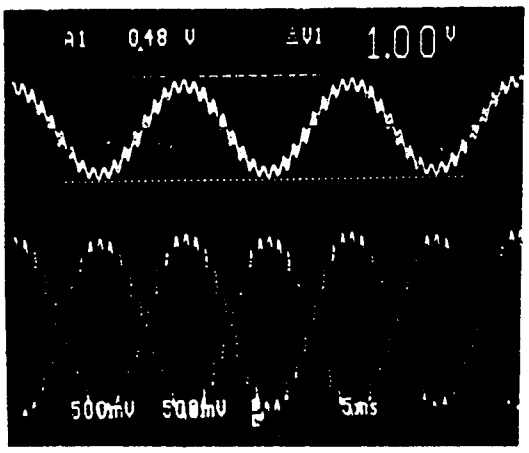

fig. 3 60 Hz noise, 1Vp-p, with a 1KΩ fault

This signal is further amplified to fit the dynamic range of the A/D converter in the PLC. Fig. 3 shows the effect of a 10 mA 60 Hz fault current at the output of the demodulator. The 60 Hz noise is seen as an ac signal by the filter and is cancelled out, leaving only the 1KHz driver signal. For

manual operation, the output goes to a terminal for connection to a DVM for measurement. If the measurement of a 60 Hz leakage current were needed, an RMS-DC converter (AD637) is connected to the output of the AD624. This value can be read by the PLC or by a DVM.

A portable wand has been designed to pinpoint the location of ground faults. This device consists of a clamp-on current probe, an amplifier, and a band-pass filter tuned to 1KHz. An audio output stage signals the presence of the fault current on the suspected cable. The monitor is placed in "Manual" mode and the faulted line is selected so that the 1KHz signal is continuous.

PLC INTERFACE/DIGITAL CONTROL

The monitor can be controlled by two different means, via either PLC control, or manually from the instrument rack control panel. PLC control allows for automatic operation from the control room. Three Allen-Bradley PLCs are used to supply digital I/O and analog measurement. The analog input PLC performs a 14 bit A/D conversion on the output signal of the sensor. Other analog inputs are used for diagnostic purposes such as monitoring the oscillator output, driver amplifier, amplitude, and ground line 60 Hz leakage current.

Two digital I/O PLCs perform:

- addressing for the driver and sensor channel multiplexors
- control the status indicator LED display
- receive switch setting inputs from the display panel
- control diagnostic tests

These PLCs are located in the monitor instrument rack. A fiber optic link is used to interface with the control room.

A monitoring program runs continuously, testing each ground line. A program operating in the Paragon Control system interprets this information. The measured voltage is converted to an equivalent ground fault resistance value and compared to two sets of limits: a warning level, and a critical level. The critical level is reached when a fault is less than 1000Ω. At this point, an audible alarm sounds. The threshhold limits can be changed for each ground line. This data is displayed on one of the PCs in the control room (fig. 4). The display shows a list of the ground lines, its measured fault impedance, and alarm status.

The monitor circuitry utilizes PLDs for the digital logic functions such as decoding the 5 bit address from the PLC, and controlling the display panel. All digital logic runs at a low clock frequency so that no high frequency noise would interfere with the analog circuit. The PLD logic is most important in the operation of the display panel. This panel is a display with different color-coded LEDs to display:

- Critical limit exceeded
- Warning limit exceeded
- Measurement OK
- Audible alarm inhibited

The audible "chime" can be inhibited for individual ground lines with a selector switch. This allows monitoring to continue without the alarm while one or more faults are present and are being investigated.

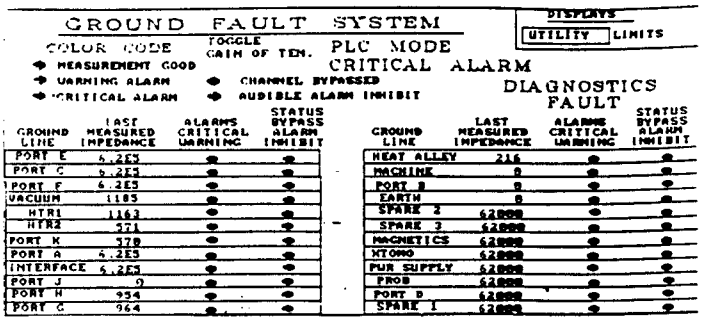

fig. 4 Control Room Display Screen

When the monitor is in "manual mode", the PLCs go off line. The operator selects the ground line to be monitored with a selector switch. Manual mode uses a PLD based state machine to scan the display panel switches and set the multiplexor addresses to the channel that has been selected. This mode is used primarily for searching out ground faults after they have been detected. Other panel switches are used for diagnostic testing.

CONCLUSION

The monitor has been in operation since June 26 and has detected many faults. The PLC interface does not operate as fast as expected. There is still some difficulty measuring phase-shifted ground lines when a dead short fault is present. Overall, the system has been quite reliable.

ACKNOWLEDGEMENT

This work is supported by U.S. DOE Contract No. DE-AC02-78ET51013.

The software for the PLC interface and the Paragon Control System were written by John Lally.

The portable wand was designed by X. Zhong.

REFERENCES

[1] Lawrence Livermore National Laboratory, MTX Project

[2] W.Parkin, "Signal Conditioning Electronics and Packaging for the Alcator C-Mod Tokamak," IEEE Proceedings 14th Symposium on Fusion Engineering, (1991).

[3] CUPL is registered trademark of Logical Devices Inc.

*David Flanary
60 Seminole Road
Acton, MA 01720

Upgrading and operating of the 80 MHz transmitter on the Alcator C-MOD Tokamak

M. Fridberg, E. Byrne, S. Golovato, M. Porkolab, Y. Takase
MIT Plasma Fusion Center
190 Albany St.
Cambridge, MA 02139

ABSTRACT

ICRF heating experiments in the Alcator C-MOD tokamak rely on FMIT transmitters as the power source. The first phase of experiments will require up to 4 MW from two FMIT units. In contrast to other projects, C-MOD is the only tokamak experiment where the original 80 MHz fixed frequency cavities have been retained. The first unit is operational and the required 2 MW, 1 sec. pulses have been run into a dummy load using both an EIMAC X2242 and X2274 for the final power amplifier. During operation of the experiment, access to the transmitters will not be possible. All control and monitoring is done remotely, using a PLC with PC interface. Data acquisition during a shot is done through CAMAC. Fast arc detection circuitry has been developed to protect the transmitter and other RF components. Details of the modification and operation of the transmitters will be presented. Future plans call for upgrading the system by adding additional units and extending the pulse length to 10 sec. A companion paper describes the Alcator ICRF antennas[1].

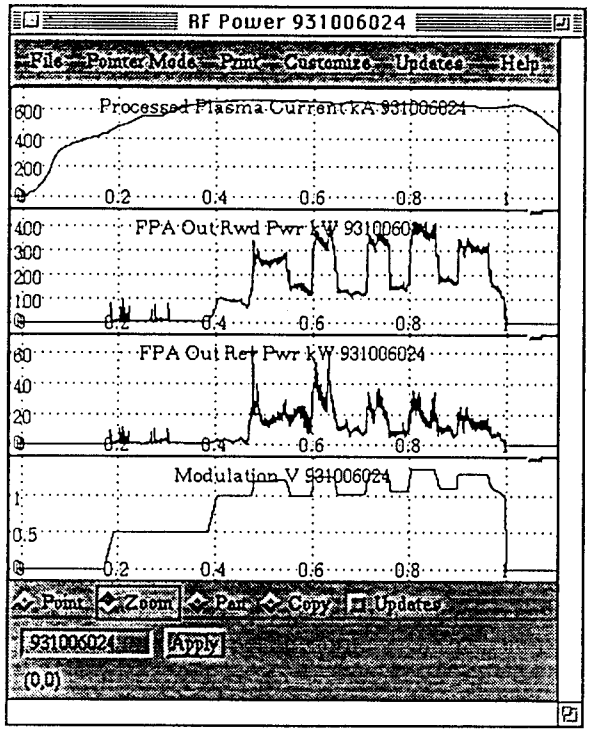

Fig. 1 Power measured on the transmitter during the shot

INTRODUCTION

The transmitter used for ICRF heating is a powerful RF signal generator, producing over 2 MW of RF power at a frequency of 80 MHz.

The Figure. 1 shows a representative plasma shot into which RF is injected. The first trace shows the plasma current, the next two traces show forward and reflected power measured at the output of the transmitter, and the fourth trace shows the programmed modulation signal.

CHANGES

The original FMIT transmitter, built by Continental Electronics Mfg. Co.[2], was designed for a maximum output power of 800 kW, which was inadequate for the experiment. The parts involved in upgrading it to 2 MW power output were:

- Final amplification stage (FPA)
- Driver amplification stage (Driver)
- Intermediate amplification stage (IPA)
- Crowbar cabinet
- High-voltage power supply (HVPS)
- FPA filament power supply
- Driver filament power supply
- Screen and control grid power supplies

Final, Driver and Intermediate Stages

The changes in the amplification stages involved using vacuum tubes with higher plate dissipation that have the same mechanical and electrical parameters as tubes used in the original unit. The plate line and decoupling fitter had to be insulated to avoid arcing in the FPA output cavity at voltages above 26 kV

High-voltage Power Supply

To provide increased power output, the plate voltage has to be increased. The original unit used 18 kV plate voltage for both FPA and Driver. The upgrade requires 30 kV plate voltage for the FPA and 18 kV for the Driver. Power requirements increased to 4.5 MW DC. The original HVPS built by Uptegraff, Mfg., was upgraded to 5 MW output power with 2 high-voltage outputs. It is possible to change voltages on both outputs semi-independently within the 12 kV- 32 kV

range for the FPA and 6 kV-18 kV for the Driver. During tests it was discovered that the modified HVPS is not capable of withstanding crowbars and it was modified once more by encasing windings in epoxy and using large copper wire for windings. Calculations performed by MIT and Uptegraff engineers show that these changes should be adequate.

Crowbar Cabinet

The modifications to the crowbar cabinet consisted of changing it to handle 2 separate high-voltage lines and to increase its voltage handling capability. To avoid corona and arcing in the small-size cabinet, very careful placement of high-voltage cables and insulation were required. Only the cabinet itself and the ignitrons were left unchanged.

Trigger circuits in the modified crowbar were designed to provide a pulse train instead of a single pulse, in the case of an arc. The modified system proved to be very reliable, with no failures during the 3 years of use.

FPA and Driver Filament Power Supplies

The Driver power supply was modified to provide filament current for the higher power tube. The upgrade consisted of rewinding the transformer and using rectifying diodes with higher current handling capabilities.

The original FPA filament power supply was a 3-phase transformer-rectifier supply with a motor-controlled variac for voltage adjustments. The controller for the motor used the AC voltage on the secondary side of the variac for control. This did not take into account the current-dependent voltage drop in the rectifier bridge, filter and cables. The controller was redesigned to use the DC voltage measured at the tube's filament leads. As a result the filament power supply now regulates voltage within ±1%.

Control and screen grid power supplies

The FPA control and screen grid power supplies had to be upgraded to handle the necessary higher grid current.

CONTROL AND DATA ACQUISITION SYSTEMS

The transmitter is located in a room that is inaccessible during operation. Thus, remote control and data acquisition are necessary for its operation.

Remote Control

To integrate transmitter operation into the ALCATOR C-MOD control system, an Allen-Bradley PLC was chosen. To provide total remote control capabilities, all control and indication signals were connected to the PLC. The system provides control of virtually all transmitter functions, as well as remote monitoring its state, with the exception of power circuit breakers.

All states of the transmitter are displayed on a PC located in the control room running Paragon[1] software as operator interface to the PLC. Different screens are used for different modes of operation. The screen used for tuning the transmitter is password protected to avoid accidental changes. The position of the tuning elements is recorded and stored on the PC's hard drive, which allows the operator to restore previous tuning.

Two 9" coaxial switches are used to connect the transmitter to different loads. The choices are an antenna on the experiment, an antenna on the test stand or a dummy load. The switches have motor drives that allow for switching loads remotely using the PLC.

Data Acquisition

All voltages and currents that need to be monitored are digitized and stored onto hard drive/magneto-optical media via CAMAC digitizers and MDSPlus system. INCAA 16-channel digitizers are used at 10 kHz sampling rate. All signals are conditioned to 0-5V, 4 kHz range to prevent overloading and aliasing and to have the maximum dynamic range available for the digitizers.

The signals, such as forward and reflected power, plate voltages and currents, control and screen grid voltages and currents are stored and can be displayed on VAX workstations.

OPERATION OF THE TRANSMITTER

Pulsing of the transmitter is done by exciting it with an amplitude modulated 80 MHz RF signal. The excitation system includes a Hewlett-Packard RF signal generator, modulator, RF preamplifier, Kalmus solid-state power amplifier, coaxial "ENABLE" switch and a gate pulse generator (Fig. 2).

The RF signal generator provides an unmodulated 80 MHz RF signal. The usual output level is -13 dbm, which is enough to cover the whole power range for the transmitter, from 10 W to 2.5 MW. The RF generator is connected to the modulator through an RF coaxial switch, which is controlled by the PLC and allows disabling or enabling the RF.

The RF signal from the generator is modulated by the modulator. It provides about 65 dB dynamic range in modulation level, which allows changing of the transmitter output power from 1 W to 2.5 MW without changing RF levels or ranges in the modulator or signal generator.

It has two feedback inputs, which allow amplitude control and high reflected wave protection. The high reflected wave feedback serves as protection for the transmitter, coaxial lines, matching system and antenna in

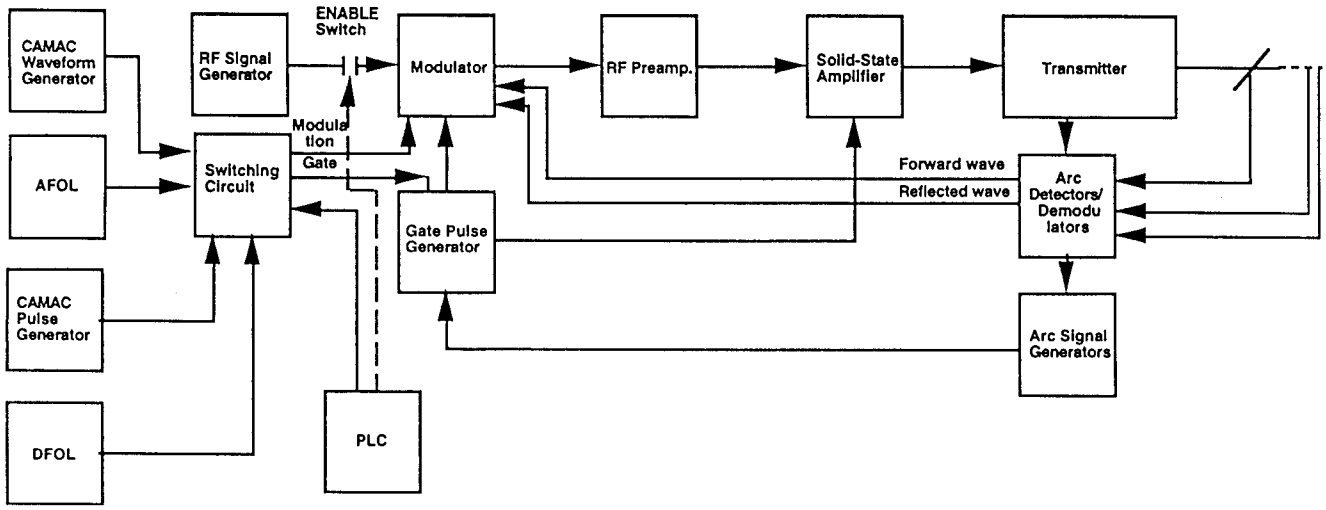

Fig. 2 Excitation system.

case of any mismatch, keeping the reflected wave power level below a specified limit. This limit can be set from 1 kW to 200 kW, the usual setting being about 50 kW. The high reflected wave feedback has priority over amplitude feedback and disables it if the reflected wave becomes too high. This feedback is not an arc protection. In case of an arc, the RF is removed unconditionally by the arc detection system for a specified time. Both feedback systems have a bandwidth of 500 kHz.

The modulator receives its modulating signal from a CAMAC arbitrary waveform generator module for pulsing during a normal shot, from an analog fiberoptic link (AFOL), for antenna conditioning or from a pulse generator for local testing into a dummy load. The switching circuit controlled from the PLC selects the signal being used in remote mode. In local mode, the pulse generator has to be connected manually.

Although the modulator can remove excitation from the transmitter, it is not fast enough for arc protection. For added safety, a gate signal is used to provide an envelope for the modulating signal.

The gate signal is generated by a CAMAC pulse generator module for a normal shot, delivered by digital fiberoptic link (DFOL) - for antenna conditioning or by a local pulse generator for local testing into a dummy load.
The gate signal from either of these sources is received by the gate pulse generator, where it is conditioned and mixed with pulses from the arc detection system. The resulting gate pulse is sent to the Kalmus solid state power amplifier, which is configured in the pulse mode. A complementary gate signal is provided to the modulator to remove the RF in case of an arc. The modulated RF signal is amplified by the RF preamplifier and the Kalmus solid-state power amplifier and fed into the transmitter.

ARC DETECTION AND PROTECTION

Three different types of arc detectors are used. One is based on detection of high VSWR, another one detects an arc if the reflected wave exceeds a specified limit, and the third one is based on RF interference caused by an arc. All three types of arc detectors use the same *logarithmic demodulator* modules with different setpoints. All of them use signals from directional couplers located near the FPA cavity before the first 9" coaxial switch. Additional arc detectors connected to the directional couplers in the experimental cell and provide redundant protection to the transmitter over a fiberoptic link.

Outputs of arc detectors are connected to the arc pulse generators. In response to input impulses, an arc pulse generator will generate a pulse with a length equal to the length of the input pulse plus some additional time -- enough for the arc to extinguish. This time can be changed in a range from 10 μsec to 100 msec. The usual time is 2 msec.

Every arc signal generator board has four inputs. Up to five boards can be connected in parallel, which provides up to twenty inputs.

The output from the arc signal generators and from the switching circuit are combined in the gate pulse generator. The gate pulse generator inserts arc pulses into the gate pulse, removing excitation from the transmitter for a time specified by the arc signal generators, then restoring it. The number of retries can be varied from 1 to 256 by a DIP-switch. The usual setting is 100 for a 1 sec pulse.

Logarithmic Demodulator

The demodulator was designed based on the requirement to provide demodulation of fast pulses (>100 nsec) and wide dynamic range. Assuming useful power output from the transmitter to be from 10 W to 2 MW the dynamic range of demodulator must be at least 53 dB. Logarithmic converters were chosen as a base for the demodulator.

The resulting demodulator has >50 dB dynamic range (Fig. 3) and 10 MHz bandwidth. As added convenience it compresses the demodulated signal so it is easier to transmit and it is more noise-resistant. Digitizers receive compressed signal and all further conversions take place in software.

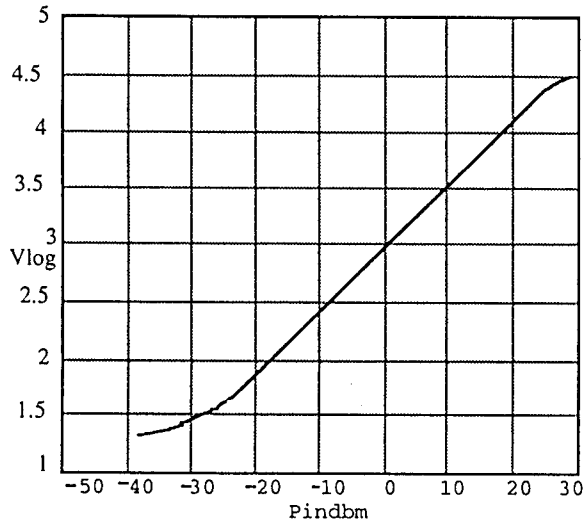

Fig. 3 Output Voltage vs. Input Power for Logarithmic Demodulator

Arc Detection Methods

Arcs, generated in the coaxial waveguide, tuning system or antenna, work as a short. This usually results in a fast and large increase in the reflected power in the matched section of coaxial line. One method of arc detection consists of comparing the forward power with reflected power and making a decision if arc happened if reflected power exceeds certain fraction of forward power. This method has its drawbacks, the main is that the arc might happen at or near the current maximum in the tuners, where short circuit does not produce any significant increase in reflected power. Multipactoring is one of the examples that can lead to such an arc. Those types of arcs will not be detected and can lead to damage to system components. The arcs of this type had happen before on other experiments with serious damage to components as a result. An arc detector that can detect such type of arc, is based on detection of RF interference caused by an arc.

The algorithm needs to check for the presence of non 80 MHz signal that would not be a harmonic component of the carrier or the modulation signal. Such a signal is a clear indication of an arc no matter where it is located. The drawbacks of this method are inability to protect the transmitter against mismatch, relatively low noise immunity, and use of complicated filters for spectrum analysis. This type of arc detector has been tested but is not currently in operation.

CONCLUSIONS

The modified FMIT transmitter is capable of providing the ICRF experiment on ALCATOR C-MOD with up to 2 MW of RF power at 80 MHz. The control system has proved to be flexible and convenient for physics experiments.

ACKNOWLEDGMENT

We wish to thank the TFTR RF group for their help and support. We would also like to thank the MIT Plasma Fusion Center technicians and engineers for their contribution to the project.

This work is sponsored by the US Department of Energy under Contract No. DE- AC02-78ET51013

REFERENCES

[1] Antennas for ICRF Heating in the Alcator-CMOD Tokamak. S. Golovato, P. Bonoli, W. Beck, M. Fridberg, M. Porkolab, Y. Takase.

[2] FMIT Transmitter Operation and Maintenance Manual. Continental Electronics Manufacturing, Co.

[1] Paragon is a registered trademark of INTEC Controls Corporation.

PERFORMANCE OF THE C-MOD SHAPE CONTROL SYSTEM.

S. Horne, M. Greenwald, I. Hutchinson, S. Wolfe, G. Tinios, T. Fredian, J. Stillerman.
Plasma Fusion Center
Massachusetts Institute of Technology
Cambridge, MA 02139

ABSTRACT

The poloidal field system for Alcator C-Mod (a high-field compact tokamak) can generate elongated, single or double null diverted plasmas. The shape control system[1] consists of hardware (hybrid multiplier, real-time control computer, and associated electronics), the user interface (a set of X-Windows applications), and the underlying algorithms used by the interface to calculate the control matrices. The shape control computer generates demands to the power supplies, based on programmed waveforms and feedback from the diagnostics. Beginning in April 1993 we have used the shape control computer to program and/or feed-back control coil currents, power supply voltages, magnetic field quantities and gas pressure during plasma breakdown, and to tailor the fields during the current ramp. Representative data from the 1993 run and an evaluation of the overall performance of the shape control computer will be presented.

Introduction

The C-Mod Tokamak presents interesting challenges in the area of startup and control. The vacuum vessel construction is thick-walled stainless steel with no insulating break, with a toroidal resistance of approximately 40 micro-ohms. Surrounding the vessel and coils is a massive steel superstructure, also conductive, which braces the toroidal and poloidal field coils. The coils themselves are liquid nitrogen cooled[2]. Just after breakdown and during most of the current ramp, the magnetics diagnostics are dominated by currents in the vessel and structure. These currents are not directly measured. Their amplitudes and spatial distribution must be deduced from the magnetics diagnostics and from their effect on the plasma shape[3].

Complicating the effect of these unknown currents in the passive structure is the fact that the poloidal field coil set is sparse, and placement of the coils is a compromise between shape control requirements and very severe engineering constraints. It is not obvious *a priori* that fields produced by currents induced in the passive structure can be canceled by the driven coils to yield a properly shaped and controlled plasma equilibrium.

This work was supported by US DOE Contract No. DE-AC02-78ET51013. Manuscript submitted October 12 1993

Figure 1.

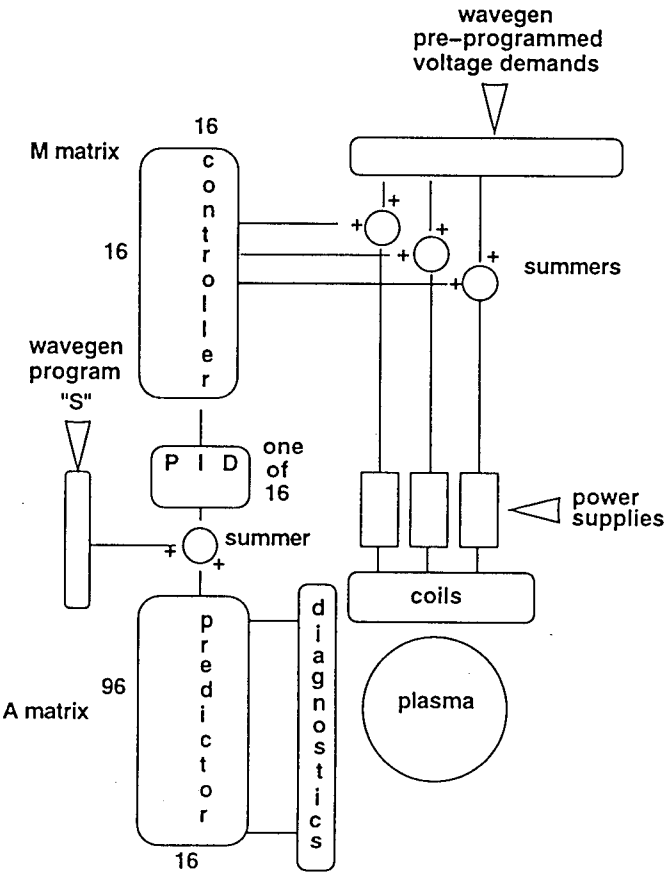

Functional diagram of the control loop.

The control computer

Real-time control of the driven coils is accomplished by the Hybrid computer – so called, because it combines an analog signal path with digitally controlled gains. The computer is assembled of blocks, each of which implements an analog matrix multiplier. The essential idea is that a digital-to analog-converter (DAC) produces an analog output voltage equal to an analog input reference times a digital number. A set of DACs connected to a summing junction produces a dot product; a combination of such sets yields an analog matrix multiplier – a device which produces as outputs a set of voltages which are programmable linear combinations of input voltages. The basic block from which the computer is assembled (a

DAC card) is a (16,4) multiplier – each of 4 outputs is a linear combination of 16 inputs. The card (a double-width Eurocard) also holds sufficient RAM to store 488 sets of 64 digital coefficients (gains), a microprocessor to control the gain switching, and assorted glue logic. A gain switch requires approximately one millisecond. Four of these cards plus a summer card form a 16 x 16 multiplier. These components are packaged into a 1/3 wide module with a front panel containing various input and output connections.

Figure 1 shows a functional block diagram of the control system, following one of the sixteen signal paths around the loop. For concreteness, we will assume this channel controls the current in the ohmic heating coil, OH1.

Diagnostics observe the plasma, producing voltages which are fed to the inputs of the computer. These include the magnetics diagnostics, and the Rogowski coils which measure the coil currents. The first processing block is the A matrix, a 96 x 16 multiplier. Its function is to multiply each of the input voltages by a digital gain, and to sum the result. In the case we are considering, all gains except that on the OH1 buss Rogowski are zero, and the OH1 Rogowski gain is set at -1. (This is the logical gain. The actual number loaded to the DAC depends on various calibration factors.) To this sum is added the wavegen programming for this channel. The analog output of this stage is the error, (programmed value - observed value). The next step provides Proportional/Integral/Derivative analog processing of the error signal. The analog gain available is [-10.,10.], with a 1.e-3 second differentiaion time constant, and a 0.1 second integration time constant. The result is distributed as demand to power supplies by the M matrix, a 16 x 16 multiplier. In the case we are considering, only the OH1 gain would be non-zero. An additional summing junction at this point allows programmed demand voltages to be added into the feedback-developed demands. This total is then fed to the individual supplies as demand voltages.

The power supplies act as amplifiers for their demand, placing their output voltage at the coil terminals. The inductance of the coils integrate their terminal voltage to produce currents and therefore fields. These soak through the structure and into the vessel. The plasma responds, the diagnostics observe, and the loop is closed.

The hybrid computer is itself the most complicated component in the control loop (with the possible exception of the plasma). To monitor its performance, the inputs and outputs of each block (A, PID, M, wavegen) are digitized and stored for post-shot analysis. Figure 2 shows digitized signals at various stages for the OH1 current. The time axis covers the pre-charge of the PF system; the coils are commutated to initiate the plasma at T=0.

Figure 2.

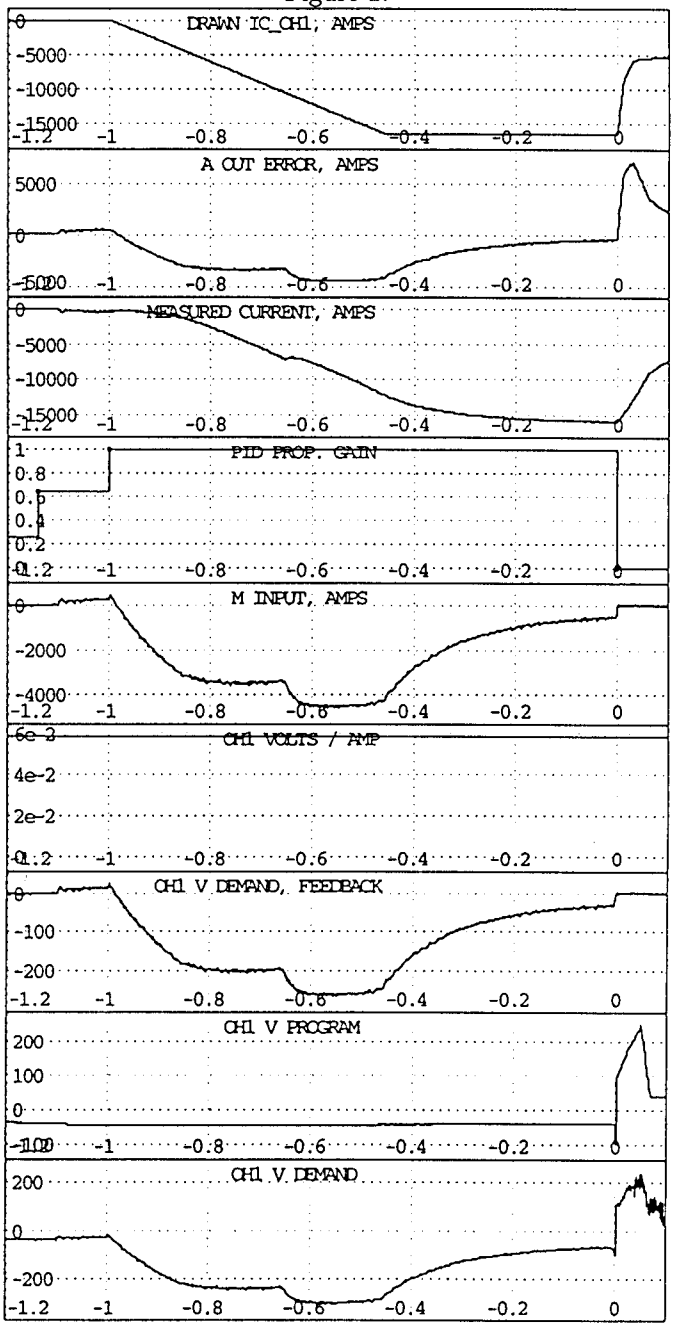

Signals recorded at various points through the OH1 current feedback path .

The top trace is the requested evolution of the current. This has been loaded into the wavegen from a trace drawn using a graphical editor which is one component of the user interface. The interface allows the user to program in physically relevant units (coil currents, plasma position, etc. are specified in SI) and hides (or tries to) the details of scaling from SI to the hybrid internal gains

and voltages.

The next trace (A OUT error) is the difference between the drawn trace and the OH1 buss current, which is shown on the third trace (Predictor). The PID proportional gain is shown in the fourth trace. Derivative and integral gain are zero throughout. The proportional gain is switched to zero at T=0 because from that point on the OH1 supply will no longer be controlled by current feedback, but instead by the plasma current and radial position.

The next trace is the input to the M matrix. To this point, analog signals have represented amperes. The controller takes error as input, and emits voltage demands. In this case, since the error has units of amperes, the controller functions as a transconductance amplifier, with an impedance which has been programmed to .058 ohms. Dividing this into the coil inductance (5.8 mH) gives a characteristic time of 0.1 second for correction of errors, and can be adjusted by varying the proportional gain. This stage contributes a term to the demand due to feedback; the voltage is shown in the next trace (OH1 V DEMAND, FEEDBACK). To this voltage is added the programmed OH1 voltage, and the total demand is shown in the last trace.

Vertical Position Control

Of all the tasks performed by the control system, control of the plasma vertical position is the most demanding, because for reasonable elongations the axysymmetric mode is unstable. Control of the vertical position thus becomes increasingly difficult as the elogation, and with it the passive growth rate, increases. As our plasmas have developed from moderately elongated, limited plasmas towards higher elongation and diverted operation, tuning each element of the vertical control loop has been a priority.

Vertical position control is accomplished using two independent control channels. On the equilibrium time scale, the OH2 and EF1 coils are used as controllers. This system has a large dynamic range, but the bandwidth of this system is limited by a combination of power supply voltage, coil inductance and power supply phase delay. Control on faster timescales is provided by the EFC coils, a low inductance pair of 10-turn coils connected in anti-series, driven by a pulse width modulated chopper. This is a two-quadrant supply, which alternately connects the coil to a 1.0 kV capacitor bank, and a 1.0 kV bank of varistors, with the duty cycle controlled by the demand voltage. This combination yields a small signal bandwidth of about 1500 Hz., falling to about 300 Hz. at full power. However the dynamic range of this system is limited by the small number of turns and the 3000 A current limit on the chopper and coil. (The current limit is constrained by compression forces due to EFC current and vertical field.) A further complication is that the unipolar nature of this supply requires that it be biased at roughly 1500 A to provide optimal operation.

Figure 3.

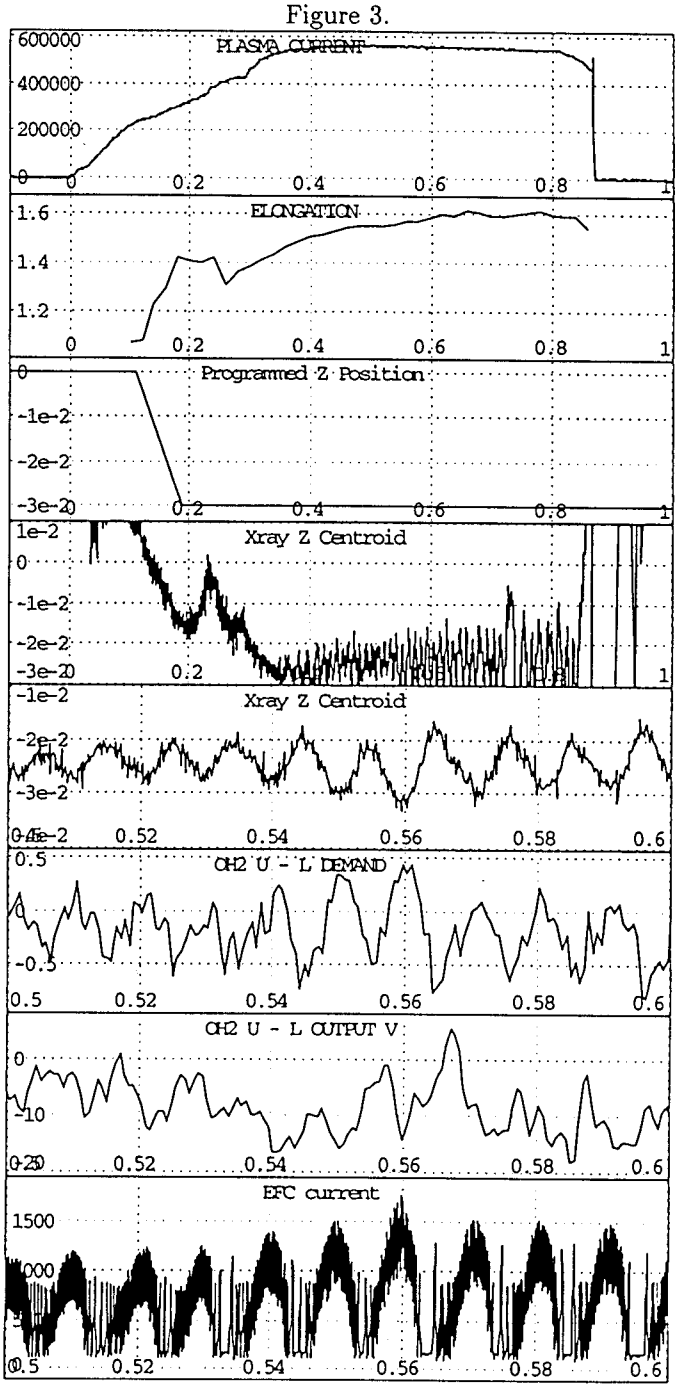

Loss of vertical position control
due to phase lag in the OH2 power supplies.

An early attempt at exploring higher elongation is shown in figure 4. Plasma current is controlled at 0.5 MA. This plasma has an elongation increasing to 1.6. The third

trace shows the programmed Z position, and the fourth the position derived through the X-ray detector arrays. The X-ray data show the Z position to average about 0.5 cm higher than requested.

Starting at an elongation less than 1.5, a vertical oscillation visible on the X-ray centroid appears and grows. On an expanded time frame, (next plot) this appears to be a coherent mode at about 100 Hz. The next frame shows the antisymmetric part of the demand to the OH2 supplies. This signal is developed by the hybrid computer via a position predictor which finds the current centroid of the plasma. It appears to be out of phase with the Z centroid, as it should. (Positive voltage in OH2 U drives positive current, which pulls the plasma up.) The actual power supply output, however, is almost exactly out of phase with the demand. The OH2 supplies show a 180 degree phase lag at 100 Hz. Convolution of the power supply output against the input confirms a .005 second lag. The power supply lag has destabilized the control loop. The last frame shows the current in the EFC system, which is attempting to hold the plasma position against the oscillation due to the OH2 supplies. The chopper is driven to zero current on each cycle, and for that period all high-frequency control of Z position is lost. The shot terminated in a vertical disruption.

Figure 4 shows a similar shot with a different control law used in the equilibrium Z control loop. The proportional gain was reduced and integral gain was added. (The negative plasma current is not a graphics error; the machine was recently reconfigured by reversing poloidal field, toroidal field, and plasma current.) The oscillations in Z position are significantly reduced, if not eliminated. Increasing the integral gain beyond this point has been seen to cause a slow (10 Hz.) vertical oscillation.

We are proceeding with analysis of the axisymmetric instability on C-Mod, using a perturbed equilibrium model of the plasma and a detailed electromagnetic model of the vessel and structure. Initial attempts to model the passive growth rates have been compared to data and factor-of-two agreement is typically seen.

Conclusions, Current problems, Ongoing work

The C-Mod shape control system is still evolving. The hybrid hardware permits great programming flexibility, but certain areas, particularly the implementation of integral gain in the PID, are being rethought. The user interface used to program the computer has been through several revisions and will develop further, in response to increasingly ambitious requirements. As the experimental program moves towards higher plasma currents and higher elongations, the consequences of vertical distruptions (or loss of control in general) become increasingly serious, and the demands placed on the control system will only increase.

Figure 4.

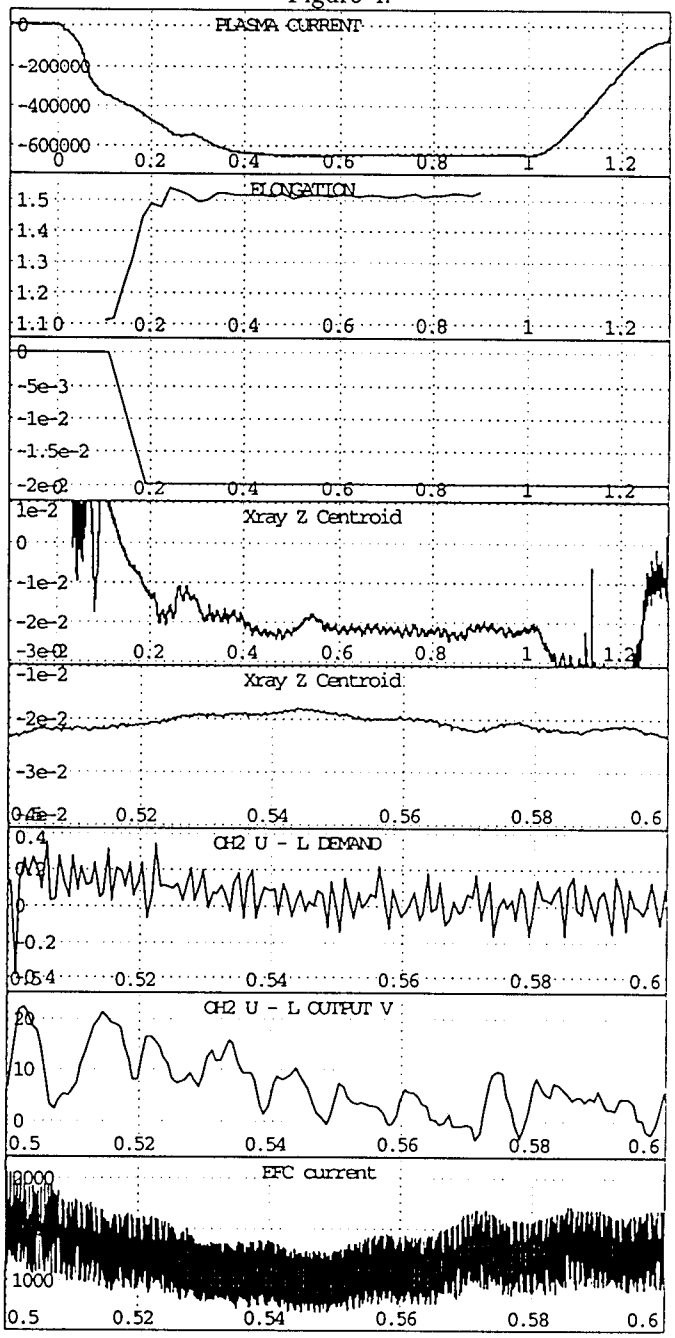

Vertical position control improved
by modifying proportional and integral gain.

References

1. P.F. Isoz, J.B. Lister, Ph. Marmillod, *A Hybrid Matrix Multiplier for Control of the TCV Tokamak*, S.O.F.T. 1990, p 1264ff
2. R. Boivin, C. Reddy, 2-PB1-10, this conference
3. Fairfax, S., 5-OB-2, this conference

THE DESIGN AND PERFORMANCE OF A TWENTY BARREL HYDROGEN PELLET INJECTOR FOR ALCATOR C-MOD

John Urbahn, Martin Greenwald, and Jeff Schachter
MIT Plasma Fusion Center
175 Albany Street, Cambridge, MA. 02139

ABSTRACT

A twenty barrel hydrogen pellet has been designed , built and tested for use on the Alcator C-Mod Tokamak at MIT. The design is the first to use a closed cycle helium refrigerator to cool the thermal system components and employs *in-situ* condensation of the fuel gas. The design of the pellet tracker a diagnostic for following the trajectory of the pellets in time is outlined. This paper discusses the design goals and engineering features of the injector as well as laboratory performance results. Tracker data obtained during injection experiments is also presented.

INTRODUCTION

Alcator C-Mod began operation in March 1992 and is the third in a series of high field, compact tokamaks built at MIT. The design is advanced over its predecessors in that it features a single null divertor with advanced plasma shaping for improved confinement. The purpose of the injector is to fire pellets of frozen hydrogen or deuterium into the Tokamak plasma. Pellet fueling is necessary to provide the high density ,peaked plasma profiles needed for optimal energy confinement. Pellet fueling experiments are an important part of the Alcator experimental program and first began in August of 1993.

DESIGN OVERVIEW

The design goals of the injector are: 1) Operational flexibility 2) High reliability 3) Remote operation with minimal maintenance.

High reliability was a necessary design goal since the primary purpose of the injector is to perform fueling experiments on C-Mod, and operation of the injector itself is not meant to be part of the experiment. Pellet fueling will , in fact, be needed consistently later on in the Alcator experimental program to help create the very high density discharges sought. A single stage light gas gun design is employed on the C-Mod injector because it is currently the most well-developed and reliable acceleration method. The injector uses *in-situ* condensation of the fuel gas to form pellets . This method was pioneered by Lafferanderie [1] and increases reliability by eliminating the need for moving parts at cryogenic temperatures .

This work supported by U.S.-DOE contract no. DE-AC02-78ET51013.

Flexibility in fueling experiments requires that the injector be capable of making pellets of different sizes and firing them either simultaneously or with any desirable time sequencing. Centrifugal or single barrel injectors do not possess this ability . The design goal was met by building the injector with twenty separate barrels allowing for five pellets each in four different size groups of 0.5 , 0.9 , 1.6, and 2.4 x 10^{20} atoms/pellet. The Alcator C-Mod design has the largest number of barrels used in any injector to date. The challenge with such a large number of barrels is to reduce both the parts count and the space requirements.

Remote operation with limited maintenance is a necessary requirement for the design because Alcator cell access is limited both during and between shots due to hazardous power supplies, possible low oxygen levels and most importantly , due to neutron and X-ray radiation from the plasma. The injector is therefore designed to operate for periods in excess of one week without direct maintenance. This requirement was met, in part, by using a closed cycle helium refrigerator to freeze the fuel gas. This is the first time a closed cycle system has been employed, the usual method being to employ an open cycle liquid helium heat exchanger. These would require cell access and expensive daily cryogenic ressupply . The closed cycle refrigerator avoids these problems but introduces other design challenges. The minimum available temperature of the refrigerator is 9 K, well above that available with liquid helium. Therefore, the thermal connection linking the refrigerator to the pellet freezing zone must have an extremely low thermal resistance in order to maintain temperatures below the freezing point of hydrogen .

ENGINEERING FEATURES

The C-MOD injector employs a total of twenty barrels having three different internal diameters, 10 of 1.8 mm and 5 each of 1.37 and 1.04 mm. Pellets are formed in place inside the barrel by opening twenty solenoid actuated fueling valves to a small plenum containing low pressure (100-350 torr) deuterium or hydrogen. This fuel flows through the barrels between the volumes on either end of the barrel. At around twenty to thirty torr the pressure equilibrates and freezing of the fuel gas begins . A small copper disk which is silver brazed to the barrel is cooled to approximately 12 K by thermal connection to a closed cycle helium refrigerator . Fuel gas pressure is below the triple point , causing the gas to freeze directly from the vapor to solid phase on the internal barrel wall in the small annular region cooled by the disk . After a few minutes, a cylindrical pellet is fully formed within the barrel, the diameter and

length of which are controlled by the barrel size and the thickness of the copper cooling disk.

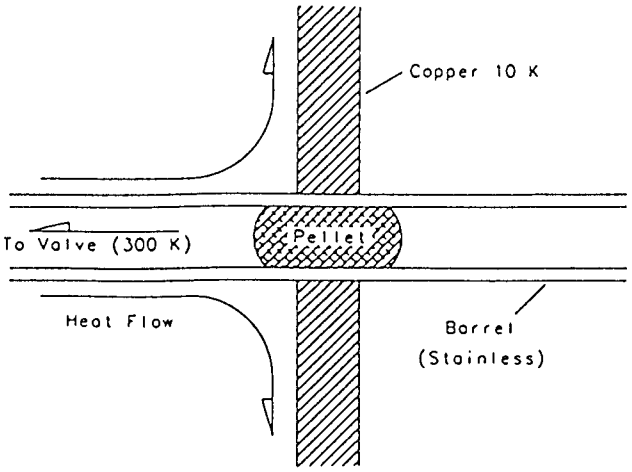

Fig. 1 : *In situ* condensation of the fuel gas.

The pellet is fired by opening high speed propellant valves which connect to a regulated high pressure gas supply. The valves were developed at the Oak Ridge National Laboratory and specifically designed for fast operation [2]. The valve body was redesigned however, to permit modular, "building block" stacking. The pressure differential applied to the pellet shears it away from the freezing zone and accelerates it down the barrel length.

The 20 barrels, cooling disks, thermal connections, propellant and fuel valves are all contained within a rectangular vacuum vessel, or cryostat which provides thermal insulation for the cold temperature components. The doors of the cryostat are removable for internal access. A closed cycle refrigerator is mounted on top of the vessel , the cold head of which is internal to the cryostat and thermally connected to the barrel cold plate.

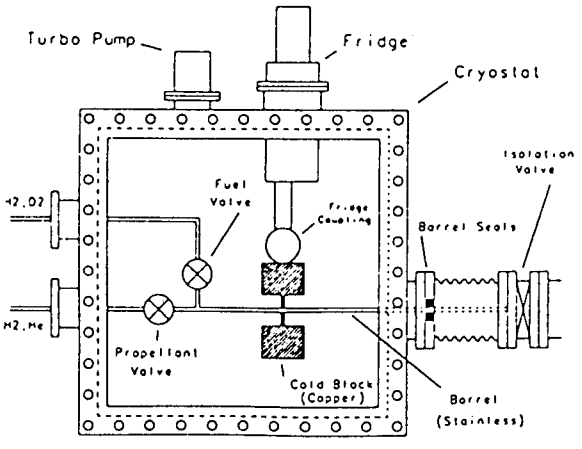

Fig. 2 : Cryostat internals

Prior to entering the plasma , pellets pass through the injection line. The injection line has two time of flight laser - photo diode gates to measure pellet velocity . The laser velocimeter is unique in its design in that each gate uses a single laser and photo diode to detect pellets from all twenty barrels.

A test cell ,used to facilitate pellet photography, is located in the forward section of the injection line . The photography apparatus are external to the injection line and consist of a CCD camera and nanolamp located on either side of the test cell windows. In flight photographs were successfully taken and used to determine pellet mass, shape and condition. The test cell is also equipped with a retractable target plate to which is attached a microphone for detecting pellet impacts. A series of baffles and pellet "guide tubes" in the injection line serve to direct propellant gas away from the tokamak and into the expansion tank where it can be pumped away.

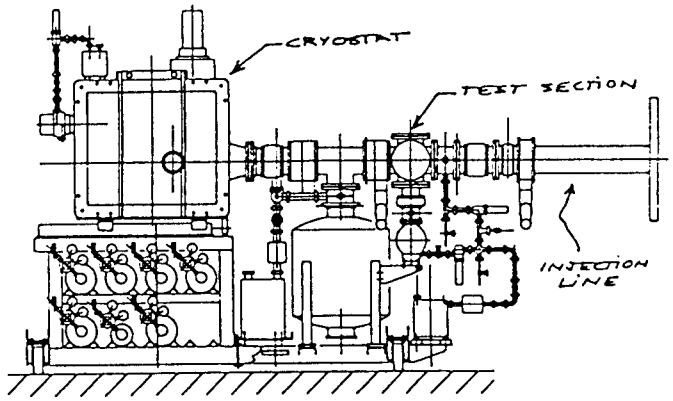

Fig. 3 : Injector side view

The injection line, cryostat vacuum system, fuel and propellant systems contain over 100 valves most of which are operated by programmable logic controllers (PLC) with a menu driven P.C. user interface. These systems allow for both the automatic control of the pellet freezing process and the monitoring of injector pressures and temperatures.

Firing of the propellant valves and high speed data acquisitions from the pellet diagnostics are made by CAMAC system timing and digitization modules. Data storage and manipulation and is via MDS software run on a network of interconnected workstations. Shot data from the injector and other diagnostics are stored in a hierarchical data structure or 'tree' which can be easily accessed by the MDS software for analysis of the shot data.

PERFORMANCE CHARACTERIZATION

The first tests of the injector were of the closed cycle refrigerator and thermal system. Cooldown of the thermal system components takes five hours, after which the low temperature equilibrium point of 9.5 K is reached. The cooling characteristics of the refrigerator indicate that the equilibrium temperature is consistent with the two watt refrigerator heat load anticipated. Average temperature near

the pellet freezing zone was 12.4 K, below the minimum necessary to freeze both hydrogen and deuterium.

Freezing experiments were successfully conducted with both hydrogen and deuterium. Extensive tests were performed to establish the effect of varying the pellet freeze time and pressure on the pellet mass. The optimum pellet "recipe" was determined for both hydrogen and deuterium and incorporated into the PLC controlled automated pellet manufacturing cycle. Repetitive pellet mass measurements were made with the pellet photography apparatus . These tests established the average deuterium pellet size from the four groups of barrels to be to be 0.5 , 0.9, 1.6 , and 2.4 x 10^{20} atoms/pellet.

Measurements were made of pellet velocities over a range of hydrogen propellant pressures from 2.3 to 8.5 Mpa (350 to 1250 psi). The results are shown in figure three below. The solid line represents the maximum theoretical pellet velocity for a fixed barrel length of 24 centimeters. The velocity difference is due to viscous forces acting on the pellet and the propellant gas.

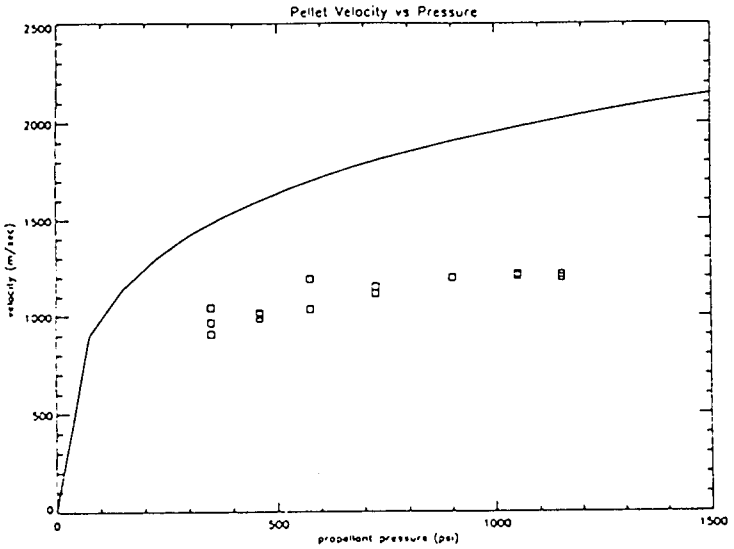

Fig. 4 : Pellet velocity vs. propellant pressure

THE PELLET TRACKER

The pellet tracker's purpose is to record the trajectory of the pellets into the tokamak plasma as a function of time . The position of the pellet in time is needed in order to correlate ablation rates to plasma properties. The data from the tracker provides the location of the neutral particle source needed to study transport issues on the pellet transit time scale (150 μ sec).

The stereoscopic tracking system is novel in its design and consists of two modified 35 mm Pentax K-1000 cameras which each have a two dimensional photo diode located in the film imaging plane. The cameras provide the imaging optics, apertures and the viewfinders needed for the tracking system. The UDT DLS-10 detectors used have an active surface area of one square centimeter and consist of p and n doped silicon semiconductor layers. Spectral response range is from 300 nm to 1150 nm with the peak around 900 nm. Sensitivity is .5 A/W at 900 nm [3]. Current flows between layers where photons are incident on the surface.

The two cameras are rigidly mounted on G-10 blocks which provide both electrical and thermal insulation between the camera and the vacuum vessel. The mounting block also contains an H-α filter holder located directly in front of the camera lens. The camera is held both at its base and at the lens ensuring a fixed and non-adjustable orientation for the camera. Cameras are mounted twenty-eight centimeters above and below the vacuum vessel mid plane on the injection port flange. The optical axes of both cameras are angled towards the mid plane by 11.9°. During operation, the cameras' lens system images photons from the pellet ablation cloud onto the photo diode surface. Each camera generates two pairs of signals, I_1, I_2 and I_3, I_4 . The difference over the sum for each pair is proportional to the position of the light image on the photo diode Y and X axes. The camera signals are amplified and digitized at a frequency of half a megahertz, providing for a two micro second time resolution . These signals are used to determine the equations of the lines of sight from each camera's optical center to the pellet's light emitting centroid. Lines of sight are computed for each voltage sample through the use of twelve fitted calibration constants. Because the lines need not necessarily intersect, the three dimensional location of the pellet in space is determined to be the midpoint of the line segment joining the lines two points of closest approach. Spatial tracking accuracy is improved over one dimensional tracking systems or cameras and is within ± 3mm in the plane perpendicular to the line of sight (Z and R* PHI) and ± 6 mm in depth or major radius. Camera orientation, and the coordinate axes are shown in Fig. 5 below.

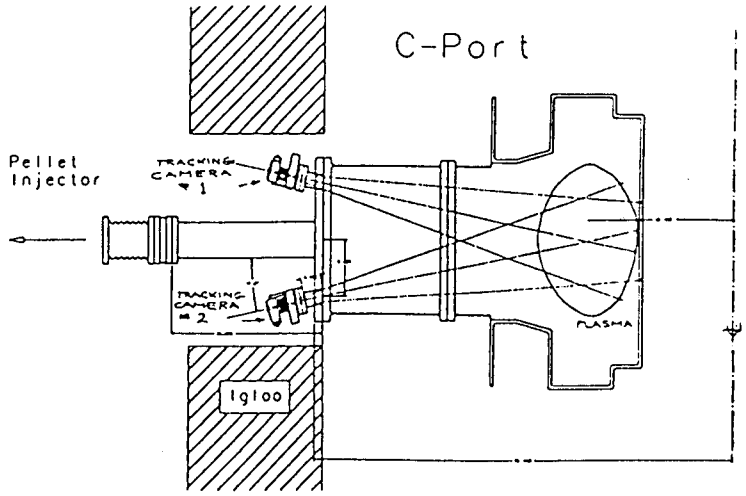

Fig. 5: Pellet Tracker apparatus and Alcator C-Mod cross section.

INJECTION RESULTS

A typical trajectory for a deuterium pellet with a size corresponding to 1 x 10^{20} atoms is shown in figure six. The data shows the pellets radial penetration into the plasma as a function of time. Total transit time for the pellet is 150 micro seconds. The dotted line depicts the pellet velocity and position corresponding to the injection line time of flight measurements.

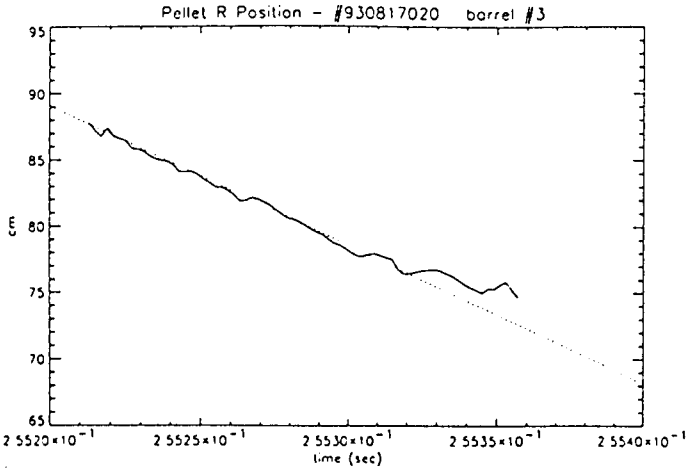

Fig. 6: Pellet radial position vs. time

Pellets typically show some deviation from a purely ballistic path, particularly towards the end of the trajectory. The deviation may be due to either non uniform ablative forces or fluctuations in the ablation cloud. Pellet penetration range is typically between 50-75 percent of the plasma minor radius for C-Mod plasmas with up to 600 K amps of current.

Figure seven depicts the line averaged central density as a function of time following injection of 1 x 10^{20} atom deuterium pellet. Immediately following injection, Plasma density was seen to rise to a level double that of the pre-injection value.

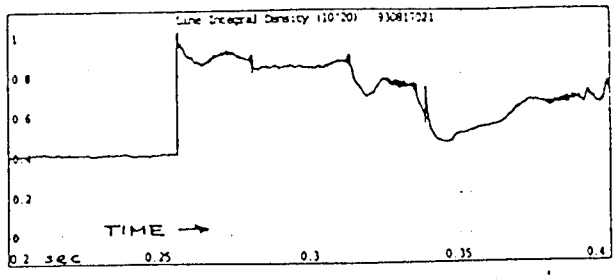

Fig 7 : Line averaged central density during pellet injection

In summary, the C-Mod hydrogen pellet injector has been shown to produce both hydrogen and deuterium pellets and inject them reliably into the Tokamak plasma. The pellet tracker has also been successfully tested during injection experiments and should prove extremely useful for pellet fueling and transport experiments.

ACKNOWLEDGMENT

Design work by Mr.. Art Gentile is greatly appreciated as is the invaluable help of Mr. Frank Silva and the Alcator Technical staff. We are also thankful for the assistance with vacuum systems given by Mr. Robert Childs and Thomas Tolland. This work was a collaborative effort with the entire Alcator Staff, and our thanks go to all of them.

REFERENCES

1) Lafferranderie. J , International pellet fueling workshop, San Diego, CA, USA ,October 30 November 3 1985

2) Combs S., Milora S. J. Vacuum Science and Technology. A4(3) 1113 (May 1986)

3) United Detector Technologies Inc., " Position Sensing Photo detectors", 12525 Chadron Ave., Hawthorne, CA. 90250